Chemische Methoden

Elemente und Elementgruppen

Alkali- & Erdalkalimetalle

Stark elektropositiv, geringe Ionisierungenergie,
reaktiv, bilden ionische Verbindungen
Oxide sind basisch

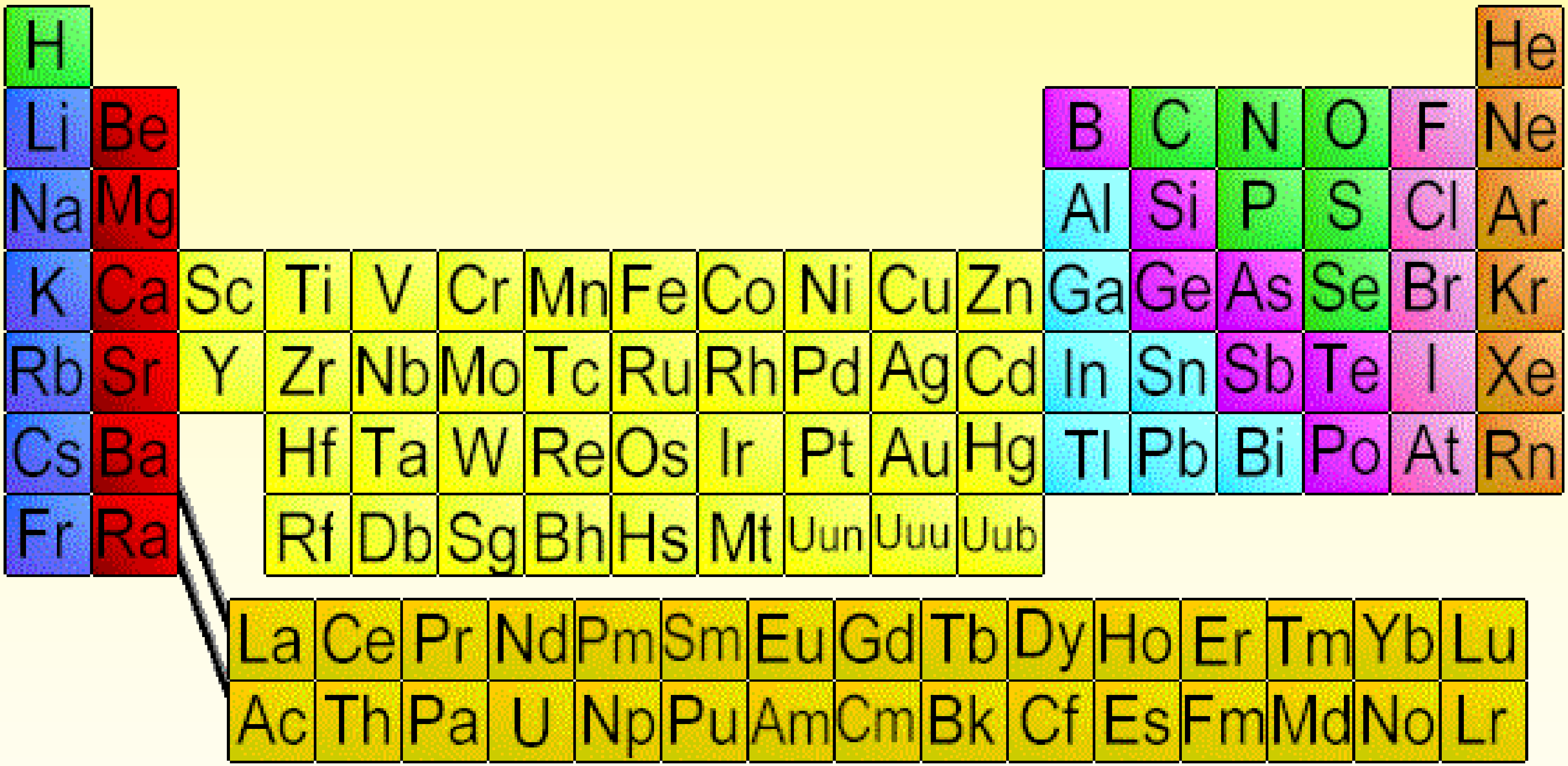

Alkali- & Erdalkalimetalle: Ionische Verbindungen

Ionenbindung zwischen Alkalimetallen und Elementen, die rechts im PSE stehen, den Nichtmetallen. Natriumchlorid klassischer Fall der Ionenbindung
Na: *e⁻ Donator (wird zu Kation),* Nichtmetall (z.B. Cl) *e⁻ Akzeptor (wird zu Anion)*

Die Ionenbindung ist elektrostatischer Natur aber nicht orientiert bzw. nicht gerichtet

Na $3s^1 \rightarrow$ **Na⁺** + e^-[Ne]

Cl $3s^2 3p^5 + e^- \rightarrow$ **Cl⁻** [Ar]

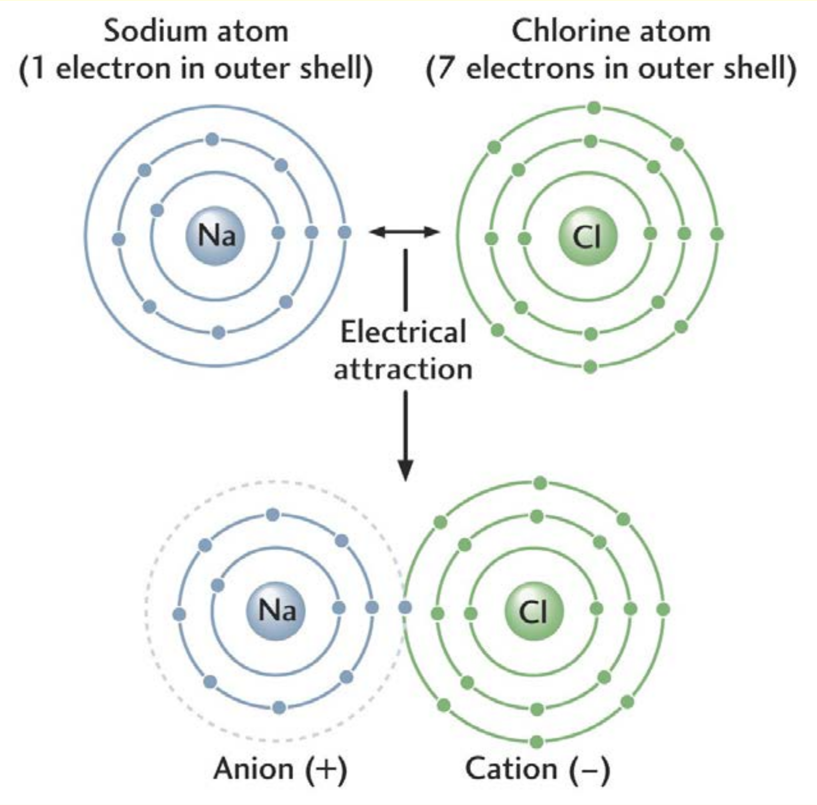

Alkali- & Erdalkalimetalle

Hohe Löslichkeiten im Meerwasser

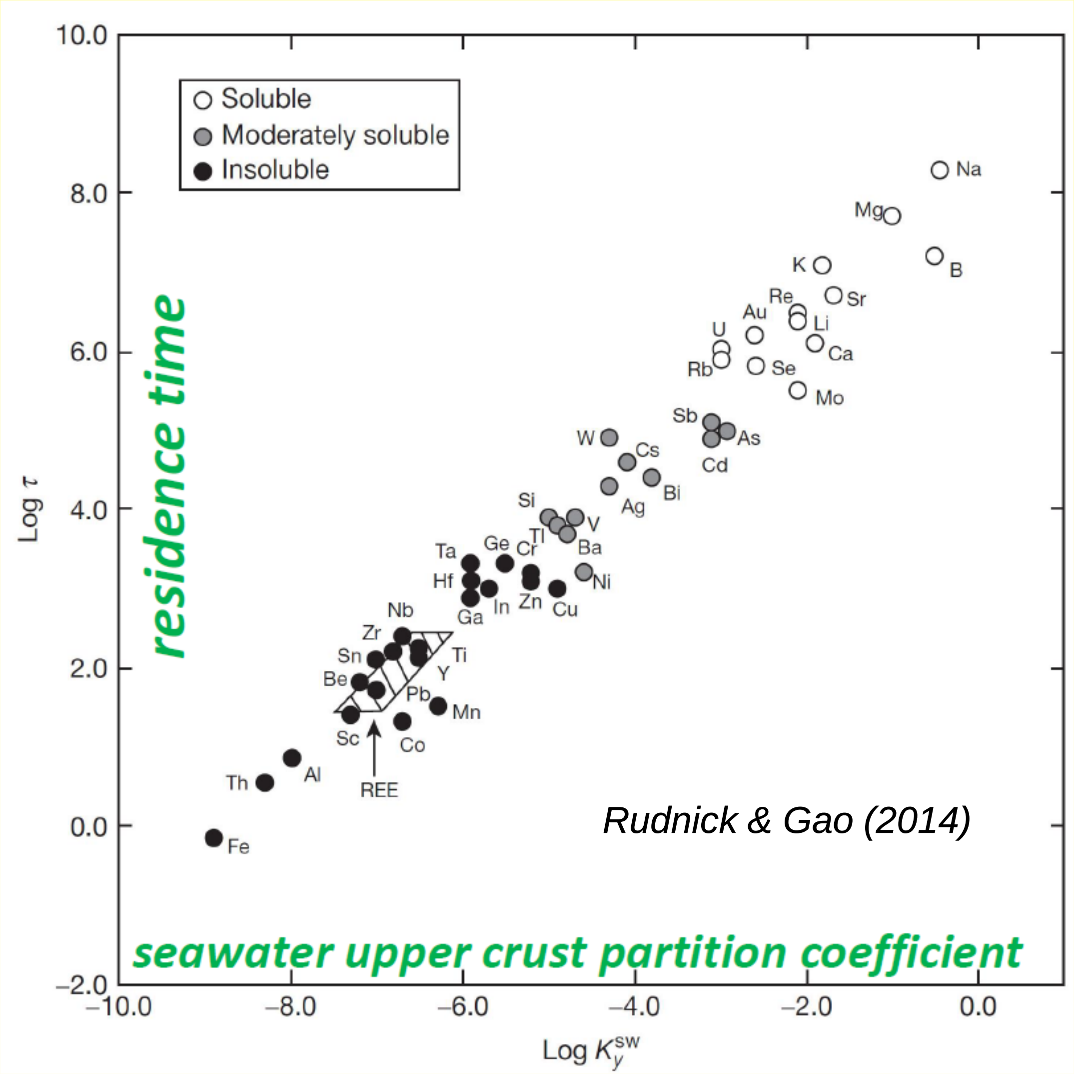

Radioaktive Alkalimetalle

Von großer Bedeutung sind **^{40}K** und **^{87}Rb**
Beide Isotope weisen große Halbwertszeiten auf (1.25 bzw. 48.8 Ga) und sind daher geeignet Erdalter zu bestimmen → isotopische Altersdatierung, Geochronologie

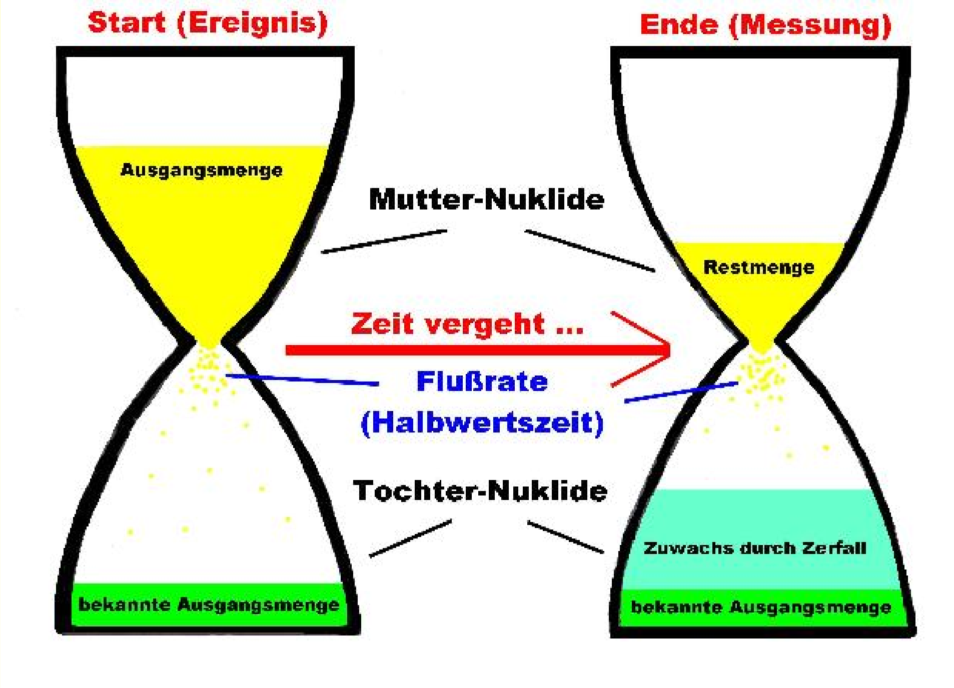

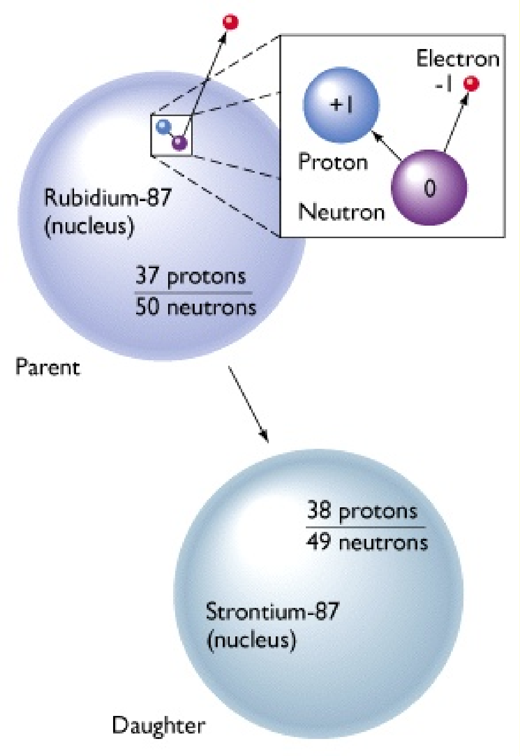

$$D = N(e^{\lambda t} - 1)$$

$$t = \frac{1}{\lambda} \ln\left(1 + \frac{D}{N}\right)$$

Wasserstoff (H)

H verhält sich **nicht** wie die anderen Alkalimetalle (besitzt z.B. eine viel höhere Ionisierungsenergie und keine Metalleigenschaften

Geowissenschaftlich wichtig als OH^- (in wasserhaltigen Mineralen wie Glimmern) und als Wassermolekül (H_2O)

Elementarer Wasserstoff besteht aus den beiden stabilen isotopen ^1H (99.984%) und ^2H (0.016%) bzw. D (Deuterium).
Ein drittes Isotop, Tritium, ist radioaktiv

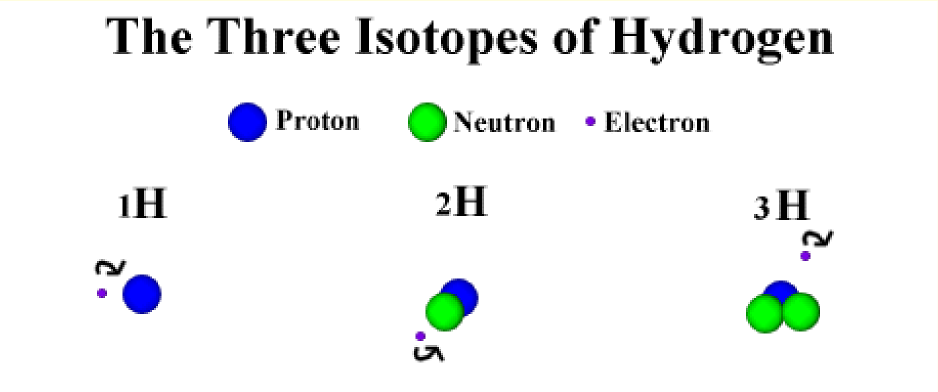

Tritium – ein hydrologischer Tracer

Bomb Tritium

Most of the tritium in the world today was produced by atmospheric testing of nuclear devices that began in 1952 and reached a maximum in 1963/1964.
The bulk of this tritium was released in the northern hemisphere, and entered the oceans.

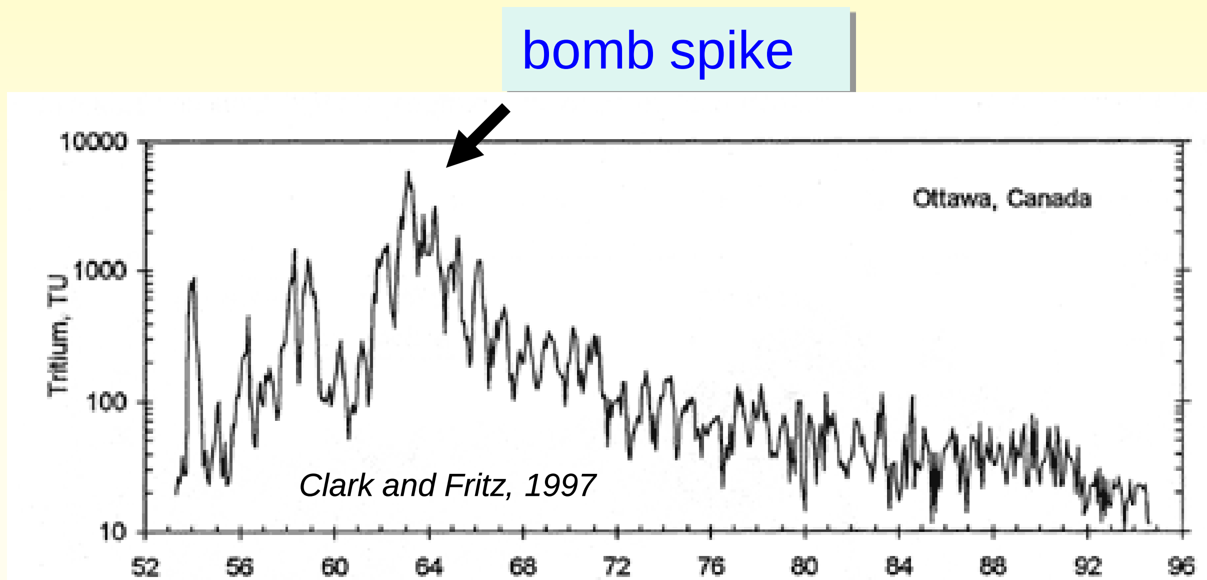

rainfall tritium concentrations

Tritium dating

- Tritium forms in the atmosphere by the interaction of ^{14}N with cosmic-ray neutrons:

  $^{14}N + ^{1}n \rightarrow ^{12}C + ^{3}H$

- Tritium rapidly combines with oxygen, forming water (HTO). Then it mixes with all other water

- Tritium decays to Helium-3; $T_{1/2}$ = 12.3 years

- Low activity ~1 part in 10^{18} (varies by region)

- Used to trace water sources; age of „recent“ materials

- Sources directly fed by rainwater will contain the same tritium levels as rainwater

Reported in units of tritium units (TU):
1 TU = 1 atom of tritium per 10^{18} atoms of hydrogen

Tritium /^{3}He age

The tritium/^{3}He age is an **apparent age**

Advantage: It is independent of the initial tritium concentration of the water sample.

Potential problem: tritium/^{3}He age is affected by mixing and dispersion

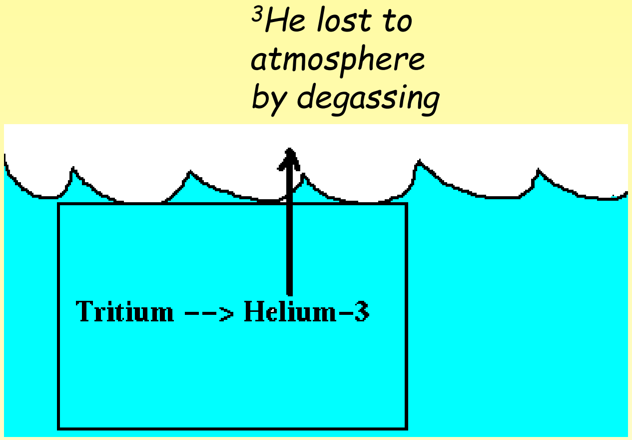

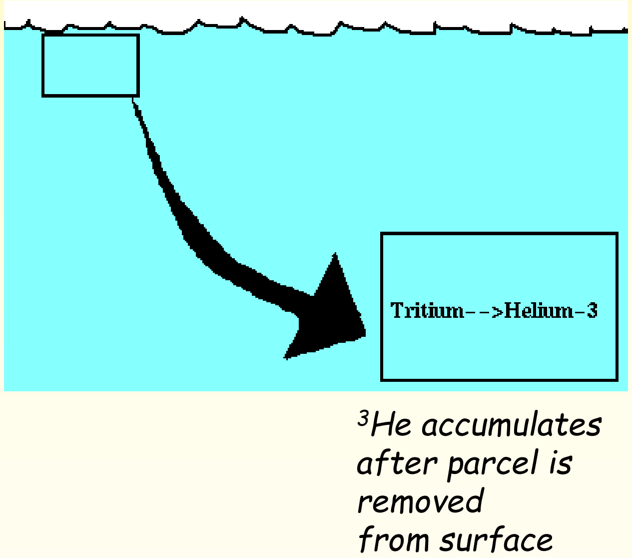

Tritium dating

Dating of ground waters

Assumptions:

(1) tritium of water was in equilibrium with atmospheric levels

(2) decrease in tritium levels is only due to radioactive decay

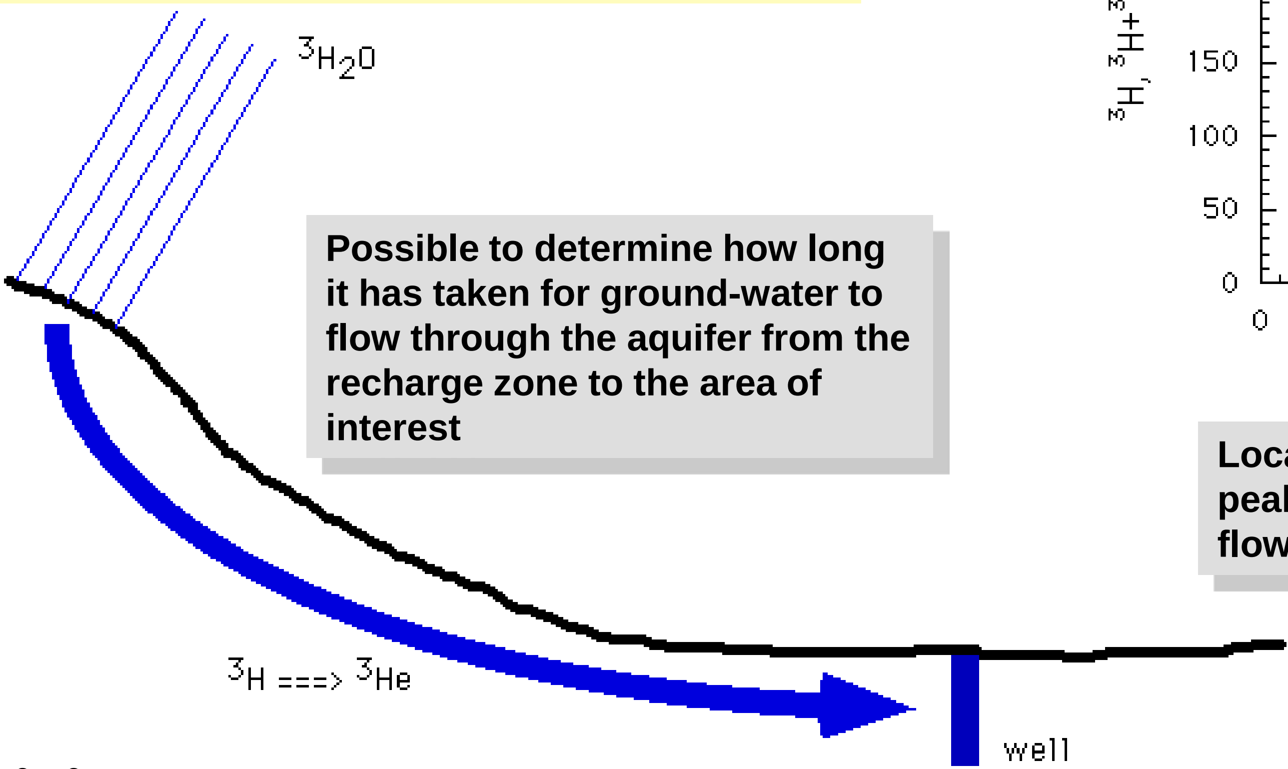

Possible to determine how long it has taken for ground-water to flow through the aquifer from the recharge zone to the area of interest

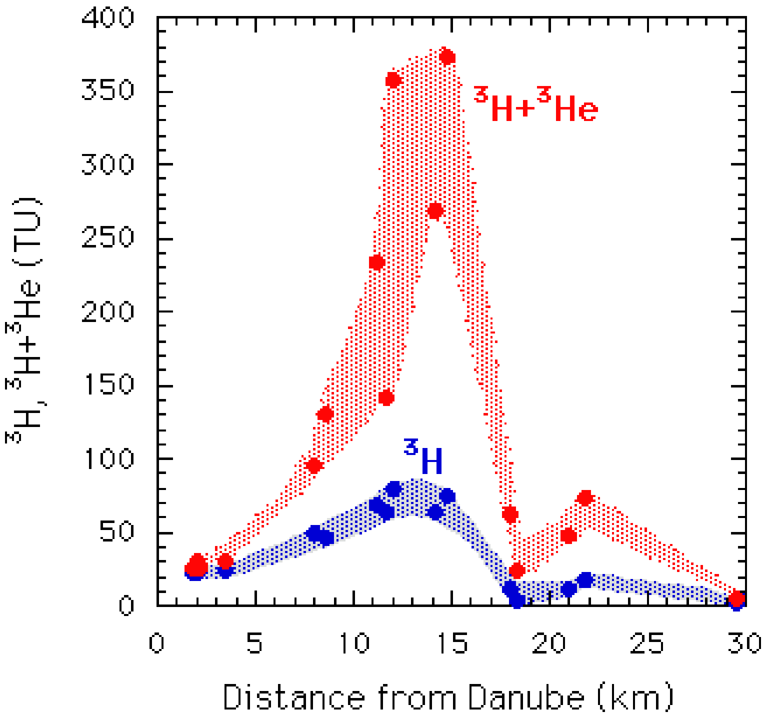

Location of the mid-1960s bomb peak provides information on the flow velocity

$^3H/^3He$ age is defined as the time elapsed since the water was isolated from the atmosphere

Erdalkalimetalle, Leichte Elemente

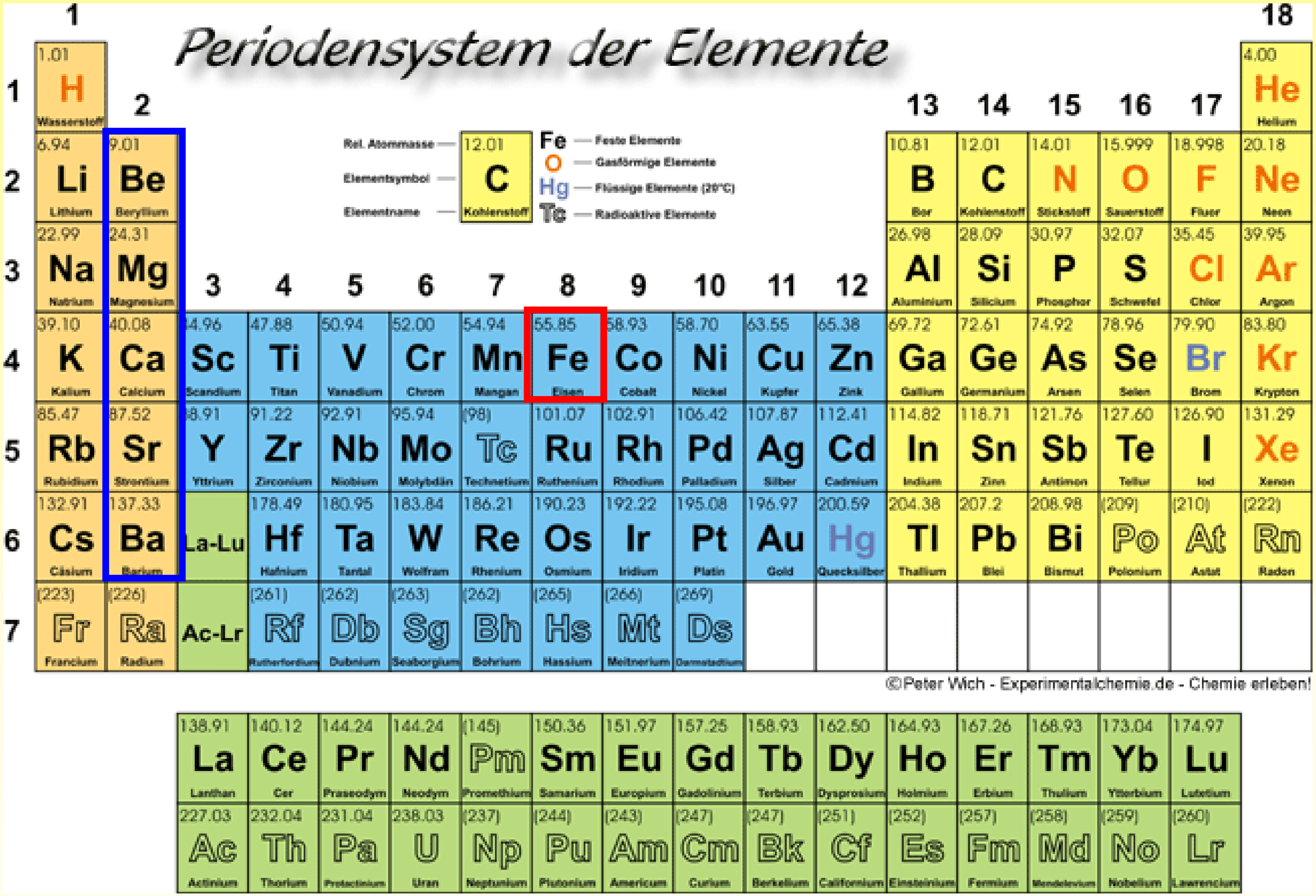

Fe-Mg Austausch

Mg^{2+} hat ähnlichen Ionenradius wie Fe^{2+}

Eisen-Magnesium Minerale wie Olivin (s. Abbildungen unten) oder Pyroxen zeigen vollständige Mischkristallbildung

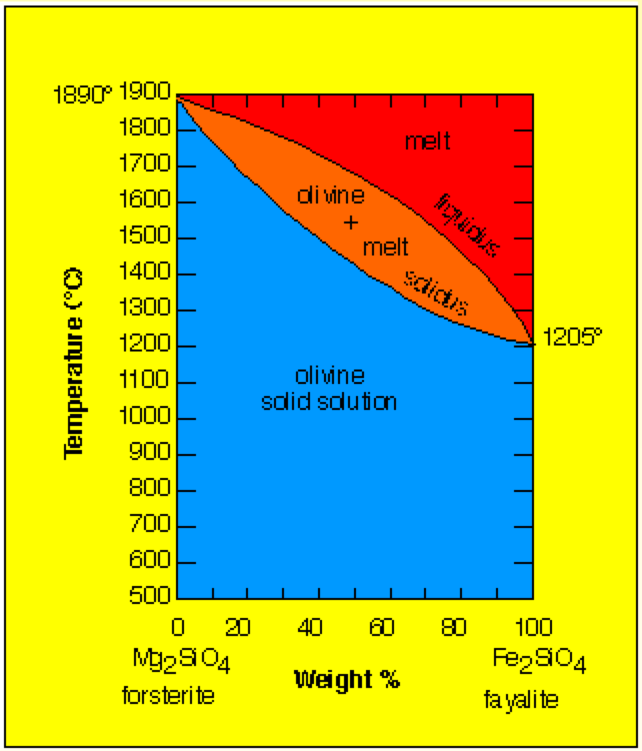

Erdmantel besteht aus Peridotit, der wiederum zu ca. 60% aus Mg-reichen Olivin

Erdmantelgestein (grün) in Basaltlava

Gleichgewichts-Schmelzbildung

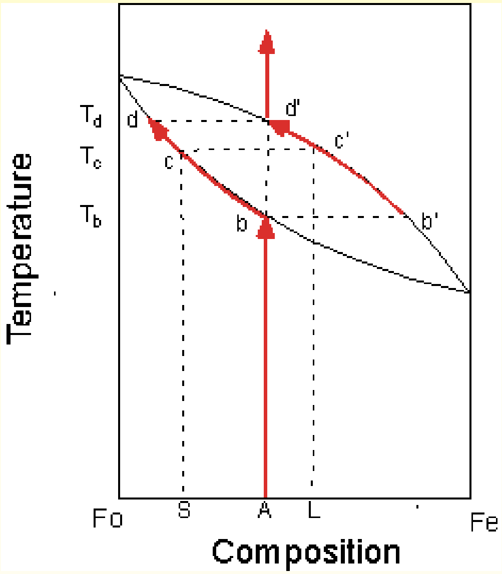

Fraktionierte Aufschmelzung

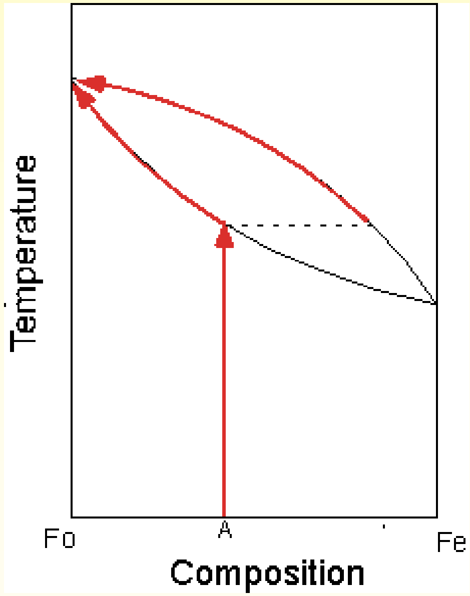

Fe-Mg Austausch zwischen Mineralen

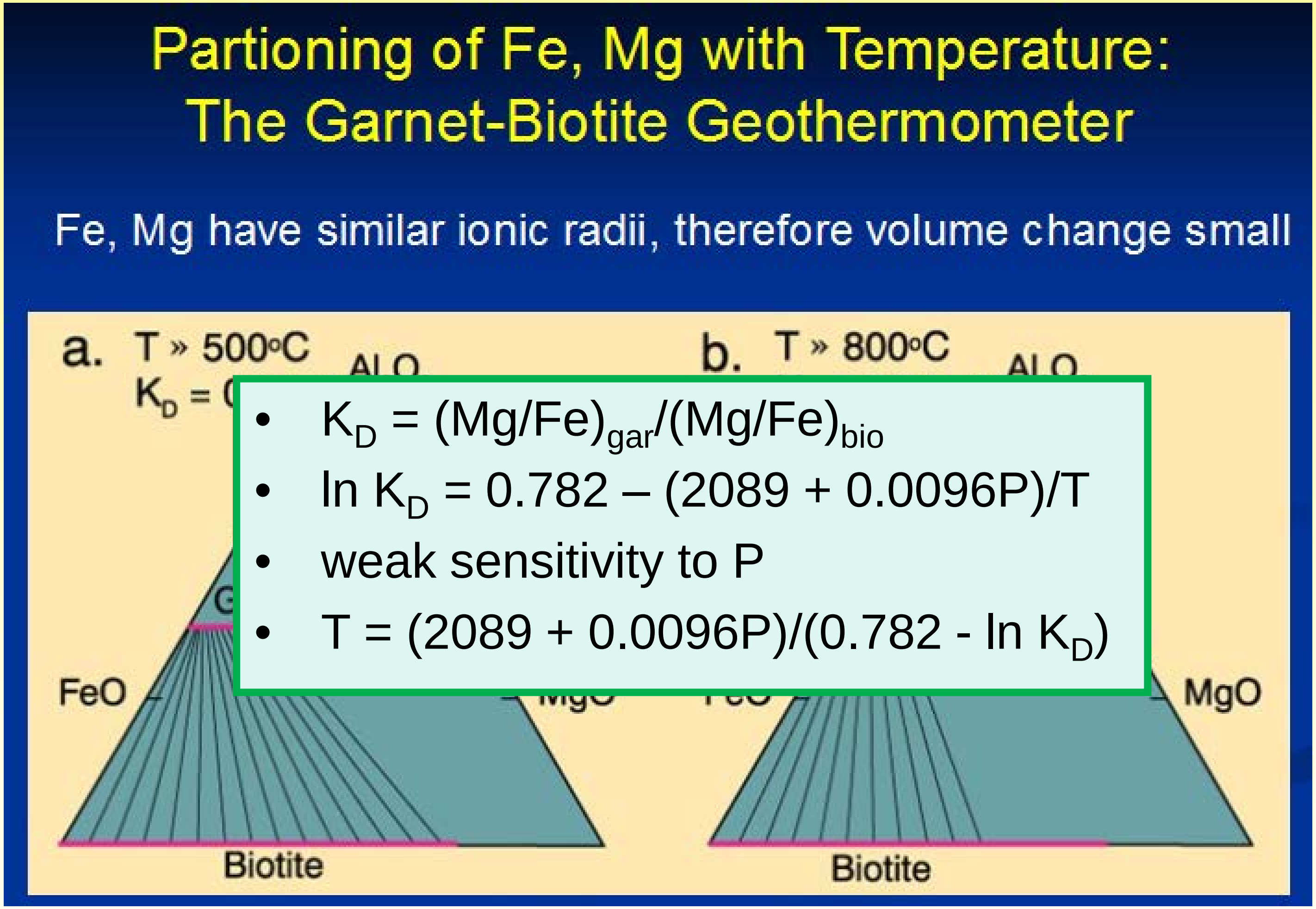

- $K_D = (Mg/Fe)_{gar}/(Mg/Fe)_{bio}$
- $\ln K_D = 0.782 – (2089 + 0.0096P)/T$
- weak sensitivity to P
- $T = (2089 + 0.0096P)/(0.782 - \ln K_D)$

$$\underset{\text{almandine}}{Fe_3Al_2Si_3O_{12}} + \underset{\text{phlogopite}}{KMg_3AlSi_3O_{10}(OH)_2} = \underset{\text{pyrope}}{Mg_3Al_2Si_3O_{12}} + \underset{\text{annite}}{KFe_3AlSi_3O_{10}(OH)_2}$$

Fe-Mg Zahl

Wichtiger Gesteinsparameter

$$Mg' = \frac{mol\,Mg^{2+}}{mol\,Mg^{2+} + mol\,Fe^{2+}}$$

$$Mg' = \frac{\frac{1}{40{,}32}MgO}{\frac{1}{40{,}32}MgO + \frac{0{,}9}{79{,}8}Fe_2O_3(Total)}$$

Oxid Gew. %	Trachyt	Phonolith	Granit	Granodiorit	Andesit	Diorit	Basalt	Basanit	N-MORB	Inselbogentholeiit	Boninit	Nephelinit	Harzburgit	MORB-Pyrolith	Lherzolith	Dunit
SiO_2	62,31	57,43	71,84	66,91	58,7	58,34	49,97	45,16	50,35	49,00	53,00	41,81	43,73	44,74	44,16	41,03
Fe_2O_3	3,04	2,85	1,22	1,40	3,31	2,54	3,85	4,02				5,64	6,0			
FeO	2,33	2,07	1,65	2,76	4,09	4,99	7,24	7,65	11,30	9,79	7,54	6,35	7,09	7,55	8,14	6,26
MgO	0,94	1,09	0,72	1,76	3,37	3,77	6,84	8,71	8,65	11,62	13,08	6,58	36,34	39,57	41,05	51,88
Mg#	0,28	0,33	0,36	0,48	0,50	0,52	0,58	0,62	0,63	0,72	0,79	0,82	0,86	0,92	0,92	0,95

Mg/Ca-Verhältnisse als Temperaturproxies

- Einbau von Mg in Calcit ($CaCO_3$) → Diadochie
- **Mg/Ca** Verhältnis in Foraminiferen ist temperaturabhängig

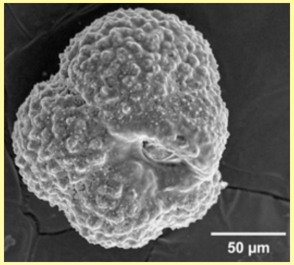

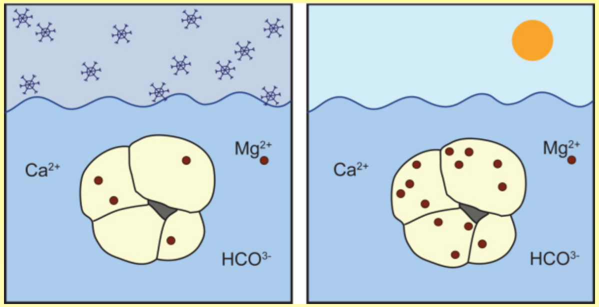

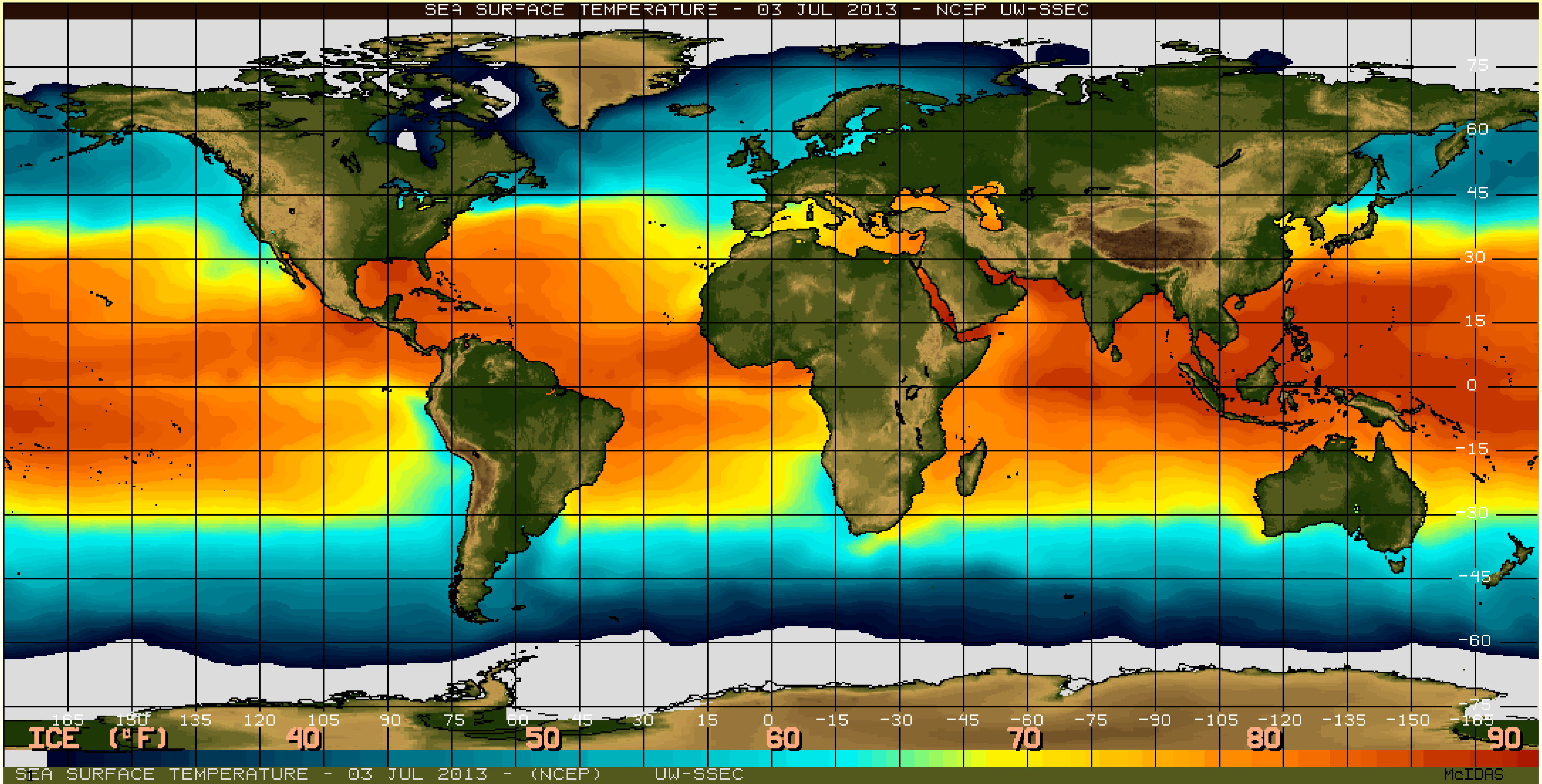

Mg/Ca-Verhältnisse als Temperaturproxies

- Einbau von Mg in Calcit ($CaCO_3$) → Diadochie
- **Mg/Ca** Verhältnis in Foraminiferen ist temperaturabhängig

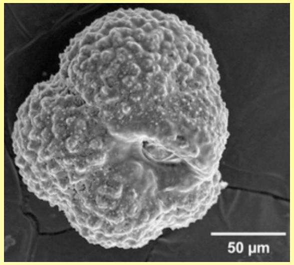

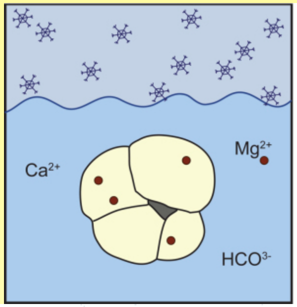

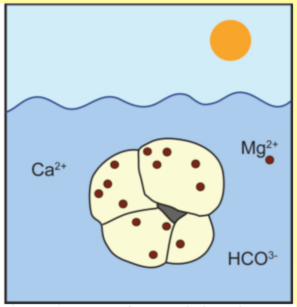

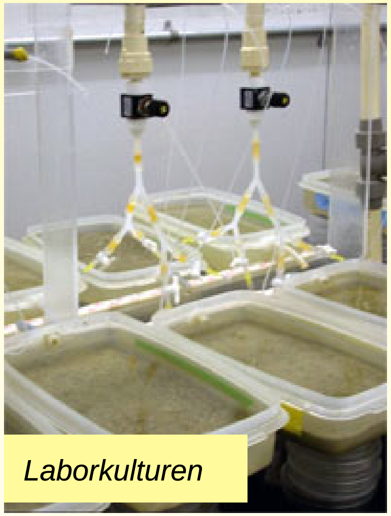

Laborkulturen

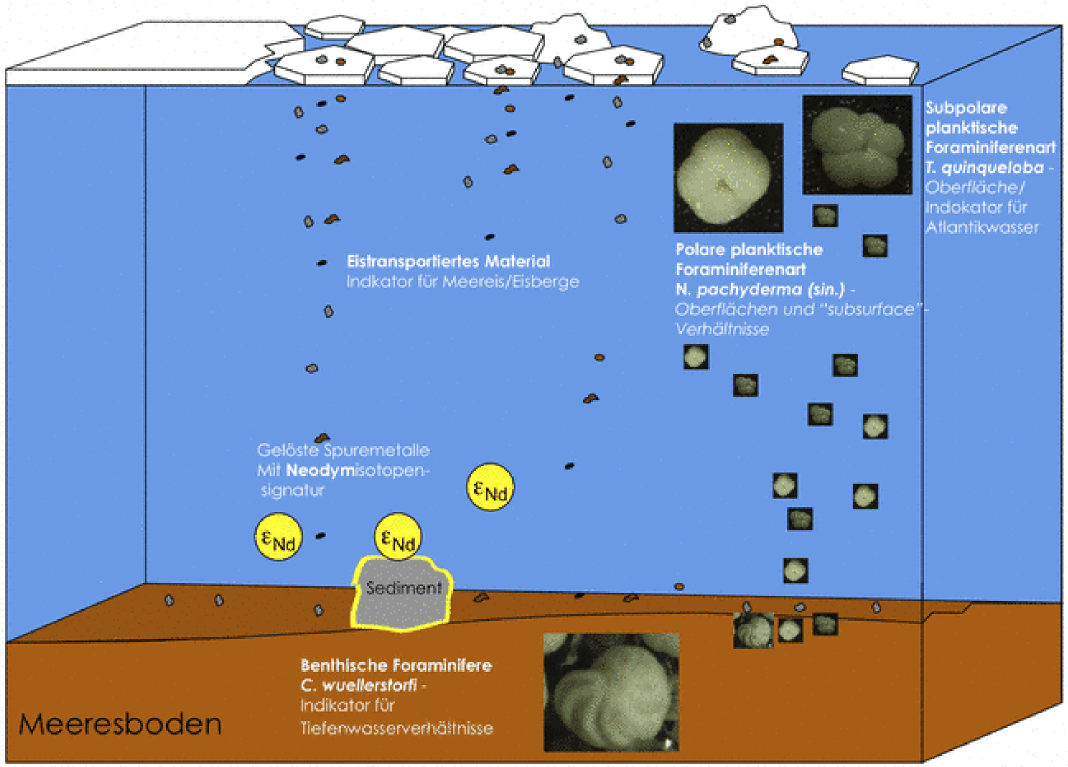

Mg/Ca-Verhältnisse als Temperaturproxies

- Einbau von Mg in Calcit ($CaCO_3$) → Diadochie
- **Mg/Ca** Verhältnis in Foraminiferen ist temperaturabhängig

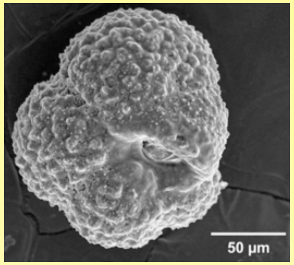

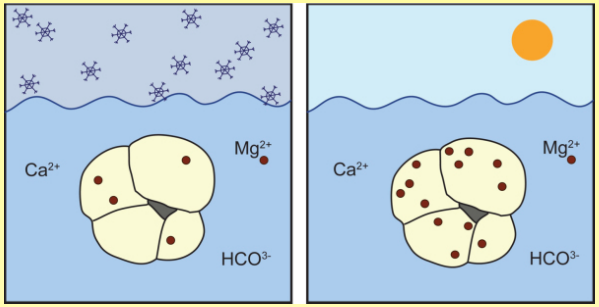

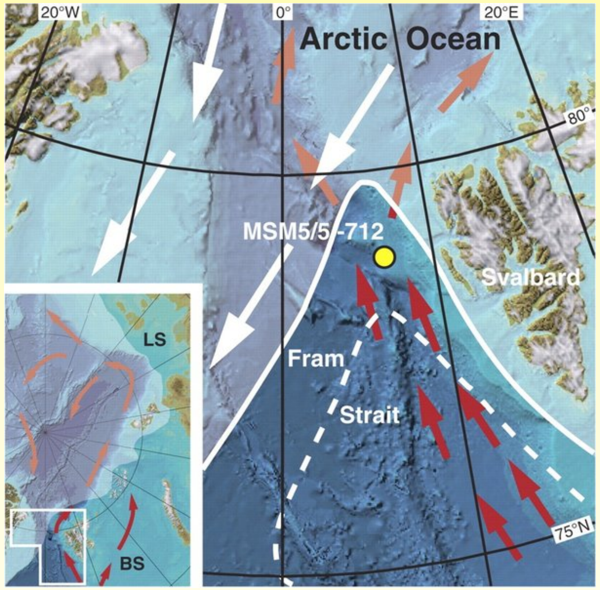

In der östlichen Framstraße dringt relativ warmes Nordatlantikwasser in den Arktischen Ozean ein (rote Pfeile)

Spielhagen et al. (2011) Science, 331, 450-453

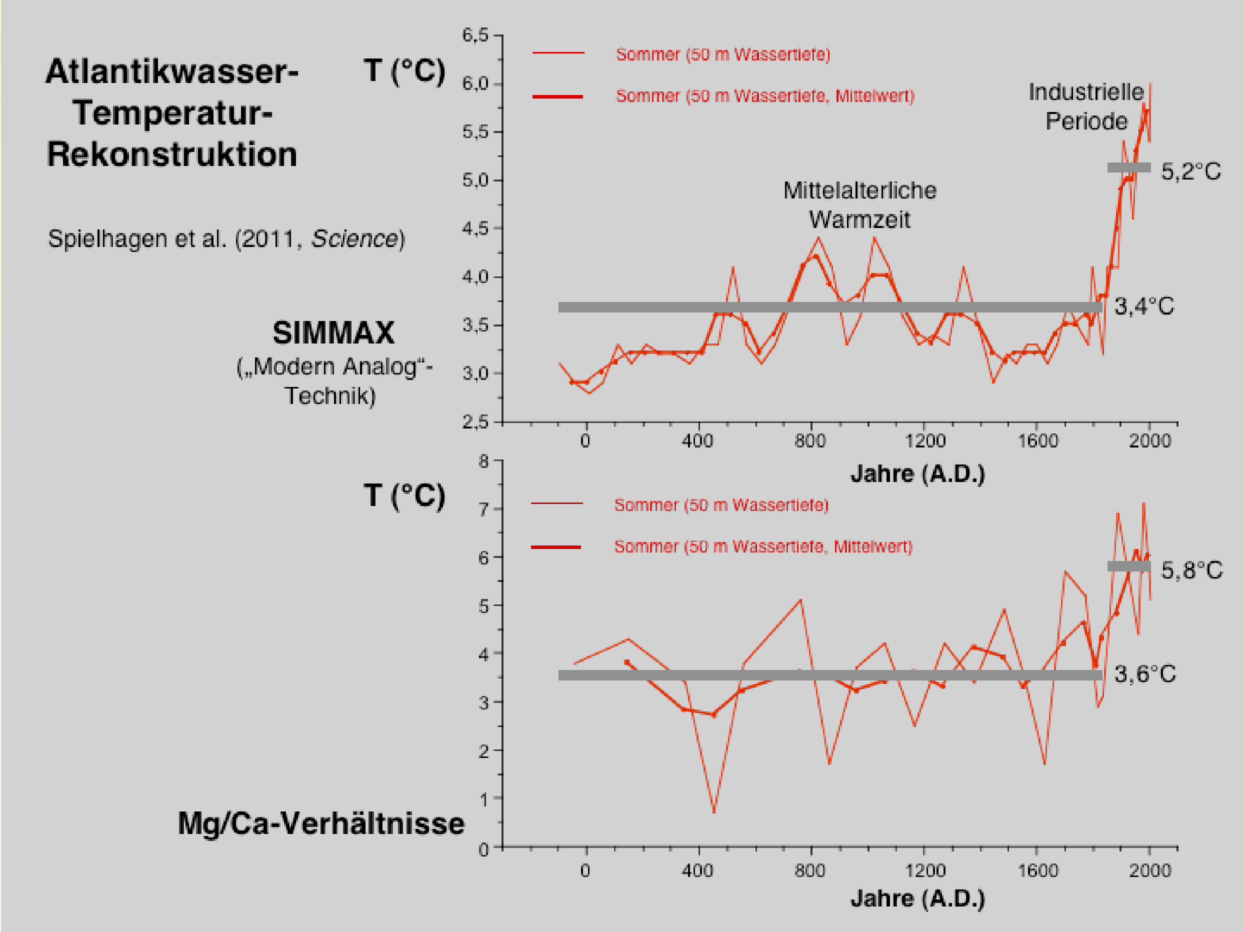

Sr/Ca-Verhältnisse in Muschelschalen als proxie für Hell-Dunkel Zyklus?

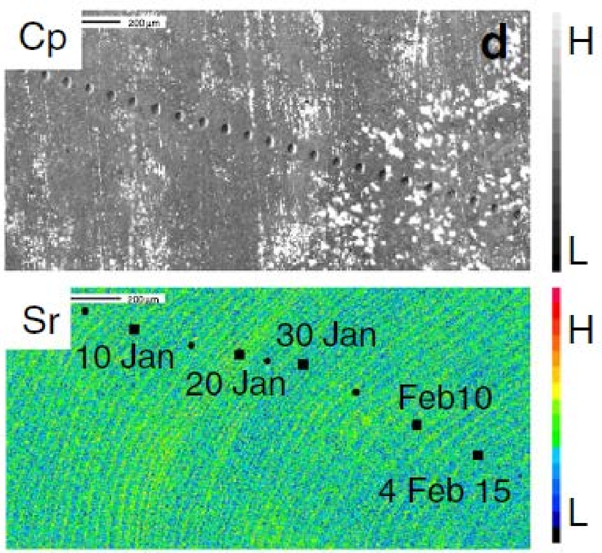

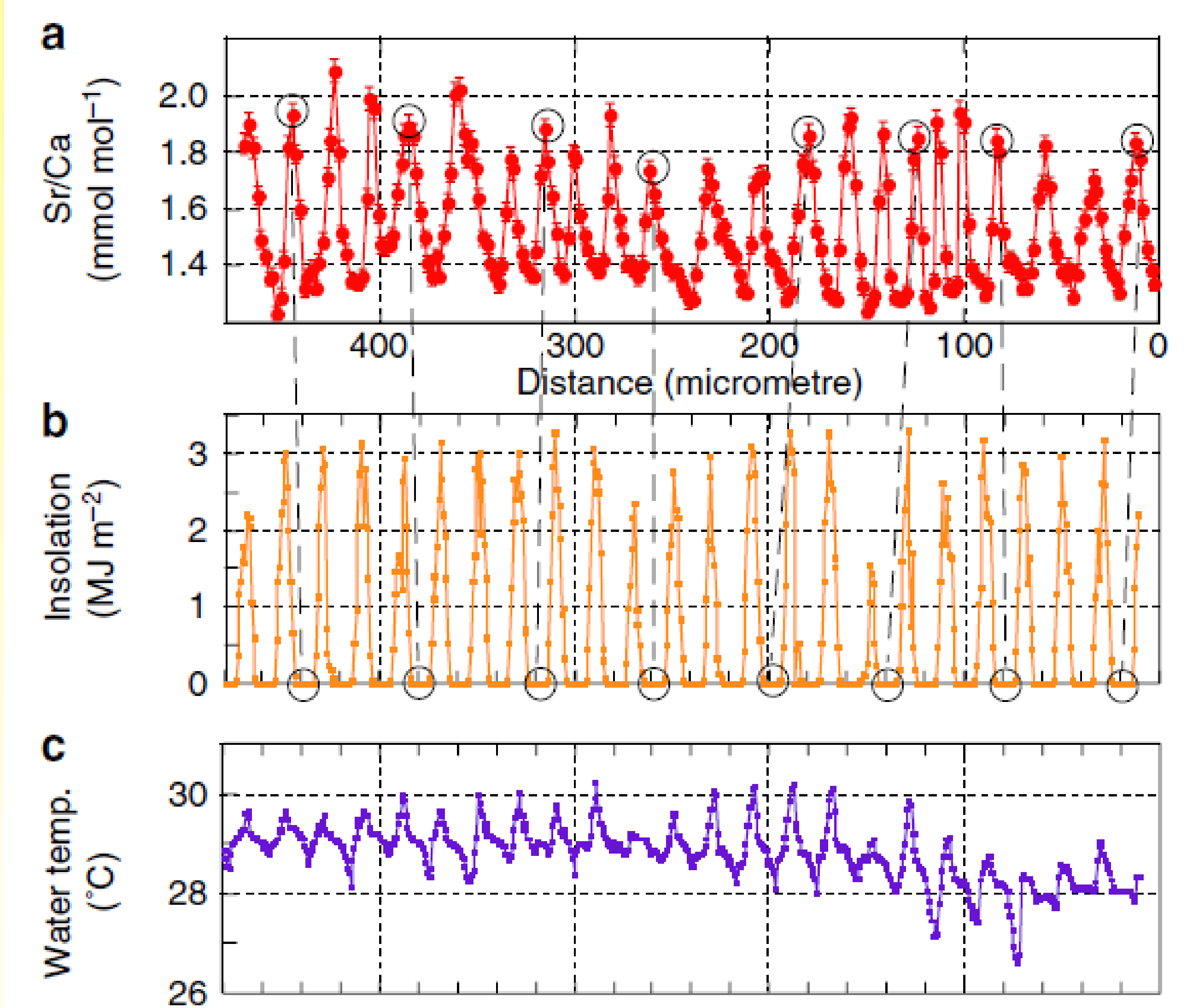

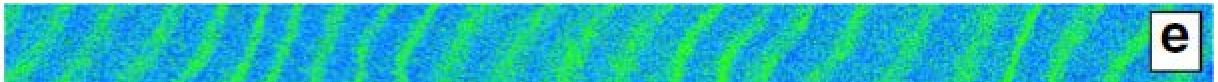

Sano et al. (2012) Nat Comm

Sr/Ca-Verhältnisse in Muschelschalen als proxie für Hell-Dunkel Zyklus?

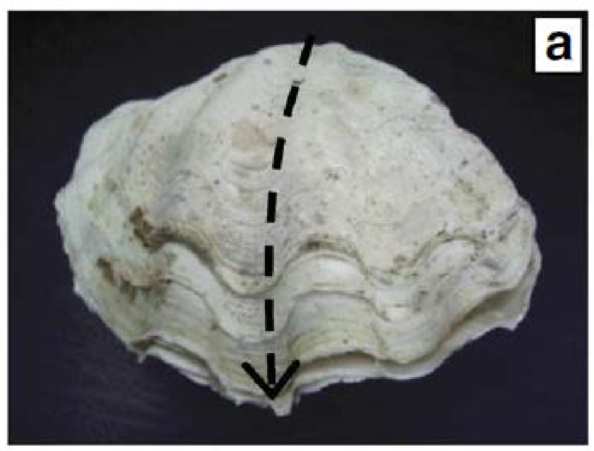

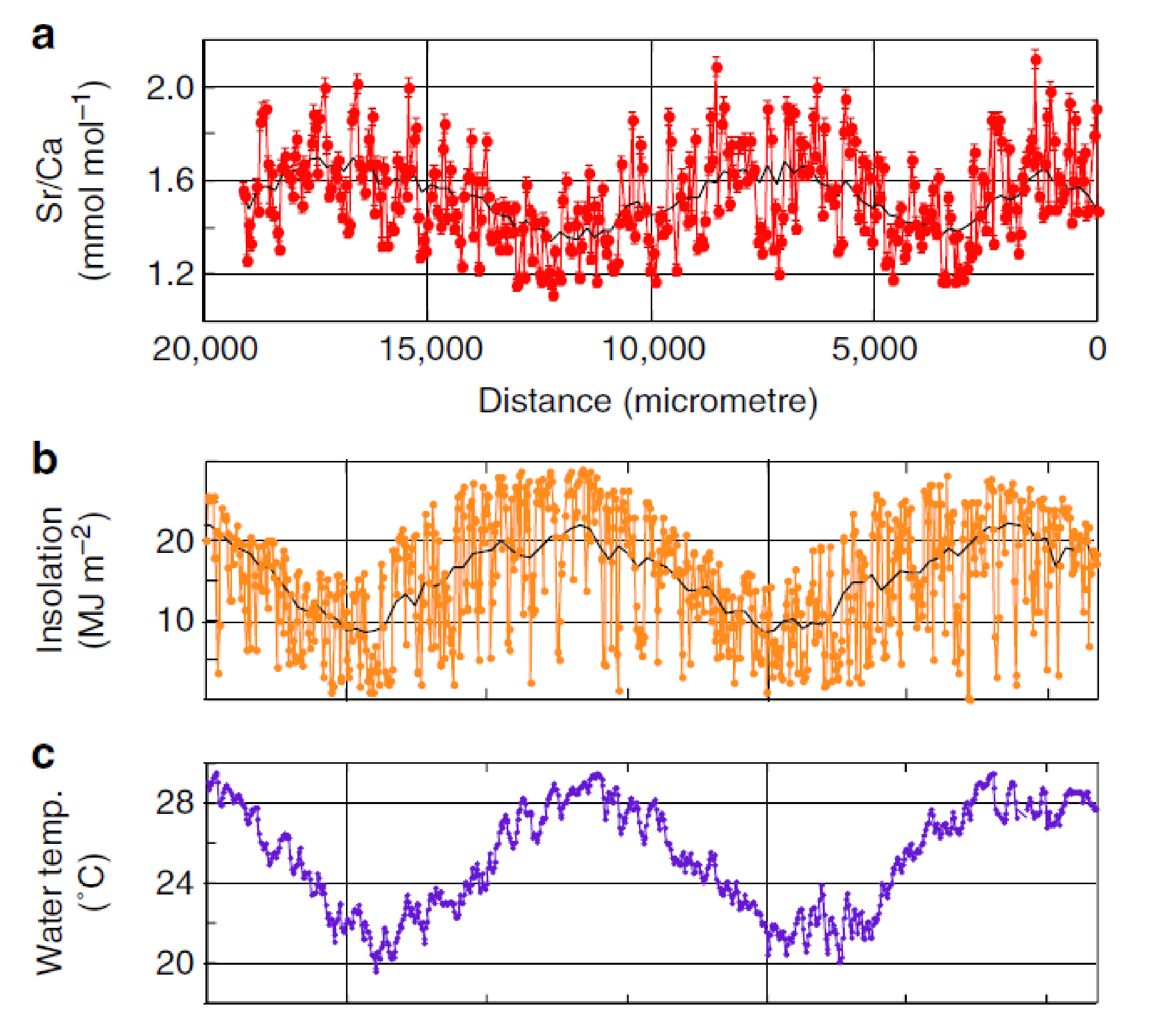

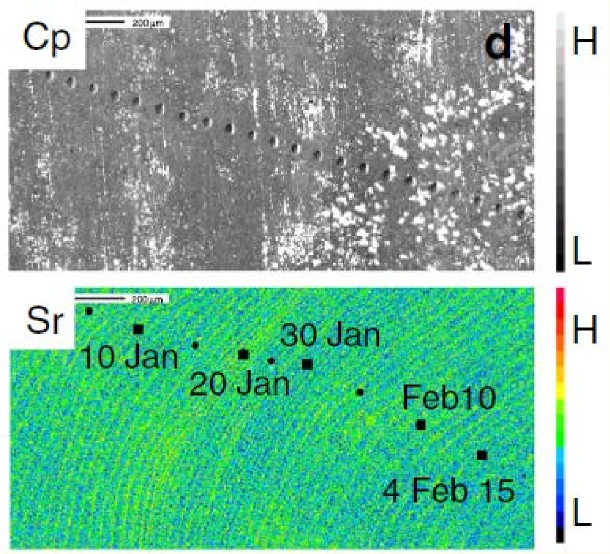

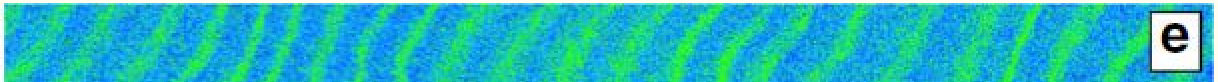

Sano et al. (2012 Nat Comm

"Knochenarbeit"

Die Physiologie fossiler Vertebraten

↓ ‚clumped isotopes' ↓

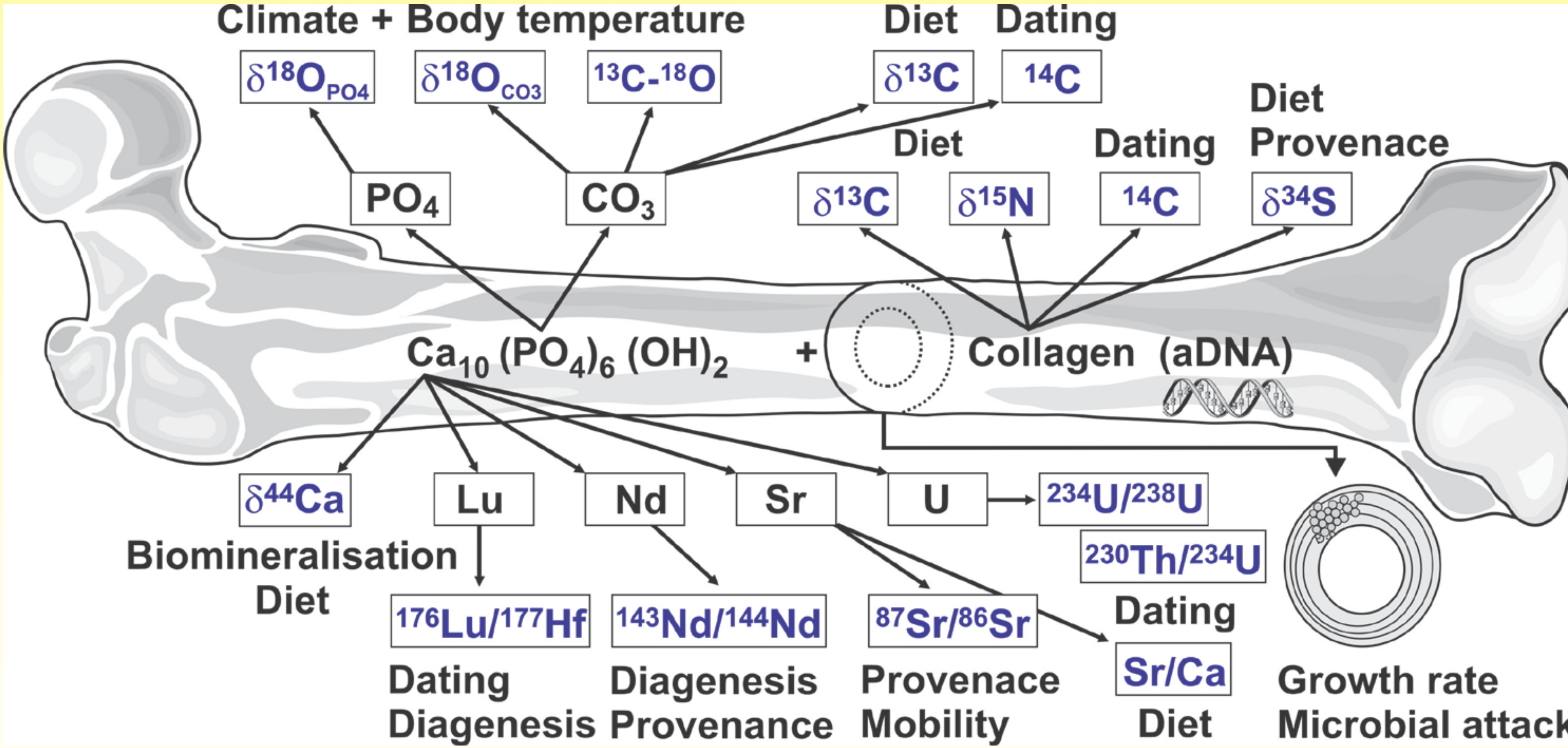

from Thomas Tütken, Mainz

Sr im Meerwasser

Sr isotope composition of the oceans is determined by the relative contributions of Sr from river waters and hydrothermal sources

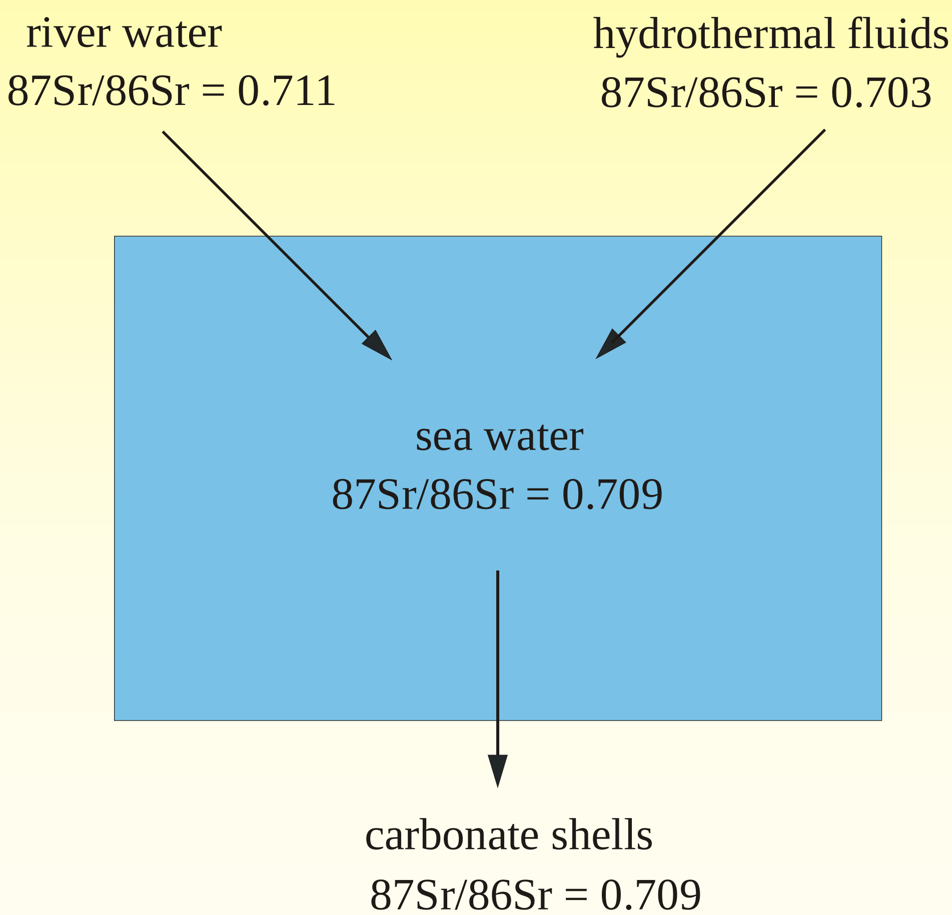

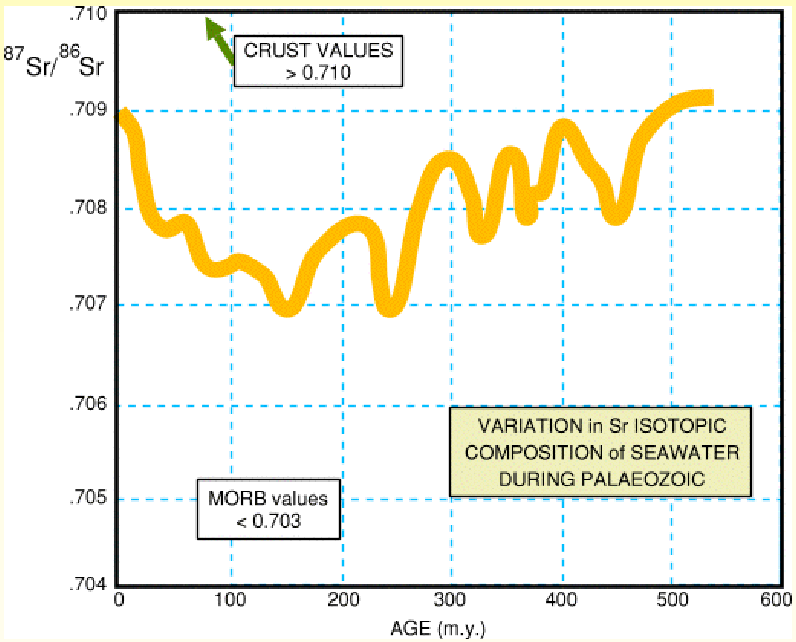

Sr-Isotopenentwicklung

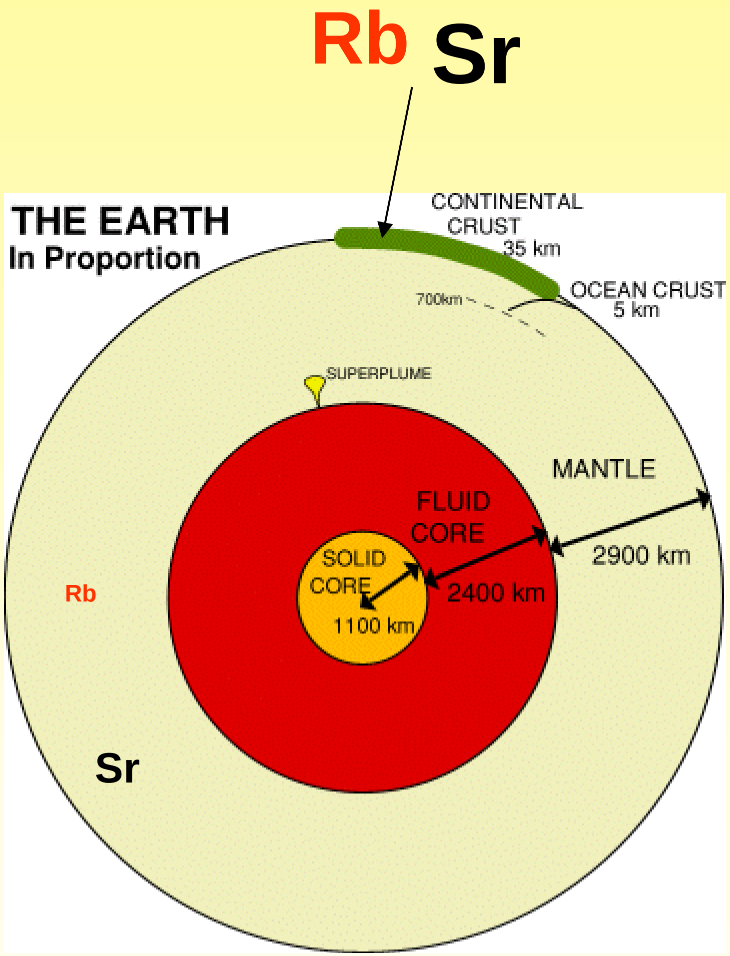

$^{87}Sr/^{86}Sr$ ratio of the crust is higher than that of the mantle due to the preferential partitioning of Rb into the crust relative to Sr.

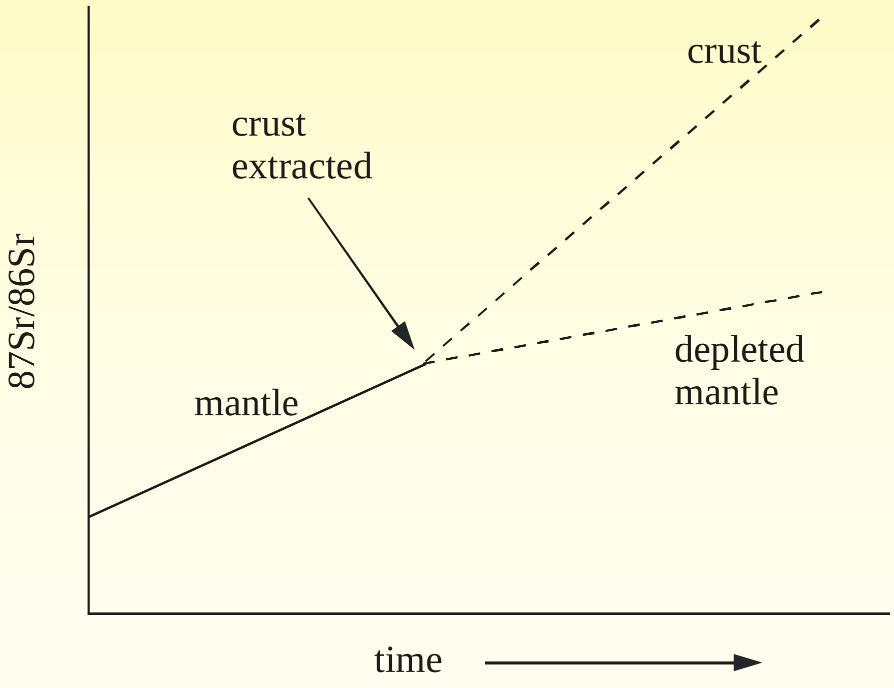

Continental crust: 32-78 ppm Rb, 260-333 ppm Sr

Depleted mantle: 0.6 ppm Rb, 19.9 ppm Sr

Sr im Meerwasser

Increase in the global ocean $^{87}Sr/^{86}Sr$ ratio since India-Asia collision

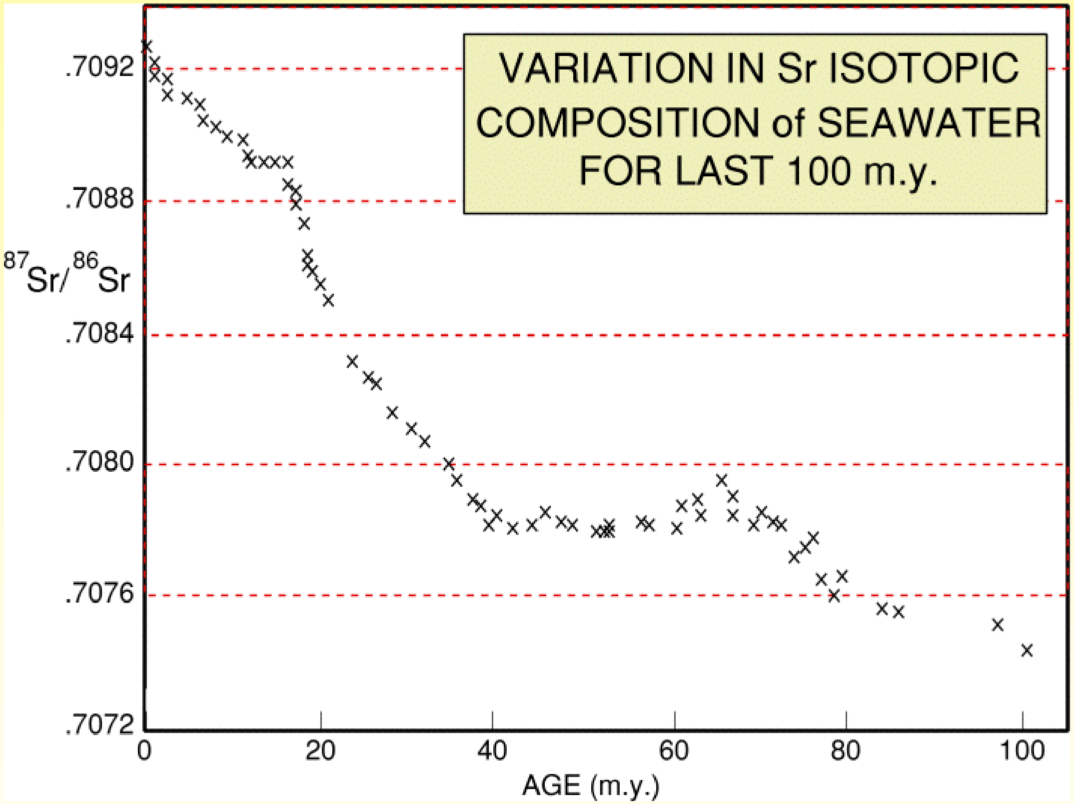

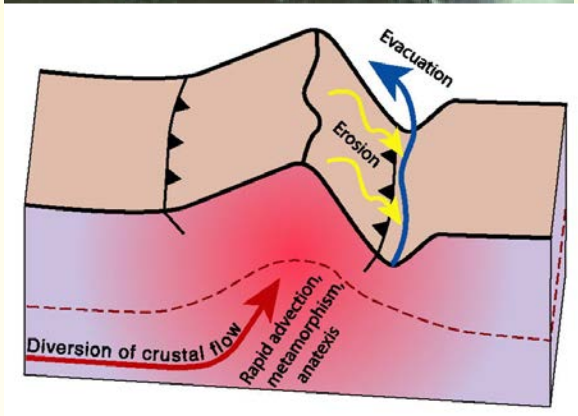

Lithium, Beryllium, Bor

leicht und selten

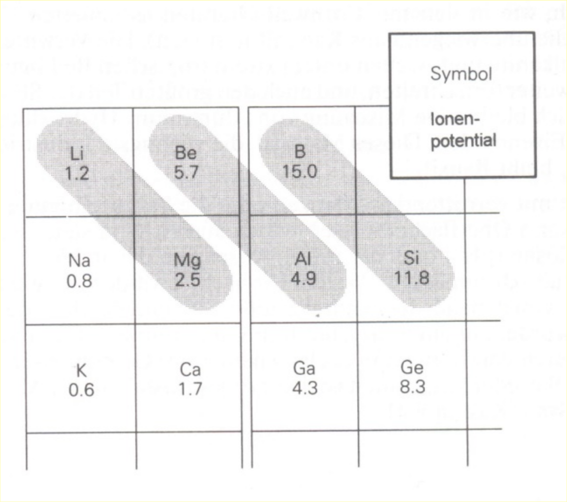

Schrägbeziehung im PSE zwischen
Li – Mg
Be – Al
B – Si

ist auf vergleichbare Atomradien und ähnliche Ladungsdichten, also ähnliches Ionenpotential zurückzuführen

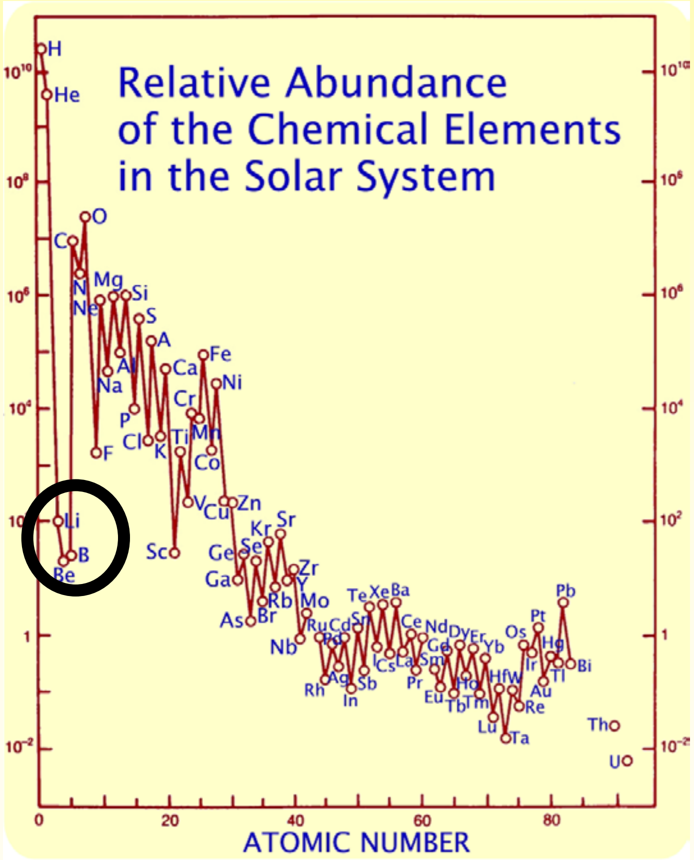

Wir erinnern uns:
Li, Be und B sind ungewöhnlich selten auf der Erde und im Sonnensystem

Lithium, Beryllium und Bor

inkompatibel, mobil und lithophil

werden über Schmelzen und Fluide transportiert

Meerwasser: Quelle und Reservoir für Li, B und Be
Kontinentale Kruste: Li in Glimmer, Bor in Turmalin und Be in ?

Tracer zur Erforschung geodynamischer Prozesse, lang- und kurzzyklische Stoffkreisläufe (z.B. in Subduktionszonen), Paläoproxy

Isotopenfraktionierung ($^{6}Li/^{7}Li$, $^{10}B/^{11}B$)

Be besitzt ein wichtiges cosmogenes Isotop (^{10}Be)

Bor Isotope als Paläo-pH Proxie

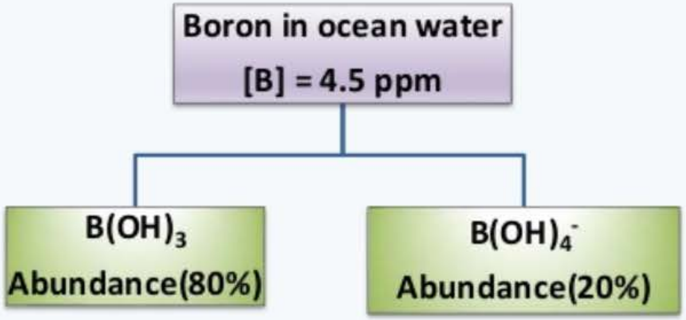

$$B(OH)_3 + H_2O = B(OH)_4^- + H^+$$

$$K_B = \frac{[H+]\,[B(OH)_4^-]}{[B(OH)_3]}$$

$$\log\left(\frac{[B(OH)_4^-]}{[B(OH)_3]}\right) = pH - pK_B$$

$$^{11}B(OH)_3 + {}^{10}(BOH)_4^- \leftrightarrow {}^{10}B(OH)_3 + {}^{11}B(OH)_4^-$$

K = Gleichgewichtskonstante < 1, d.h. trigonale Spezies ist isotopisch schwerer im Vergleich zur tetraedrisch koordinierten Spezies;

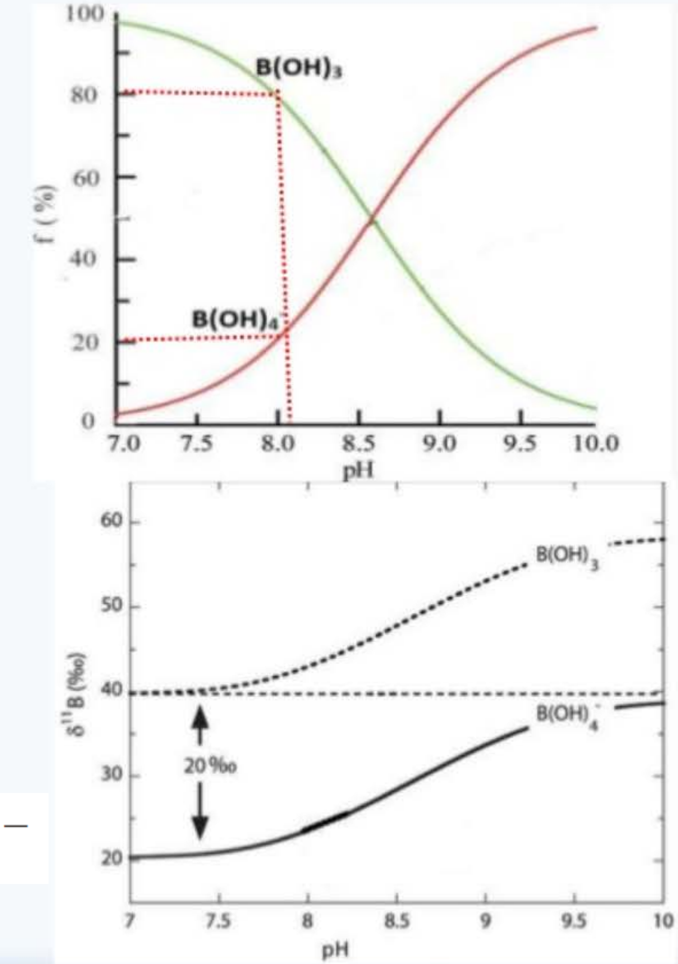

Hemming & Hanson 1992, ***Geochimica et Cosmochimica Acta***

Bor Isotope als Paläo-pH proxy

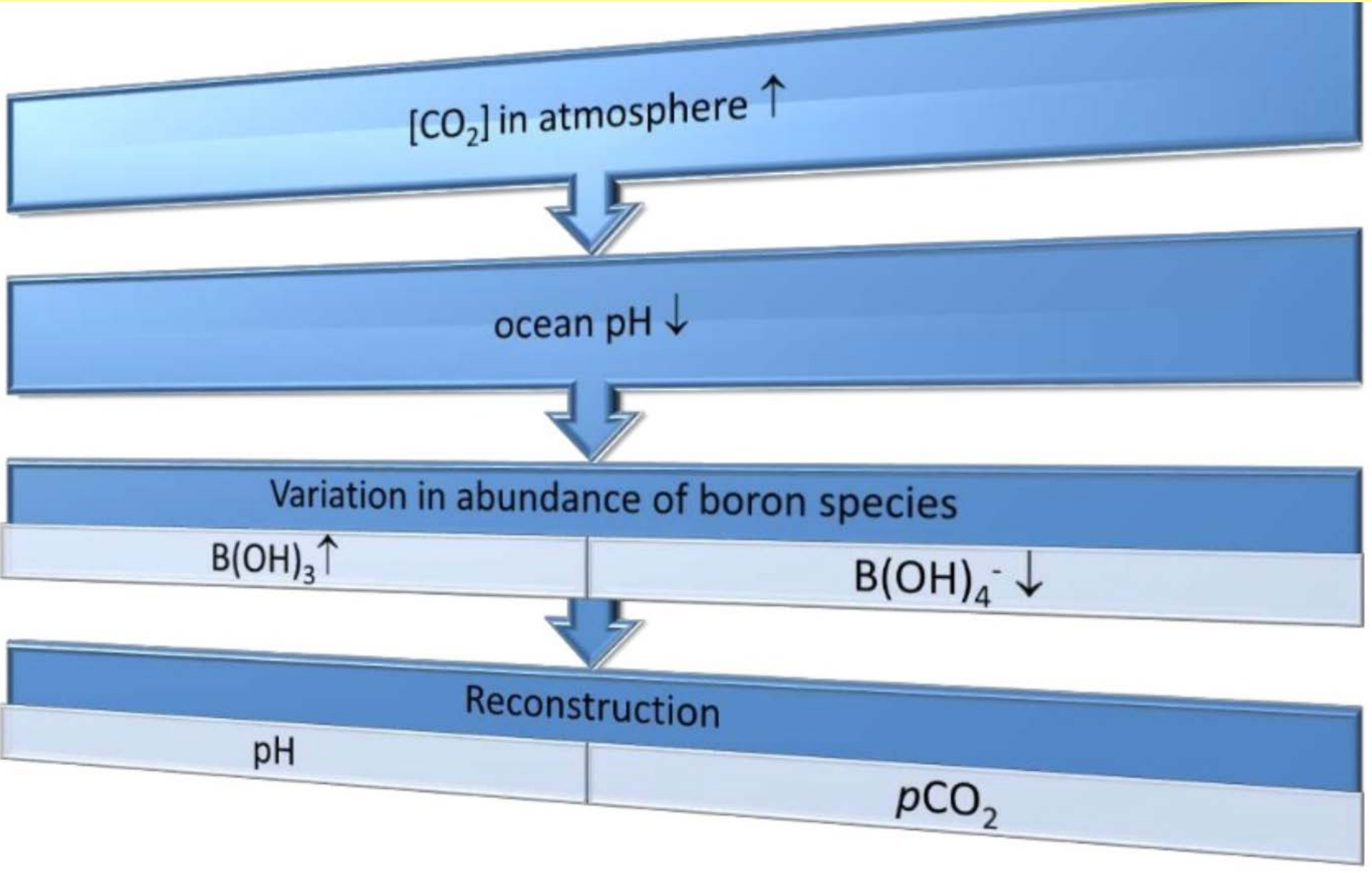

Bor Isotope als Paläo-pH Proxie

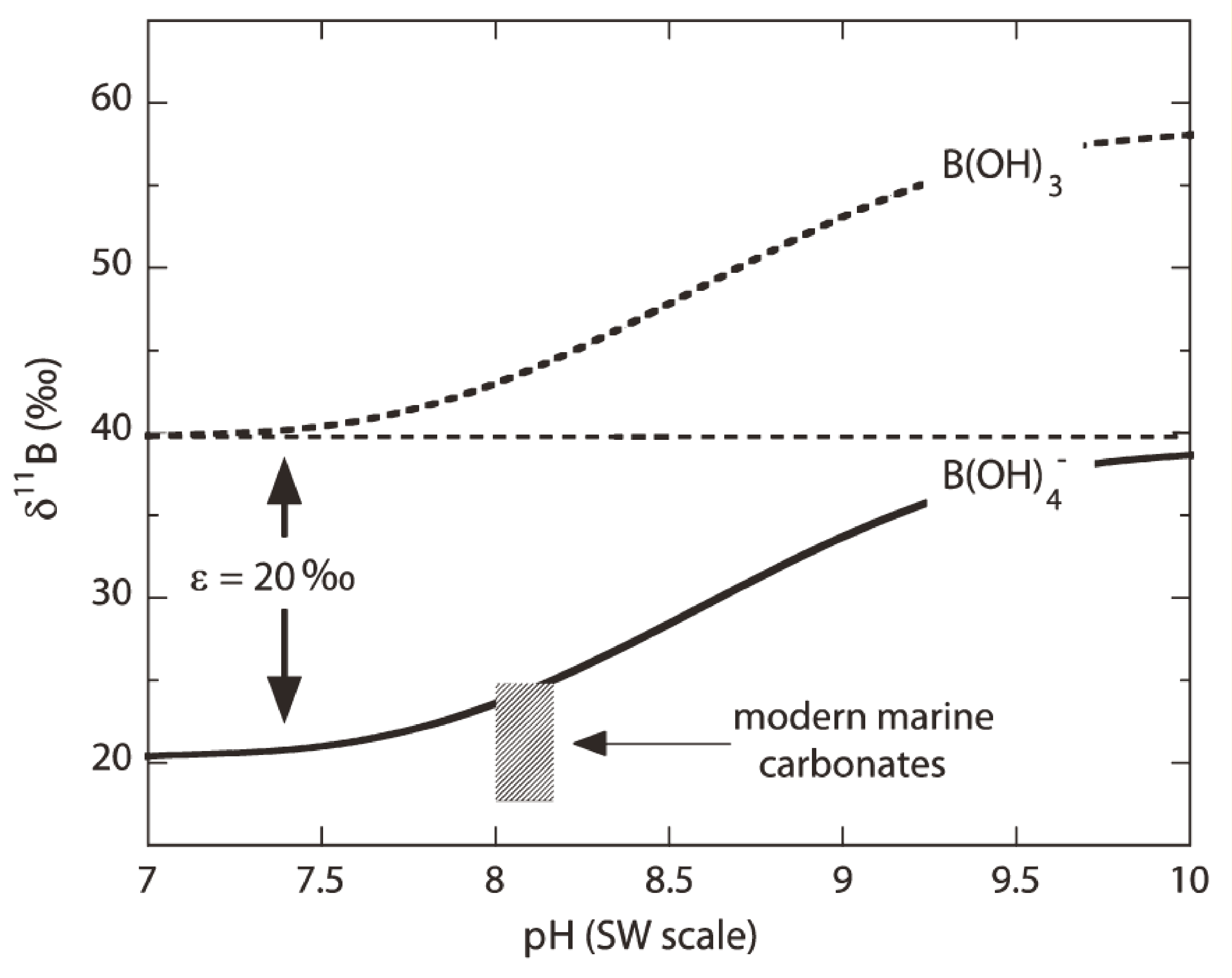

$CaCO_3 + B(OH)_4^- \leftrightarrow Ca(HBO_3) + HCO_3^- + H_2O$

Bor Isotope als Paläo-pH proxy

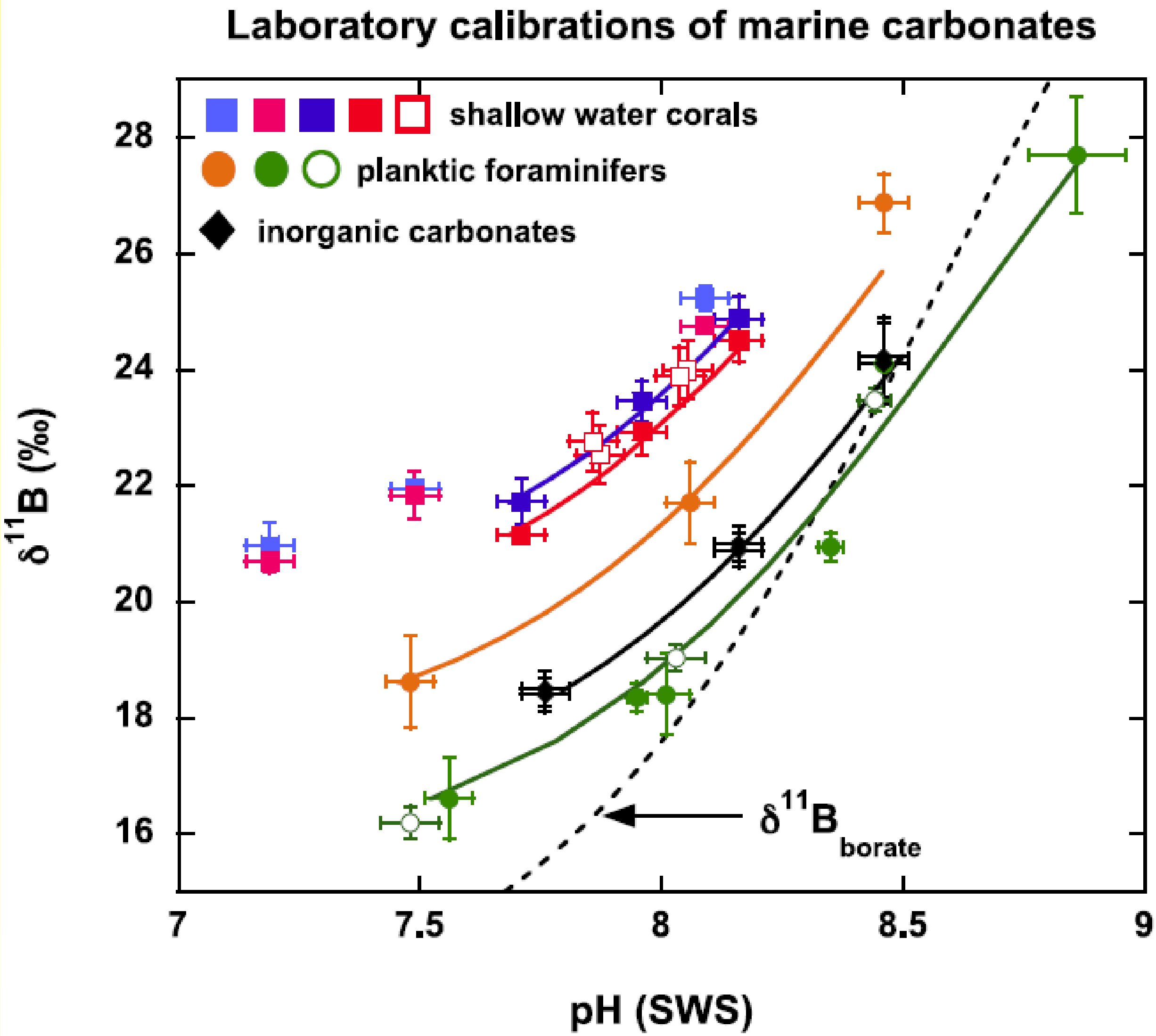

MC-ICP-MS

S. pistillata (Krief et al. 2010)

Porites sp. (Krief et al. 2010)

O. universa (Hönisch & Rae, unpubl.)

N-TIMS

P. cylindrica (Hönisch et al. 2004)

Acropora sp. (Reynaud et al., 2004)

A. nobilis (Hönisch et al. 2004)

G. sacculifer (Sanyal et al. 2001)

inorganic calcite (Sanyal et al. 2000)

O. universa (Sanyal et al. 1996)

Source: http://www.pmc.ucsc.edu/

Bor Isotope als Paläo-pH proxy

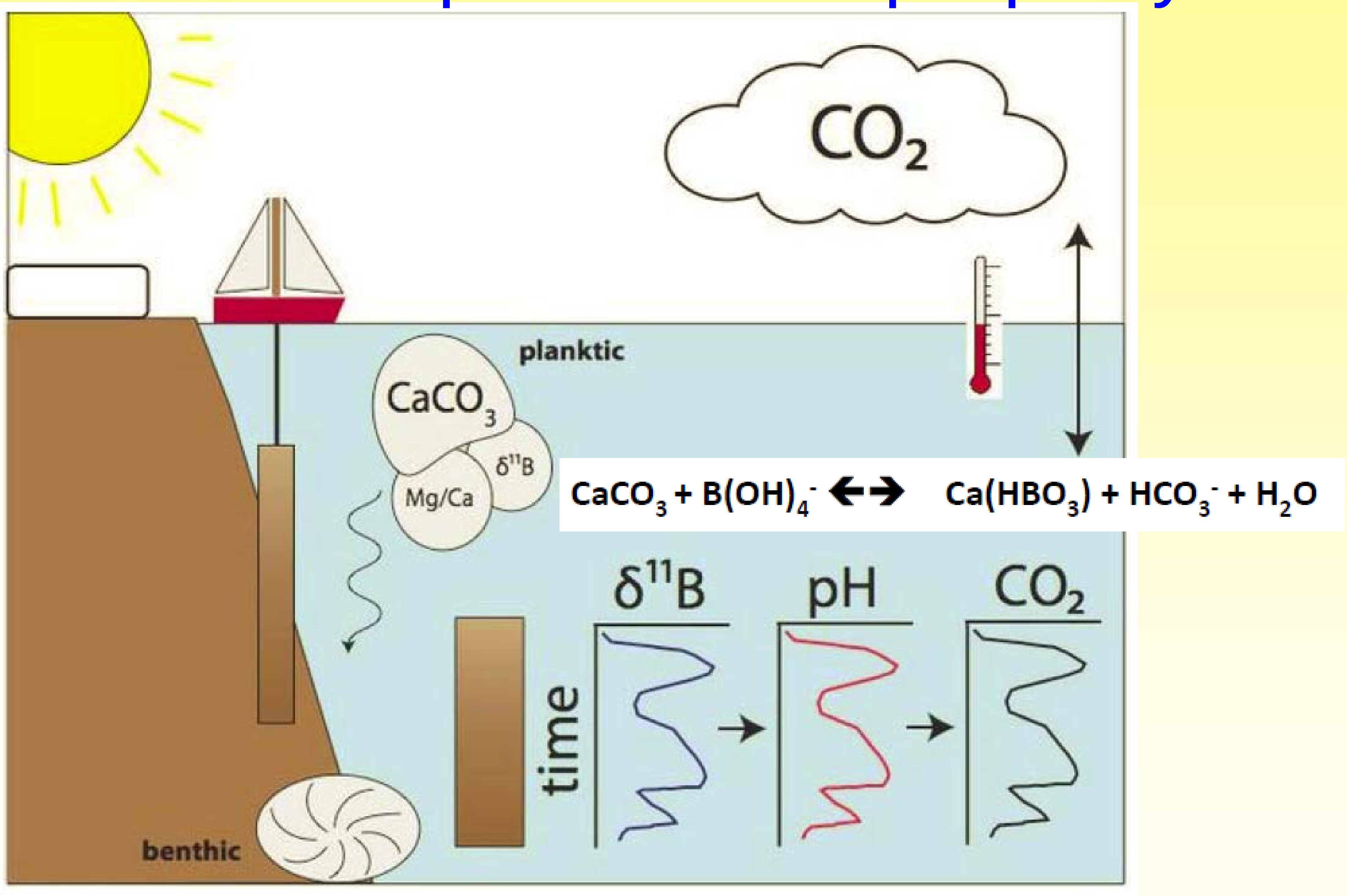

Source: http://www.pmc.ucsc.edu/

Bor Isotope als Paläo-pH proxy

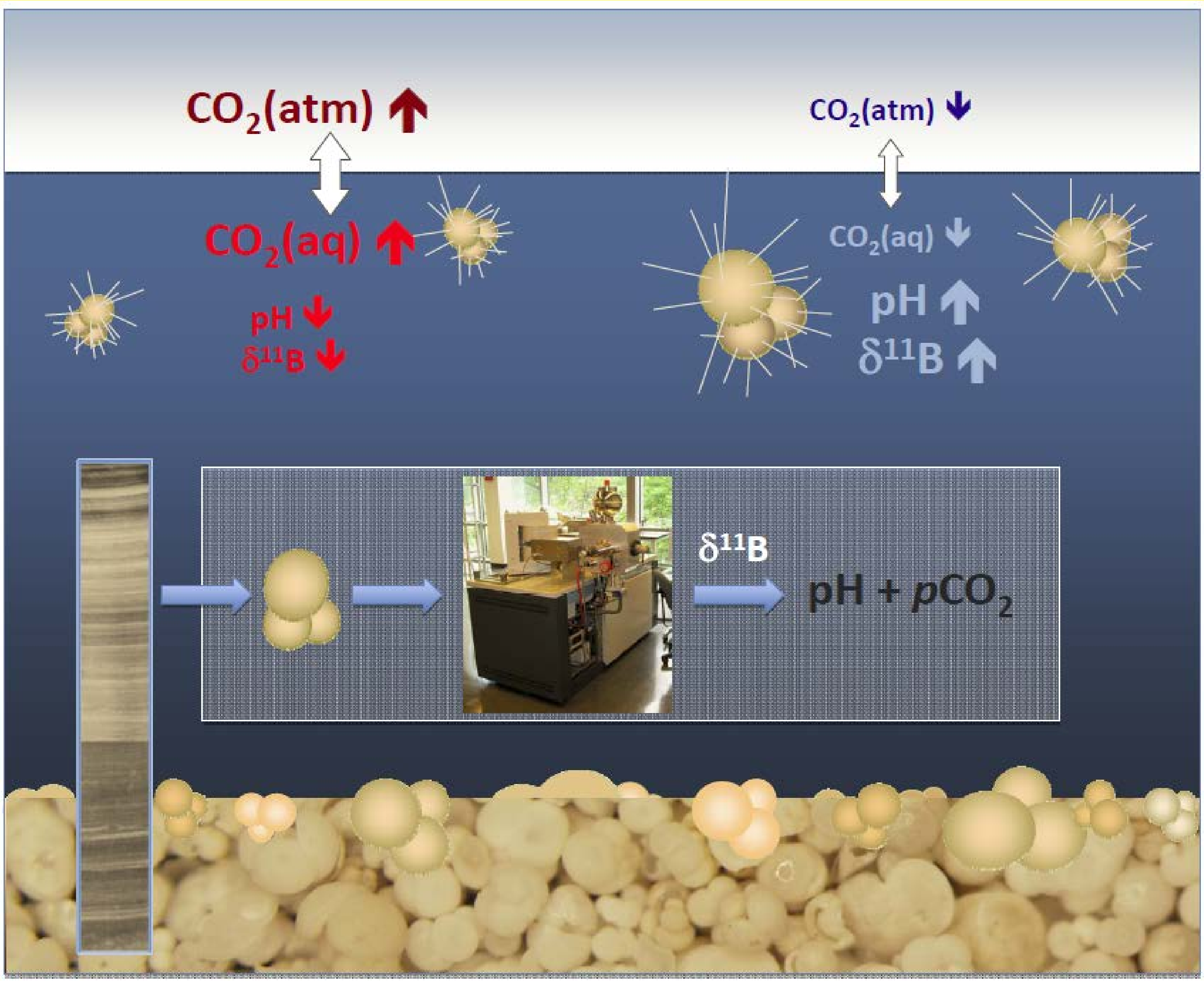

Source: http://www.pmc.ucsc.edu/

Bor Isotope als Paläo-pH proxy

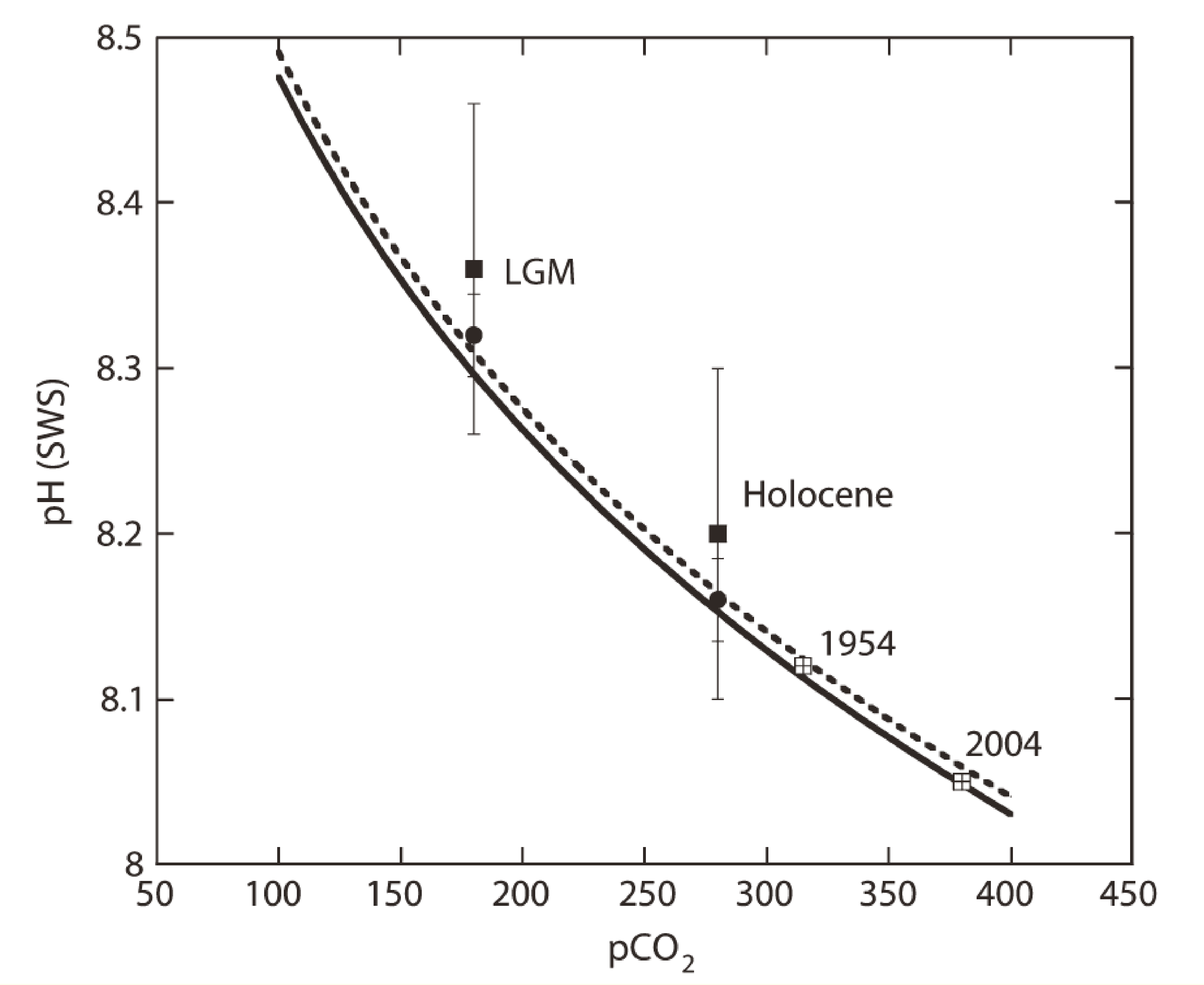

Source: Hemming & Hönisch (2007)

Bor Isotope als Paläo-pH proxy

Data from ODP site 668B, eastern equatorial Atlantic (sediment core) with atmospheric pCO2 variations (Vostok ice core)

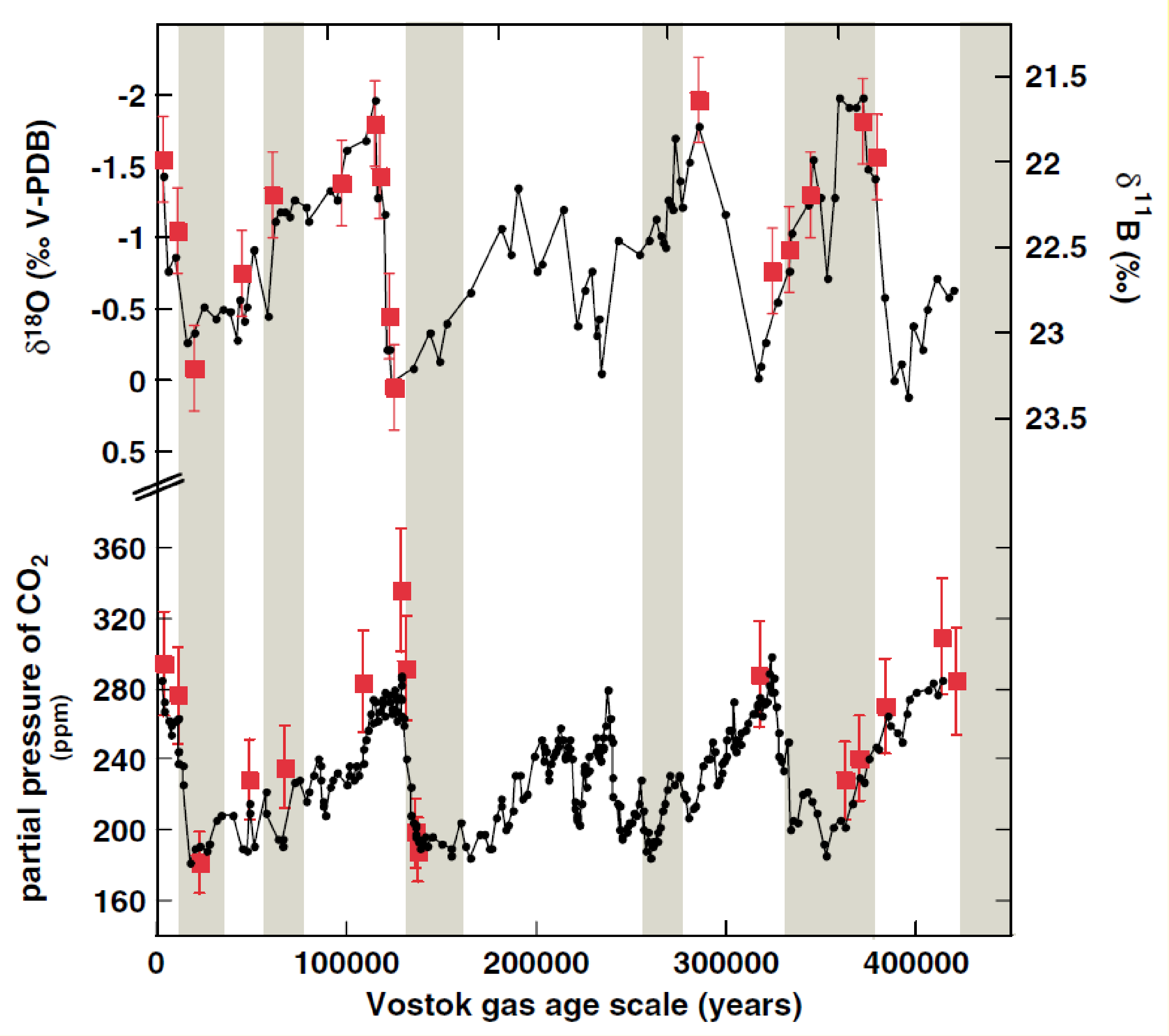

Hemming & Hönisch (2007)

Bor Isotope als Paläo-pH proxy

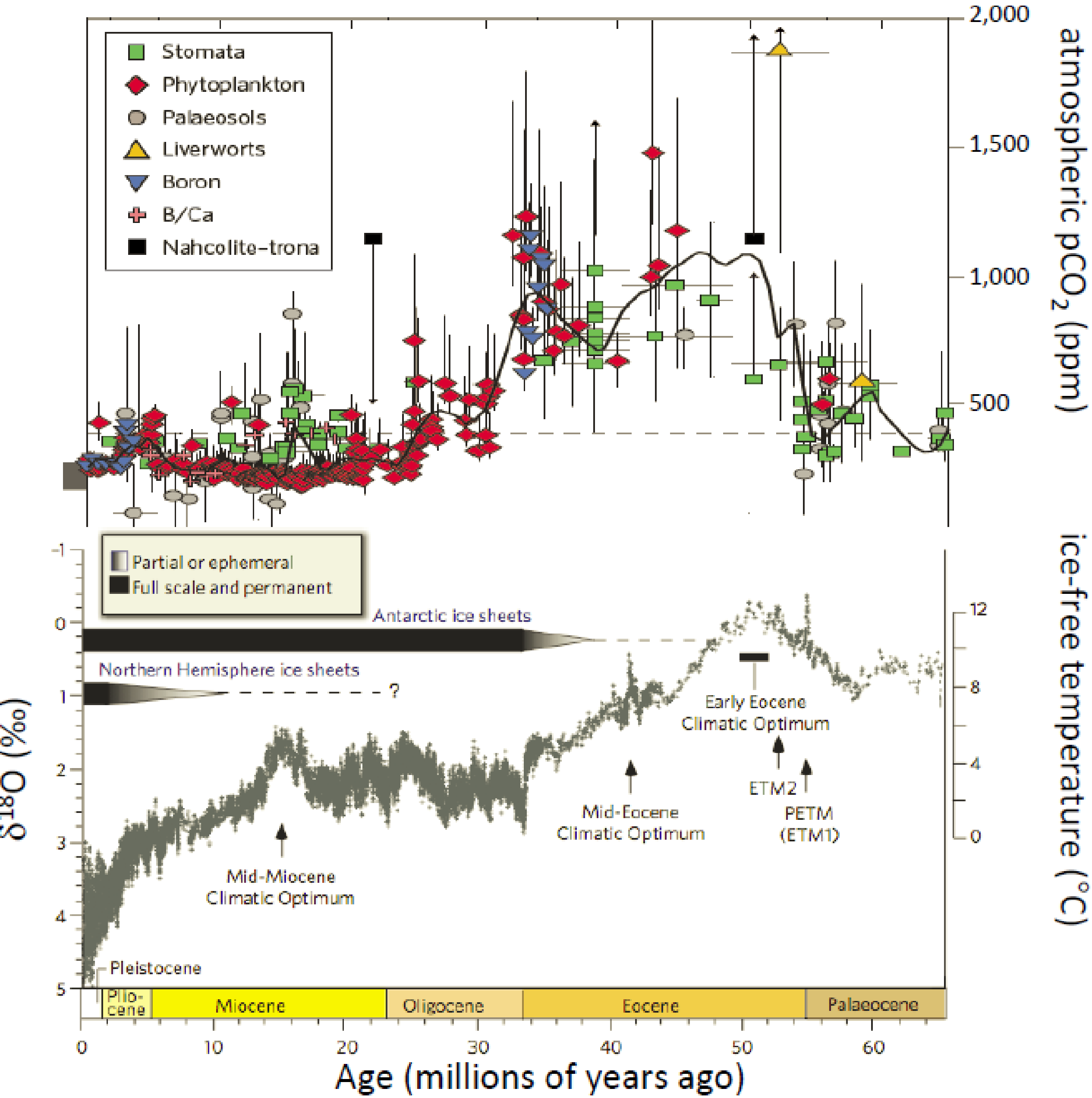

Beerling & Royer, Nature Geoscience, 2011

Streuung der Mess-werte durch ^{11}B Sekularvariation im Meerwasser?

Zachos et al., Nature, 2008

Übung – Alkalinität und pH

$$H_2CO_{3(aq)} \leftrightharpoons H^+_{(aq)} + HCO^-_{3(aq)}$$

$$K_1 = \frac{aH^+ \cdot aHCO_3^-}{aH_2CO_3} = 10^{-6.4}$$

$$HCO^-_{3(aq)} \leftrightharpoons H^+_{(aq)} + CO^{2-}_{3(aq)}$$

$$K_2 = \frac{aH^+ . aCO_3^{2-}}{aHCO_3^-} = 10^{-10.3}$$

Berechnen sie das Verhältnis Hydrogenkarbonationen (HCO_3^-) zu Karbonationen (CO_3^{2-}) für Gewässer mit ph-Werten von 8, 9, 10 & 11 und zeichnen sie ein Diagramm mit den prozentualen Anteilen der beiden Ionenarten für die verschiedenen pH-Werte

pH = -log10aH^+

für pH 8 (pH = -log10aH^+) gilt:

$$aHCO_3^- = \frac{10^{-8} . aCO_3^{2-}}{10^{-10.3}} = \frac{1 \times 10^{-8} . aCO_3^{2-}}{5 \times 10^{-11}} = 200\, aCO_3^{2-}$$

Alkalinität

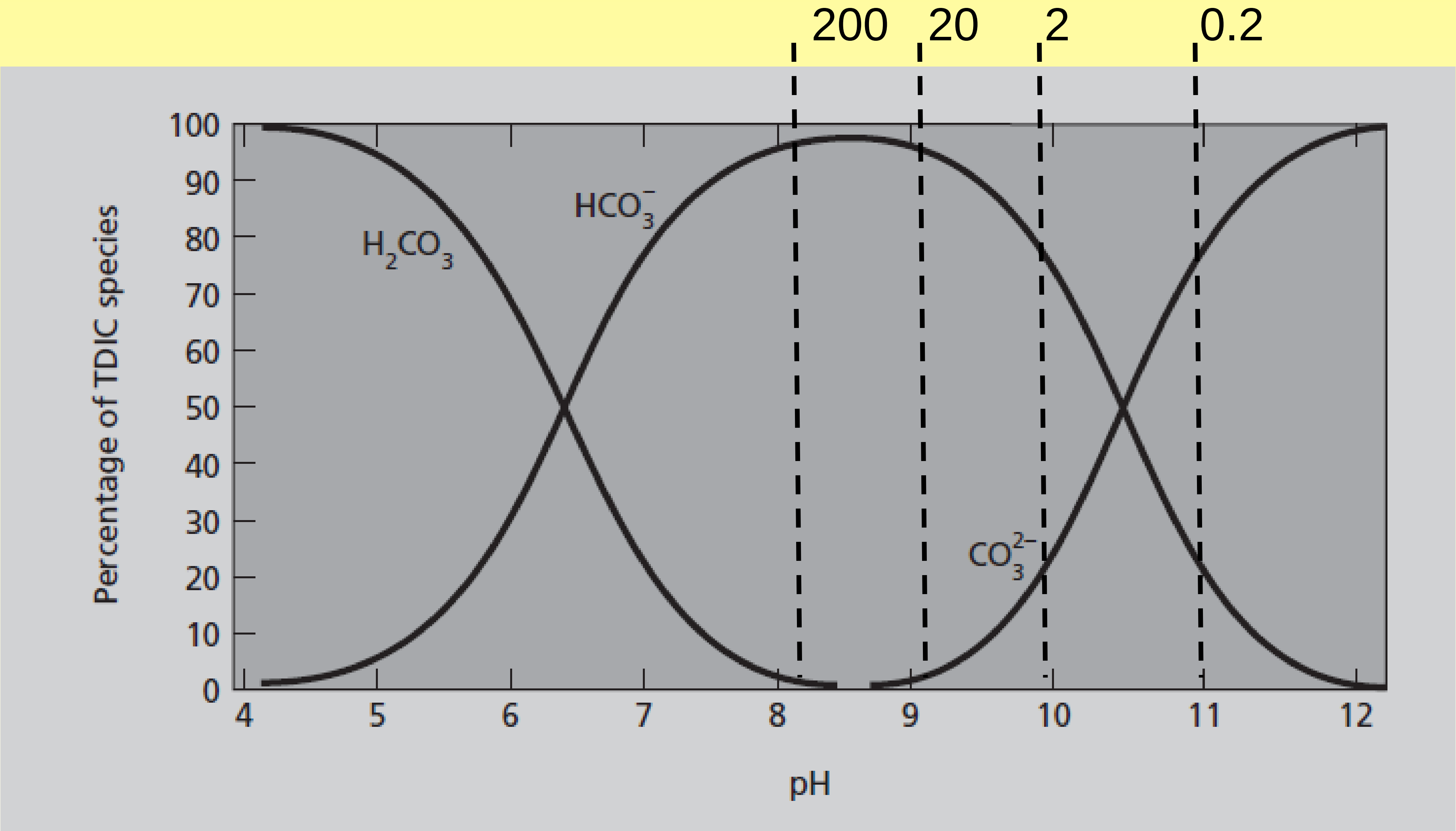

Li-, Be- und B-Kreislauf

Li-, Be-, B-Stoffkreislauf:

Meerwasser →
ozeanische Kruste →
Subduktionszone →
Fluide →
Mantelkeil →
Schmelze →
Vulkanischer Bogen →
Verwitterung, Erosion →
Meerwasser
(hier schließt sich der Kreislauf)

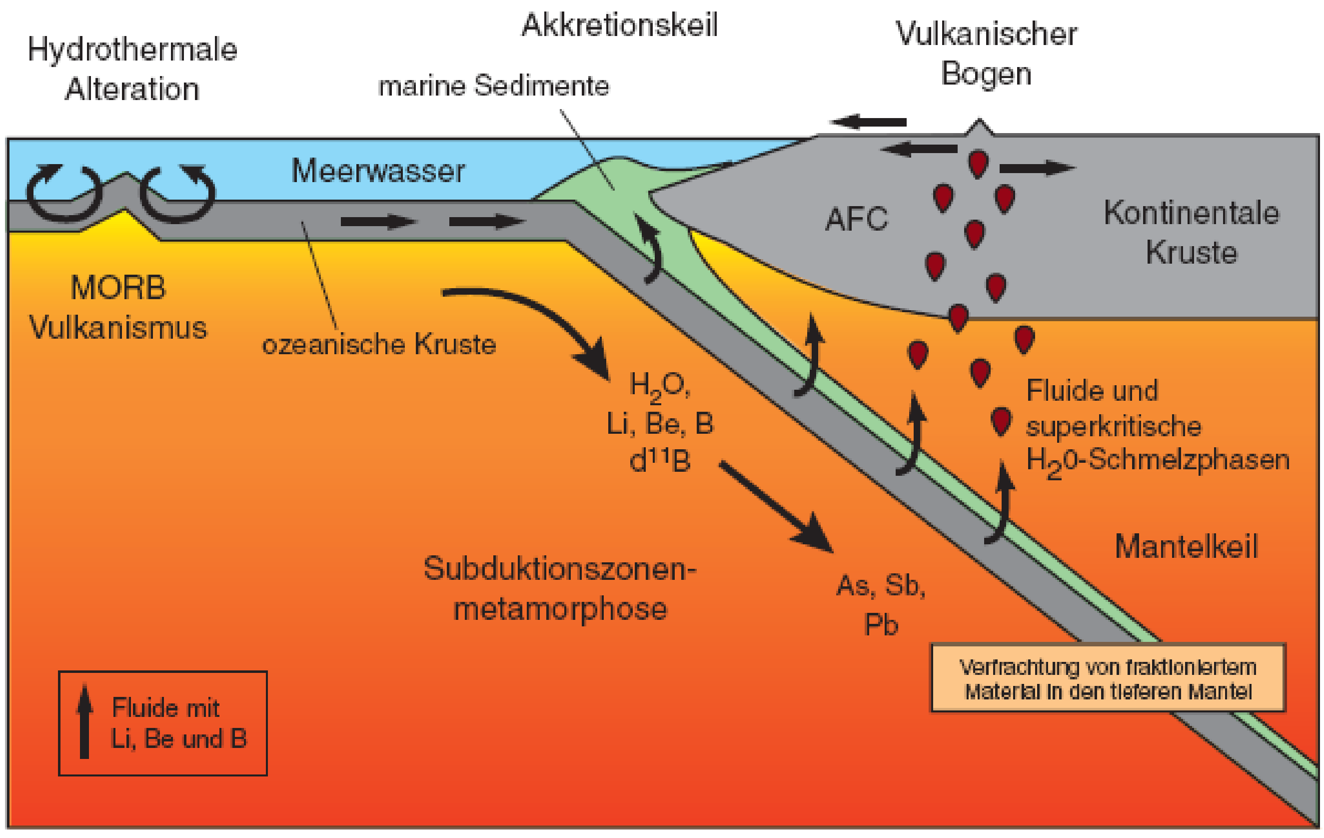

Abb. 1-1 Stoffkreislauf leichter Elemente (Li, Be, B) an Subduktionszonen (nach Bebout 1996)

Li-, Be-, B-Trägerphasen in Subduktionszonen: Tonminerale, Lawsonit, Omphazit, Phengit, Amphibol, Chlorit, Chloritoid, Paragonit, Epidot, Serpentin, d.h. viele OH-haltige Minerale

Bor-Konzentrations- und Isotopenvariationen

$\delta^{11}B = \{[(^{11}B/^{10}B)_{sample}/(^{11}B/^{10}B)_{standard}] - 1\} \times 1000$

Meerwasser wichtige Quelle für Bor

Alterierte ozeanische Lithosphähre mit hoher Bor-Konzentration

In Subduktionszone entwässern Bor-haltige Fluide →temperatur-abhängige) B-Isotopen-fraktionierung

Frontale Arc-Magmatite mit hohen Bor-Gehalten

e.g. Izu arc: Ishikawa & Nakamura (1993) Nature 370

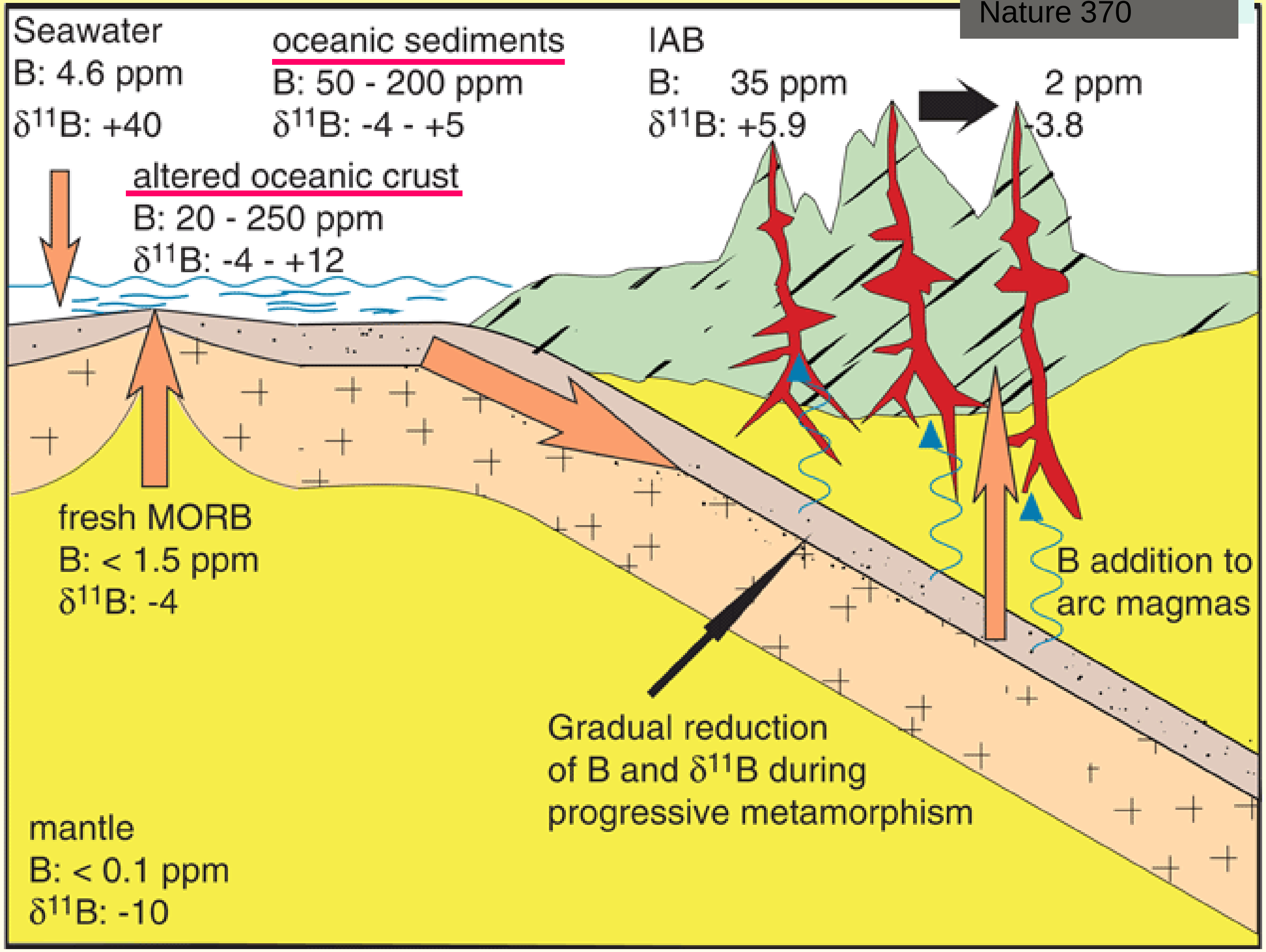

Quelle: GFZ

in wässrigen Fluiden (T > 50°C) ist Bor trigonal koordiniert – angereichert an ^{11}B

Bleiisotope – andere Methode andere Aussagen

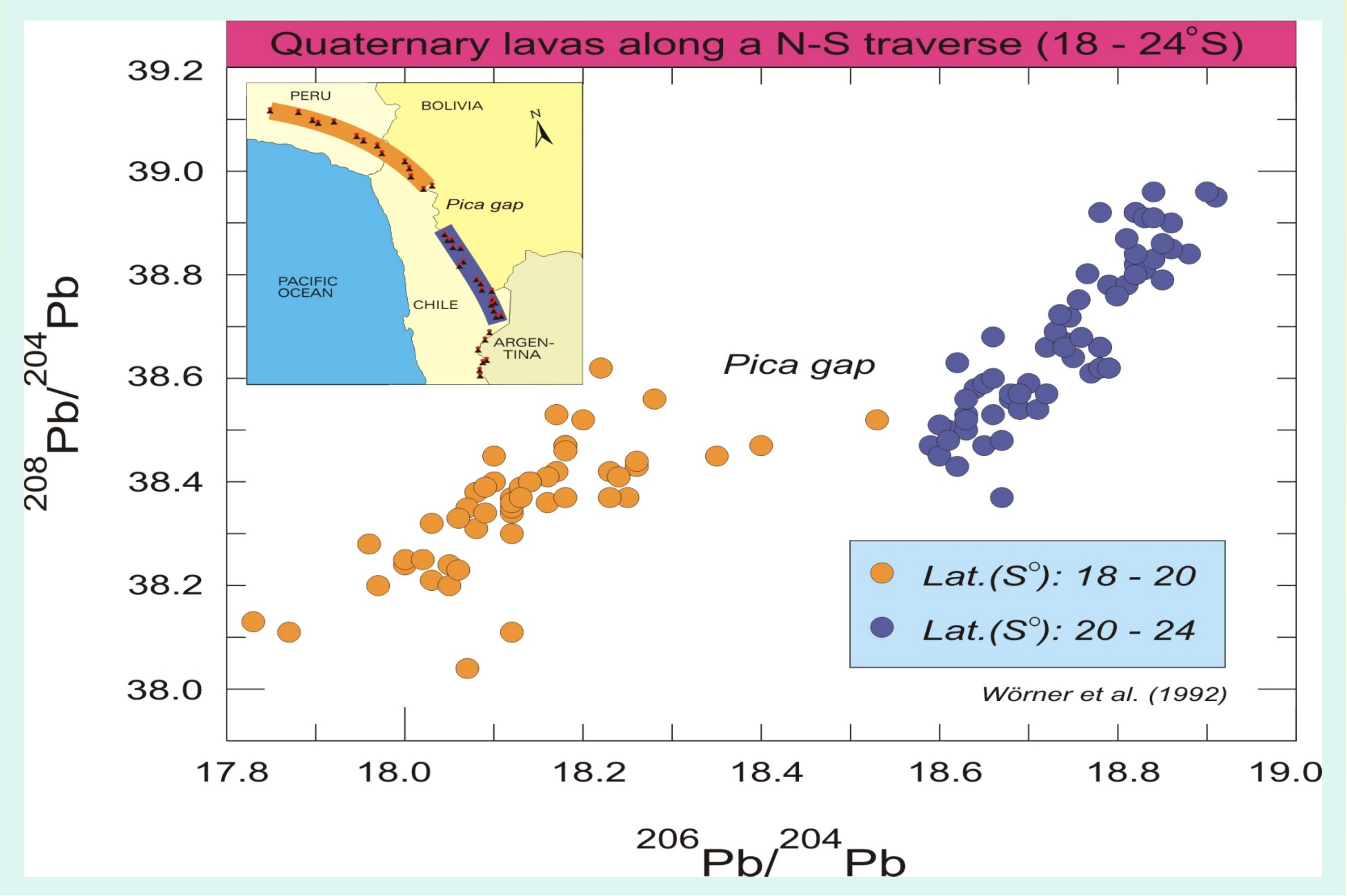

Cosmogene Nuklide

Discovery of cosmic-rays

Victor Hess discovered the „cosmic rays“ in his balloon voyages of 1911-1912 (received Nobel Prize in physics in 1936)

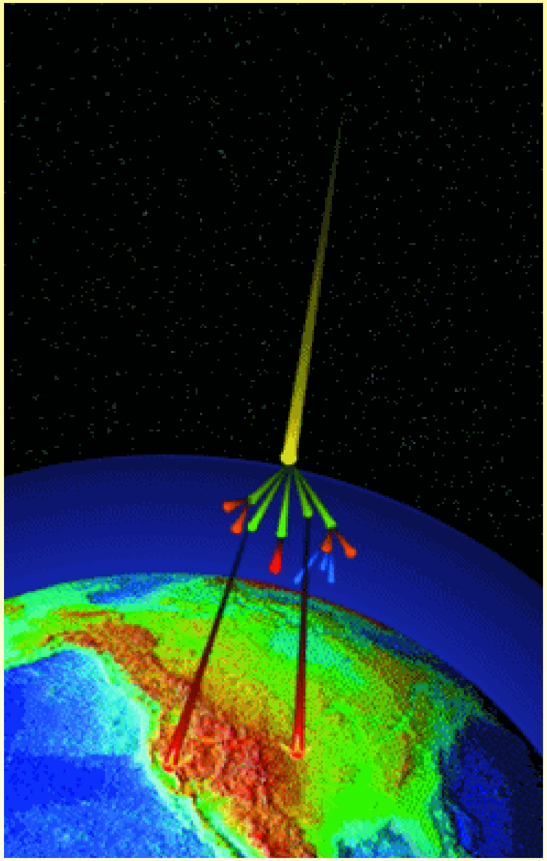

Libby introduced radiocarbon dating (^{14}C) in 1947 (Nobel Prize in 1960)

Discovery of ^{10}Be, ^{7}Be (1956-1957) Arnold (Chicago) Peters, Lal (Bombay)

Terrestrial cosmogenic isotopes

The “centre of mass” of many geoscience departments has shifted from solid Earth subfields towards surface processes (Bruce Watson, Elements 2009)

Cockburn & Summerfield 2004

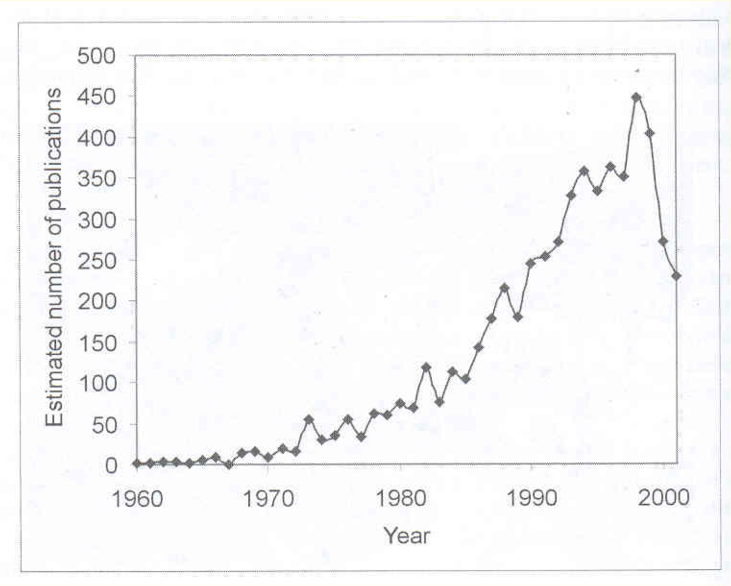

Davis et al. 2003: papers containing “U-Pb” and “zircon” as key words

Cosmic rays protons interact with nuclei in the upper atmosphere, producing neutrons which in turn interact with atmosphere and rock surface

GMIT 33, 2008

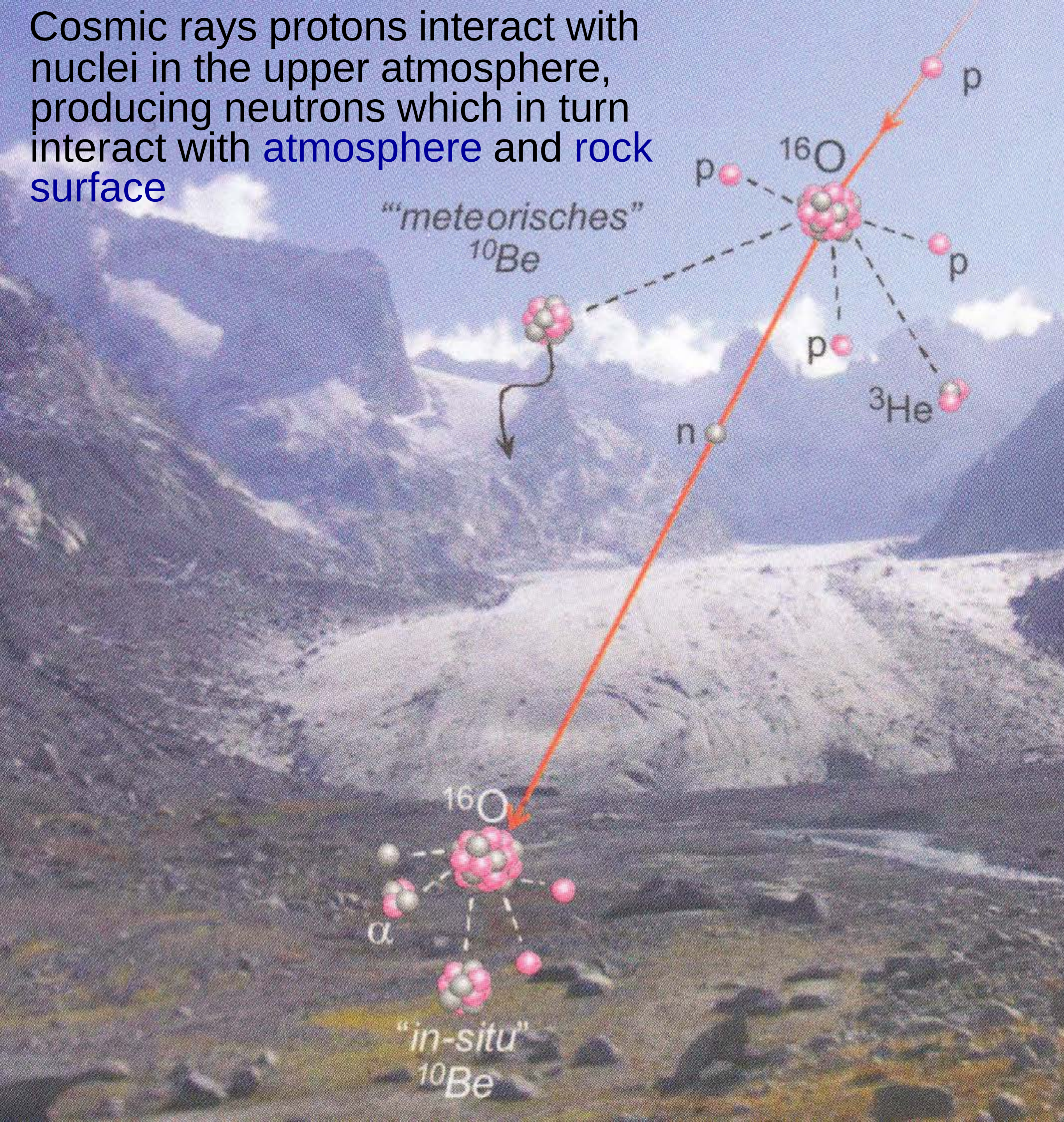

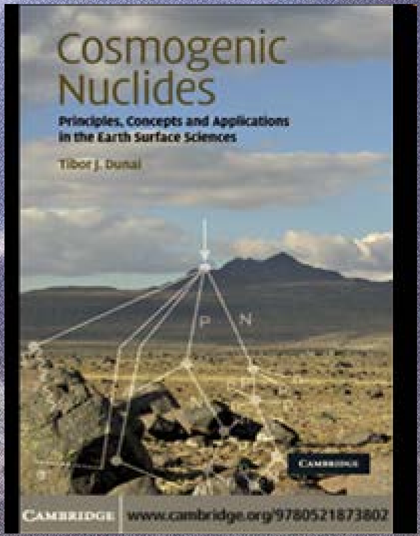

Cosmic-rays

Galactic cosmic rays derive their energy from supernova explosions

Crab nebula (Krebsnebel)

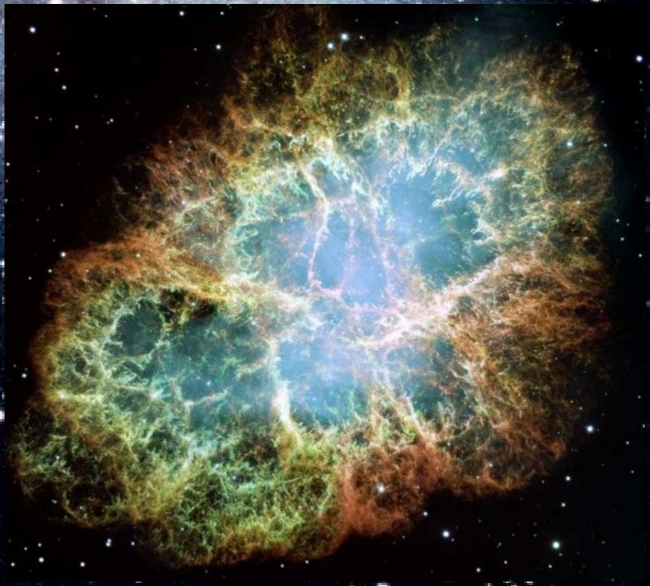

http://www.spacetelescope.org/images/html/heic0515a.html

Galactic cosmic rays: originate in sources outside the solar system, throughout our Milky Way galaxy.

Solar energetic particles: nuclei and electrons accelerated in association with energetic events on the Sun

Variation of production rate

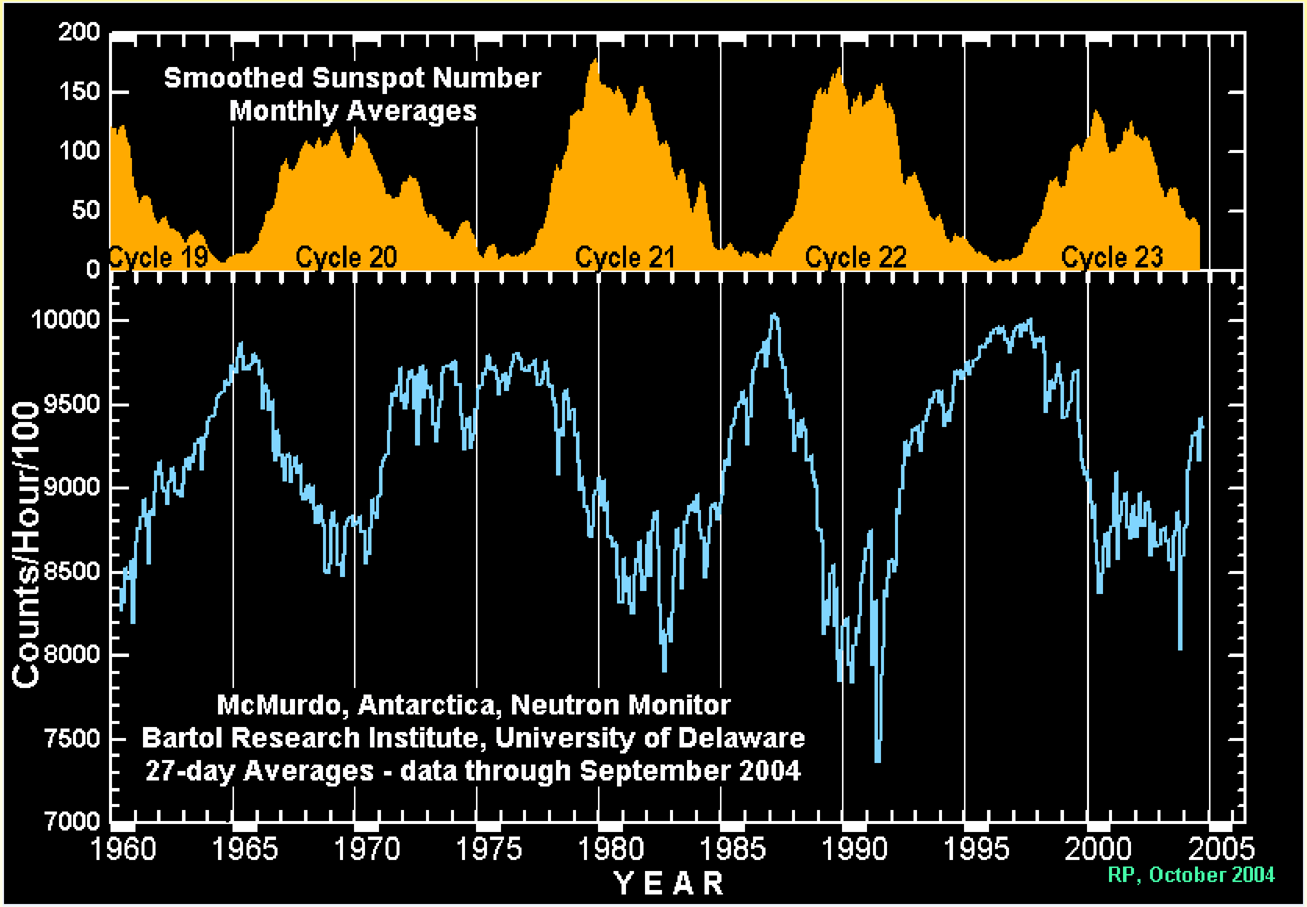

When the sun is active, we get fewer cosmic rays here

Energy of cosmic-rays

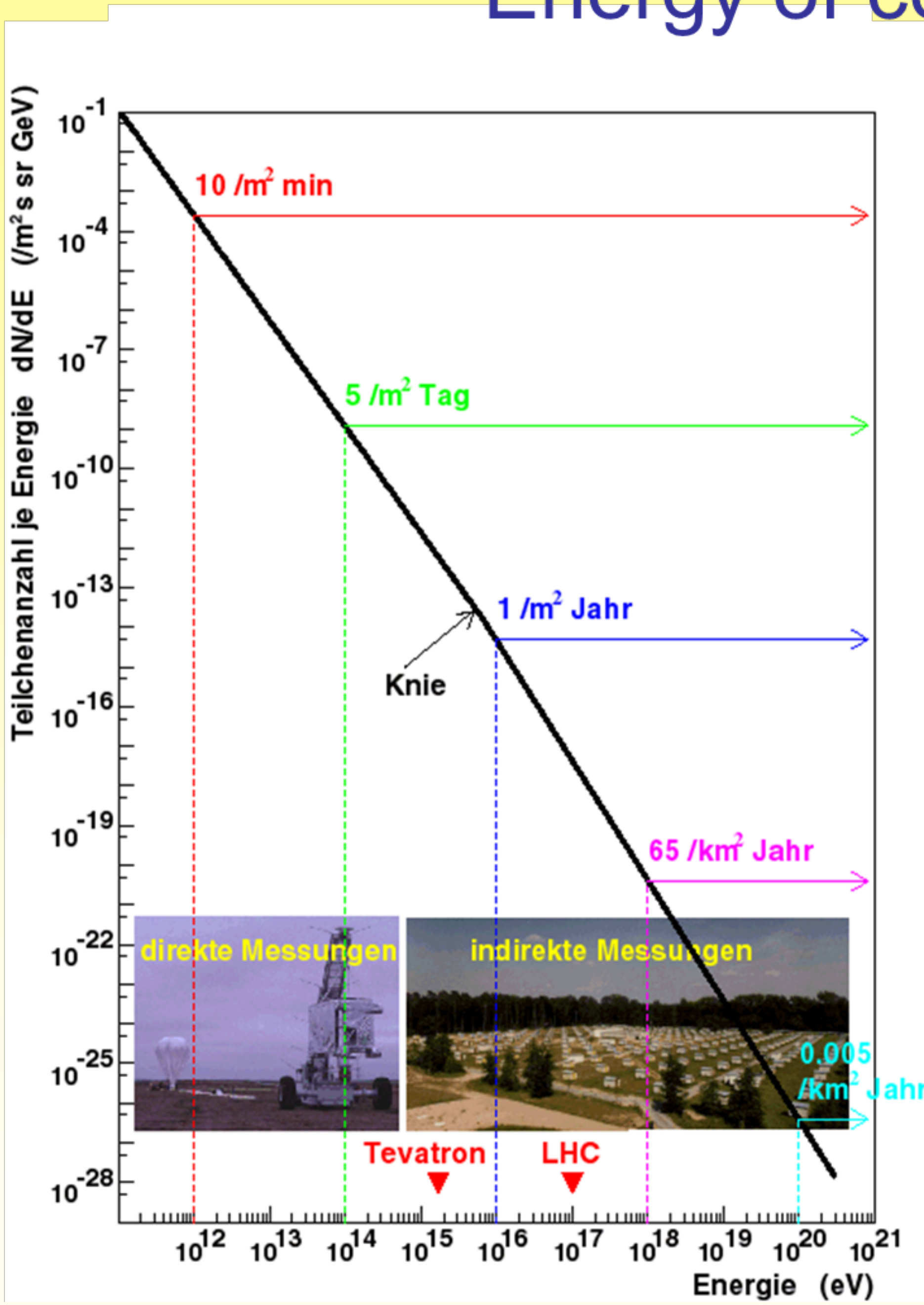

Components of galactic cosmic-rays

87-89% protons

10-12% α-particles

1-2% electrons

1% heavier elements

Secondary cosmic-rays

Pions → muons, neutrinos, γ-rays

electrons

positrons

Particle colliders

Tevatron, Fermilab, Chicago, USA
LHC, CERN, Geneva, Swizzerland

Cosmogenic isotopes

Major *in-situ* produced cosmogenic nuclides in terrestrial materials

Isotope	Production rate (atoms / g / year)	Half-life (years)	Target elements in terrestrial rocks
^{3}He	75 – 100 (olivine)	stable	O, Si, Al, Mg
^{10}Be	5 – 7 (quartz)	1.5×10^{6}	O, Si, Al, C
^{14}C	18 – 20	5730	C, O
^{21}Ne	18 – 21 (quartz)	stable	Mg, Na, Si, Al
^{26}Al	30 – 36 (quartz)	0.71×10^{6}	Si, Al
^{36}Cl	8 – 10 (basalt)	0.30×10^{6}	Cl, K, Ca
^{53}Mn	?	3.7×10^{6}	Fe

Cerling & Craig (1994) Annu. Rev. Earth Planet. Sci. 22

Major target minerals:
^{3}He: olivine, pyroxene hornblende
^{10}Be, ^{14}C, ^{21}Ne, ^{26}Al: quartz
^{36}Cl: calcite, K-feldspar

Cosmogenic isotopes are produced in near surface rocks by collisions of high energy neutrons and muons with specific target elements in rocks and minerals. All production rates scaled to sea-level high latitude (>60°)

Production of cosmogenic isotopes

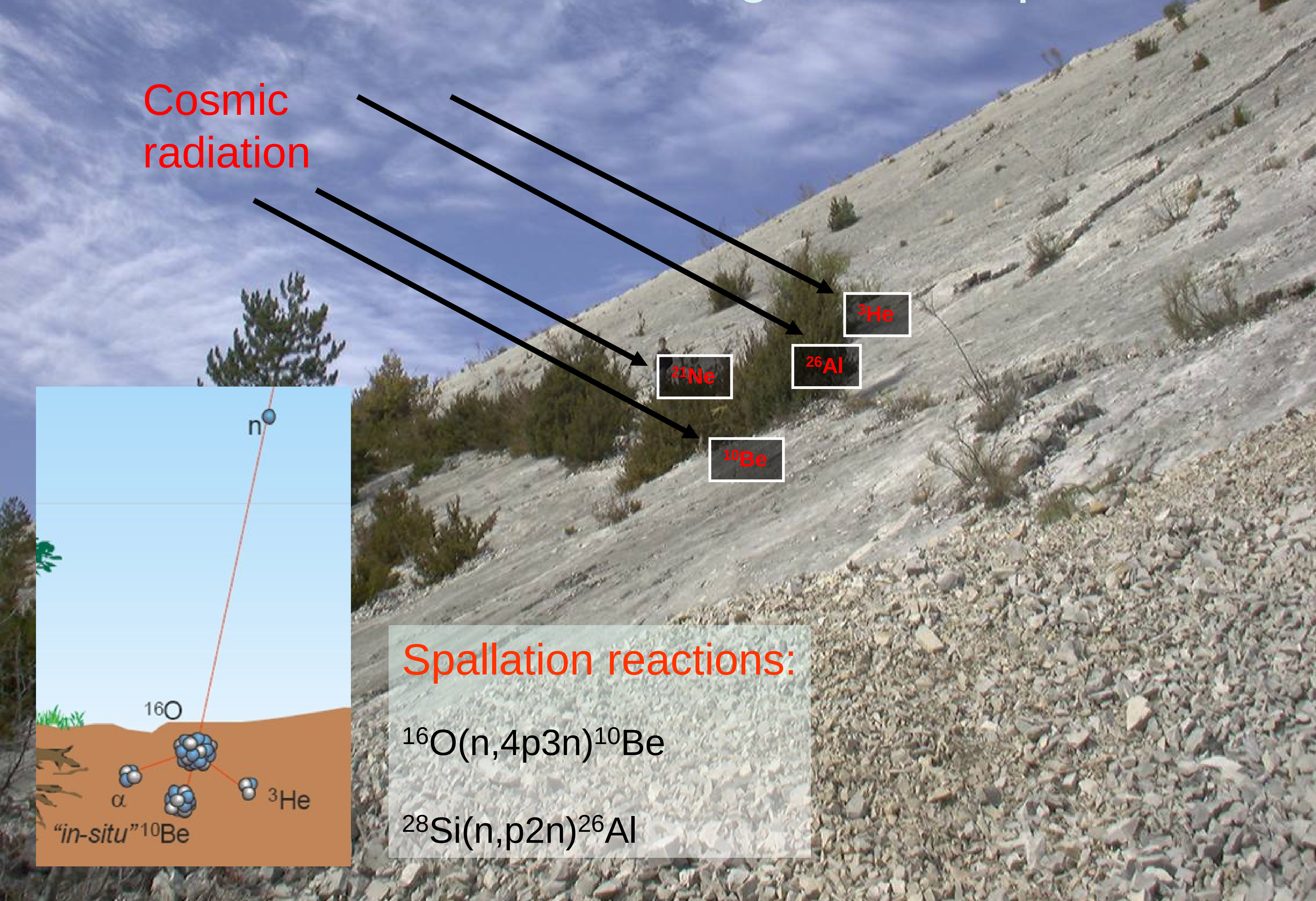

Spallation reactions:

$^{16}O(n,4p3n)^{10}Be$

$^{28}Si(n,p2n)^{26}Al$

Variation of production rate

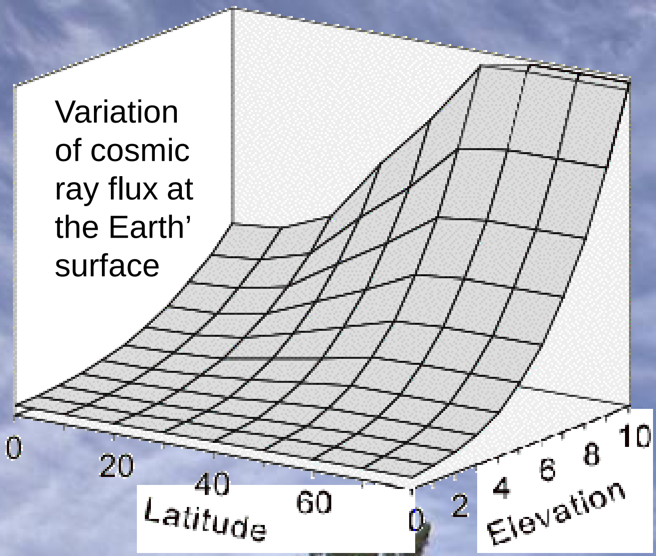

The **rate of production** of cosmogenic isotopes depends on the concentrations of the target elements (O, K, Ca, Mg), elevation, surface orientation, and geomagnetic latitude

Comparison with redness of a person's skin (suntan)

Gosse and Phillips (2001)

Suntan – wears away

Cosmogenic nuclide – decays

Suntan lotion shields skin from radiation

Atmosphere and snow shields a landform from radiation

Not everybody tans to the same degree of redness

Nuclide production varies in different minerals

Production rates

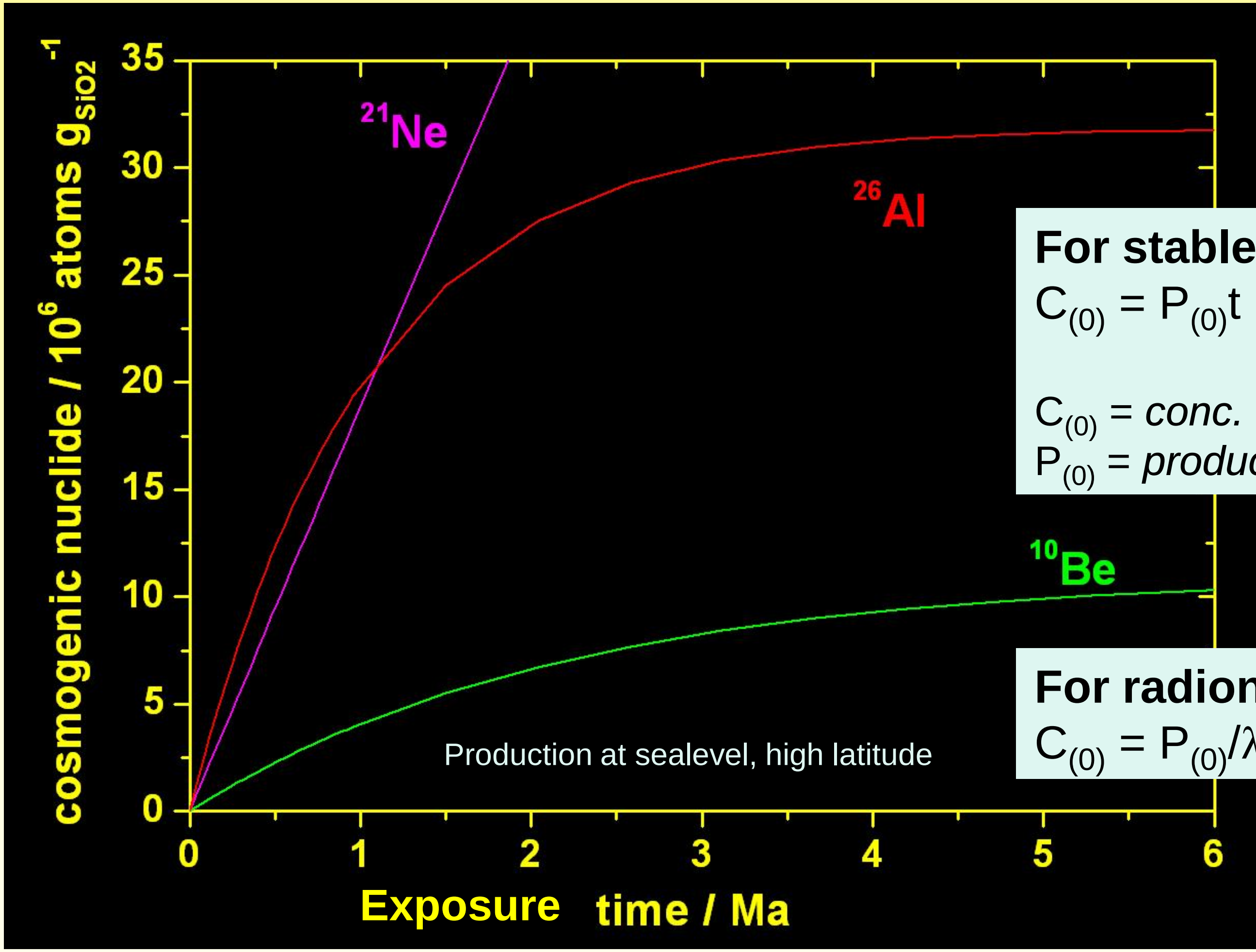

For stable nuclides (e.g. ^{21}Ne):

$C_{(0)} = P_{(0)}t$

$C_{(0)}$ = *conc. at surface*

$P_{(0)}$ = *production rate at surface*

For radionuclides (^{26}Al, ^{10}Be):

$C_{(0)} = P_{(0)}/\lambda(1–e^{-\lambda t})$

build-up of cosmogenic nuclides in case of **no erosion**

^{10}Be

^{10}Be is produced by reactions of cosmic ray protons with N_2 and O_2 in the upper atmosphere

Be is a particle reactive element → becomes concentrated in clay-rich oceanic sediments

^{10}Be then undergoes decay to ^{10}B with a half-life of about 1.5 Ma (long enough to be subducted, but quickly lost to mantle systems)

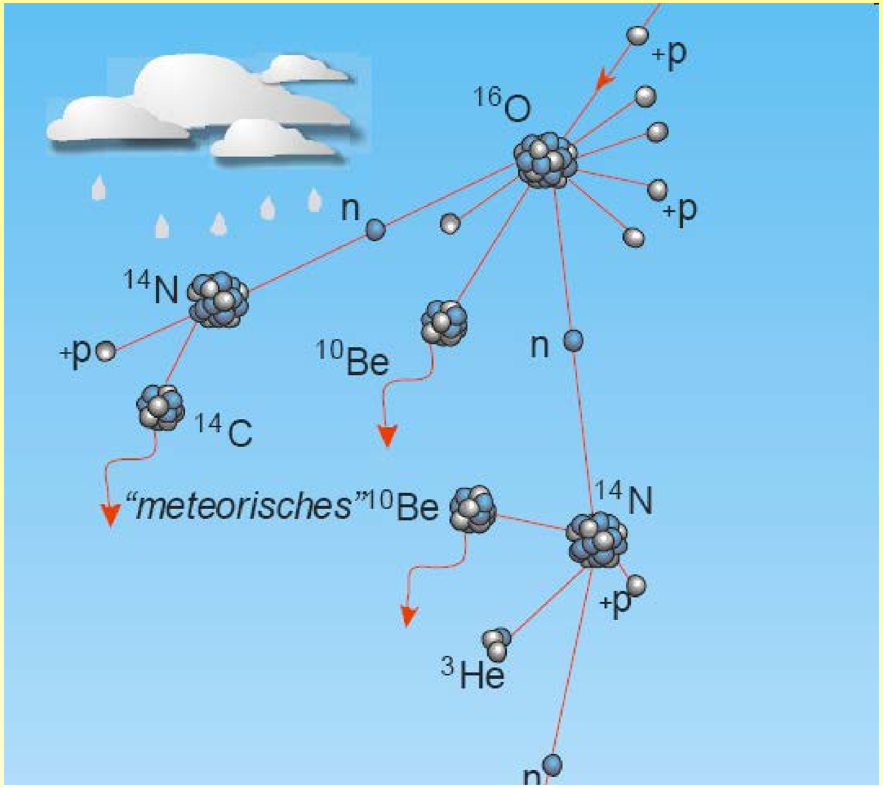

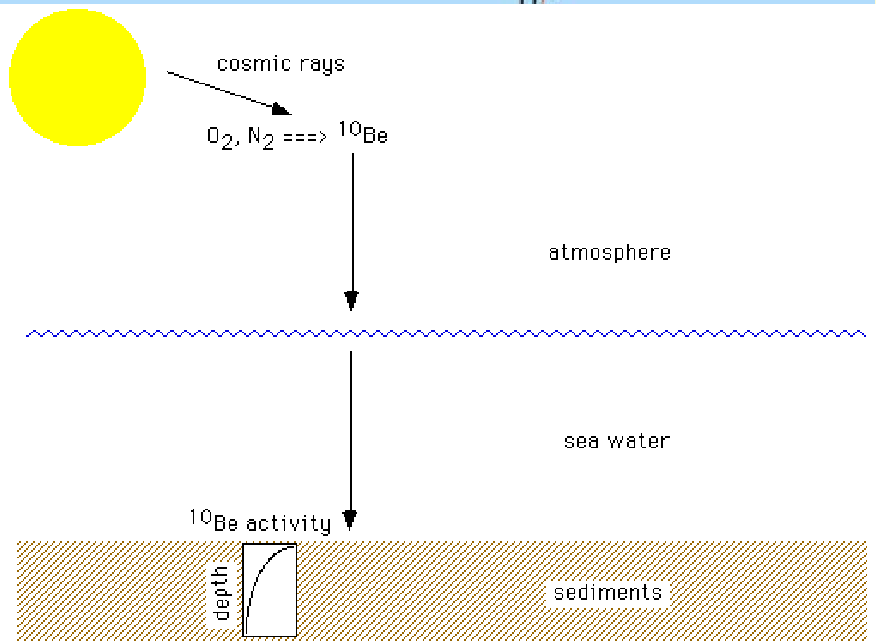

^{10}Be

Incorporation of cosmogenic ^{10}Be in island arcs?

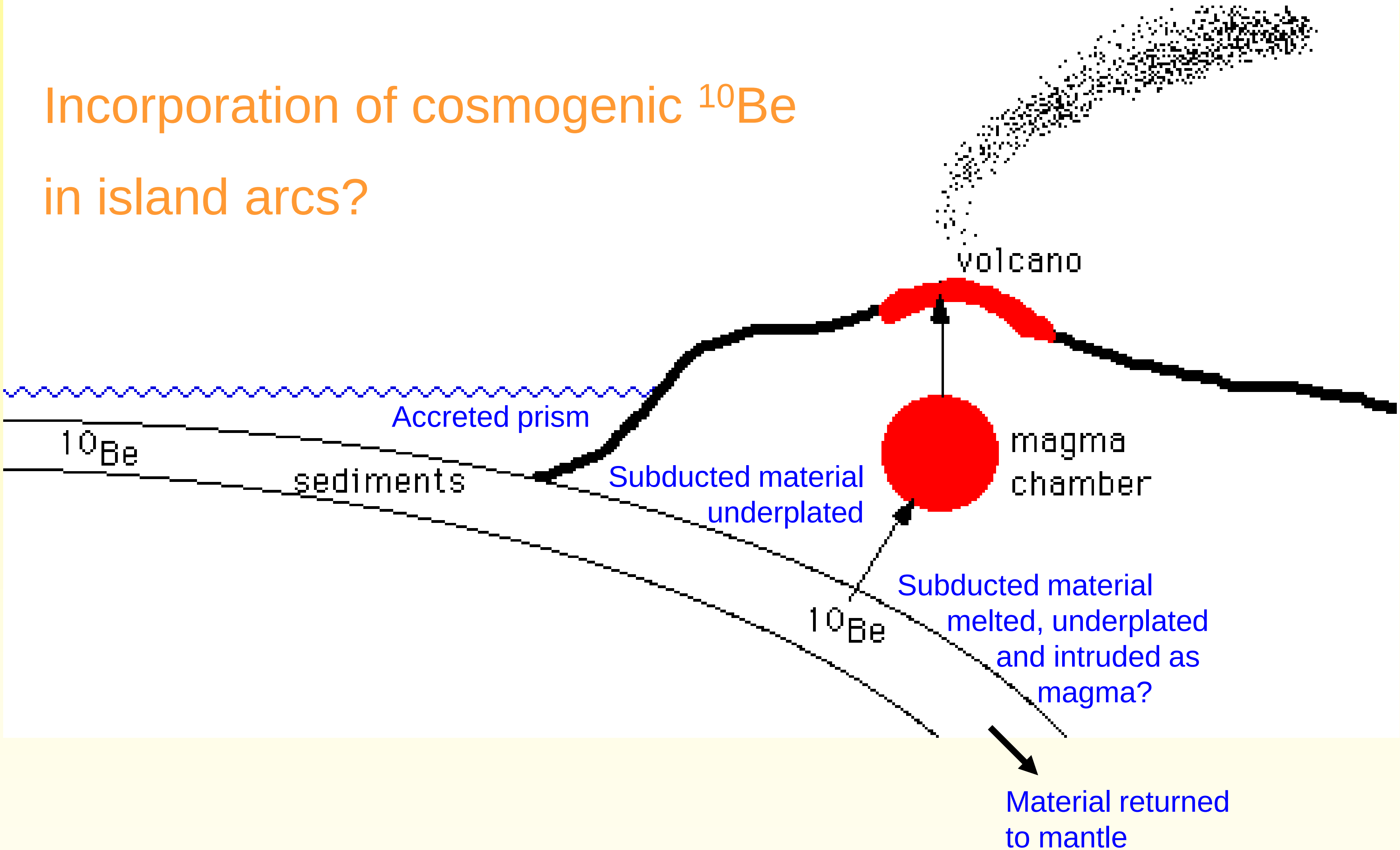

^{10}Be in arc lavas

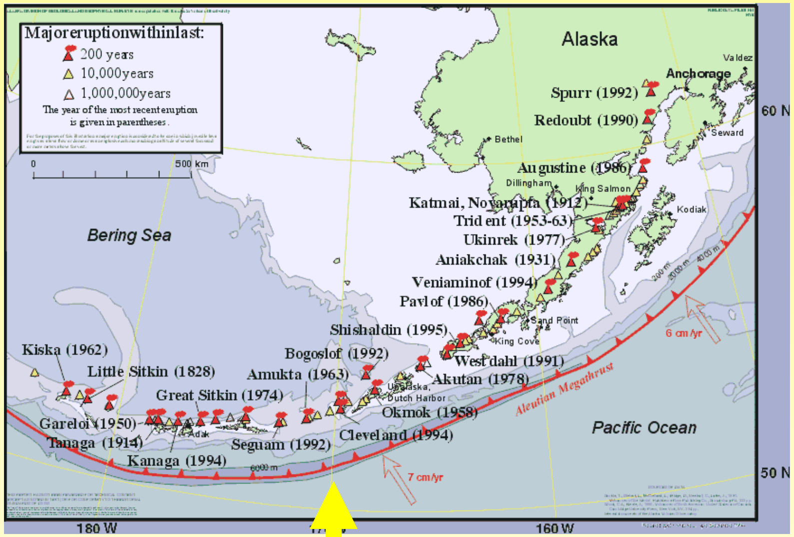

Smoking gun evidence for sediment subduction

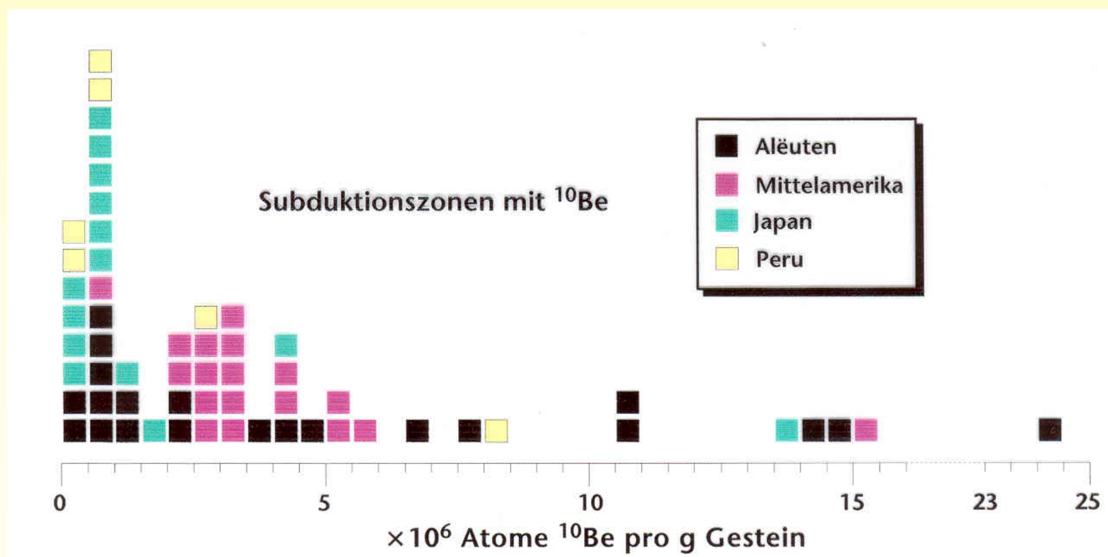

Brown et al. (1982) Nature 299; Tera et al. (1986) GCA 50

Measurement

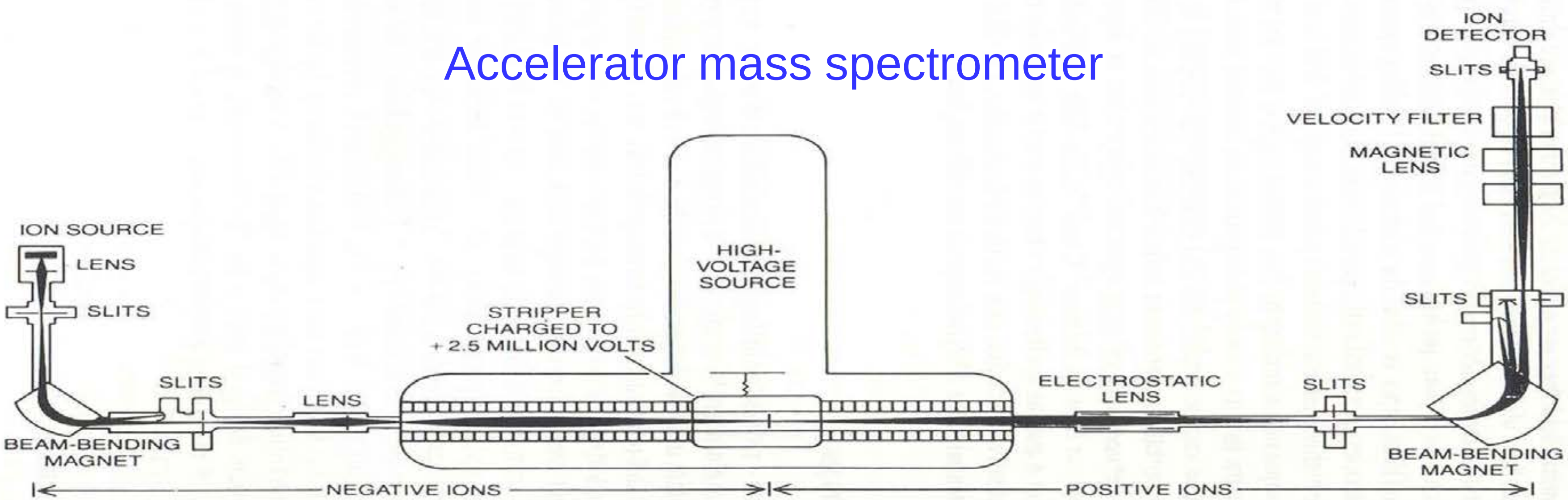

Fig. 37. Principal components of an accelerator mass spectrometer. (After Hedges and Gowlett 1986)

AMS has a factor of a millon lower detection limit for ^{14}C, ^{36}Cl, ^{10}Be, ^{26}Al compared to counting methods

How to determine production rates of TCN?

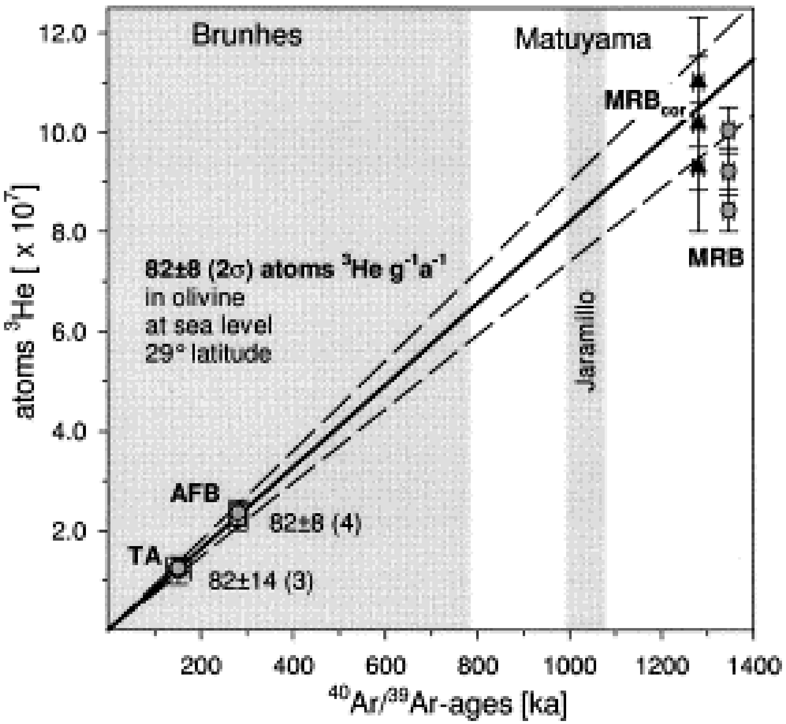

Production rate of ^{3}He in olivine derived from 3 lava flows dated by the $^{40}Ar/^{39}Ar$ technique at 152, 281 and 1350 ka (from Dunai & Wijbrans 2000).

Production rates

Nucleoneic production profile with depth P(d):

$P(d) = P_{(0)} e^{-d/L}$

$P_{(0)}$ = production rate at surface
d = depth
L = absorption length scale
L = 160/ρ cm (ρ = overburden pressure)

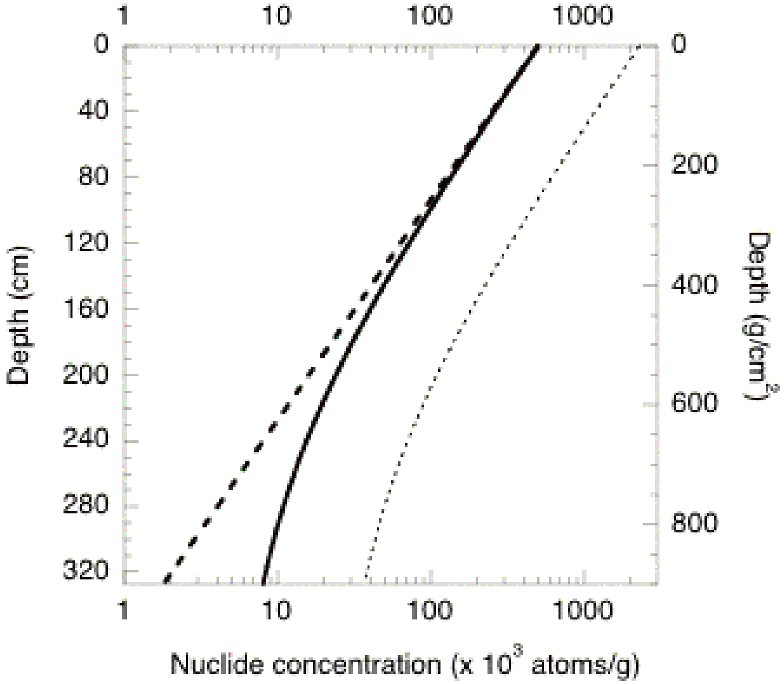

^{10}Be concentration vs. depth after 100 ka exposure calculated for nucleon production (dashed line) and for combined nucleon and muon production (solid curve) with a surface production rate of 5.1 atoms g^{-1} a^{-1}, a rock density of 2.75 g cm^{-3} and **no erosion**.

Production rates

Nucleonic production profile with depth P(d):

$P(d) = P_{(0)}e^{-d/L}$

$P_{(0)}$ = production rate at surface
d = depth
L = absorption length scale
L = 160/ρ cm (ρ = density of overburden)

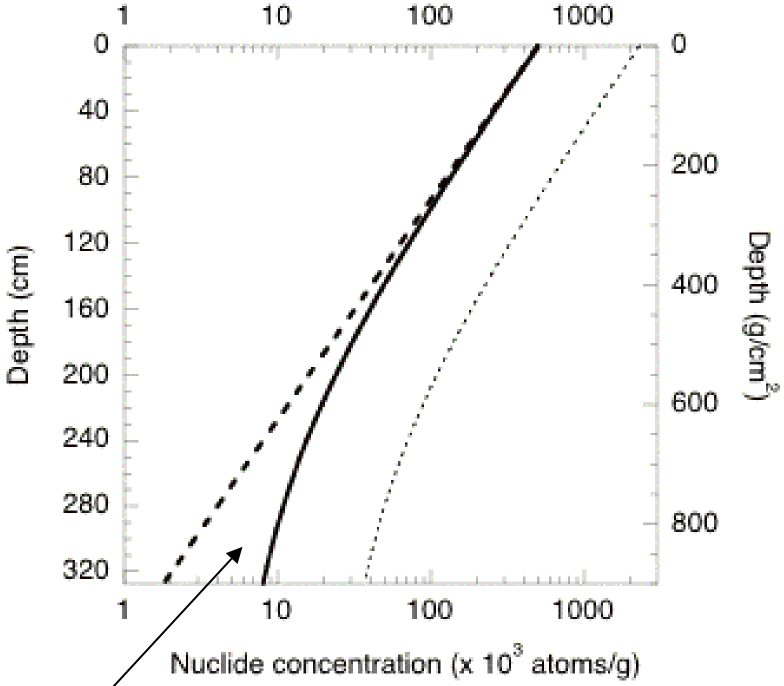

In situ cosmogenic isotopes are produced near the surface of the earth because the cosmic flux is attenuated by rock at depths that exceed 2-3 m.

For nucleon and muon production (solid curve in fig.):

$$P(d) = P_{(0)}e^{-d/L0} + P_{(1)}e^{-d/L1} + P_{(2)}e^{-d/L2} + P_{(3)}e^{-d/L3}$$

Production rates

Production profile with depth P(d):

$P(d) = P_{(0)}e^{-d/L}$

$P_{(0)}$ = production rate at surface
d = depth
L = absorption length scale

$P(d) = P_{(0)}e^{-d/L0} + P_{(1)}e^{-d/L1} + P_{(2)}e^{-d/L2} + P_{(3)}e^{-d/L3}$

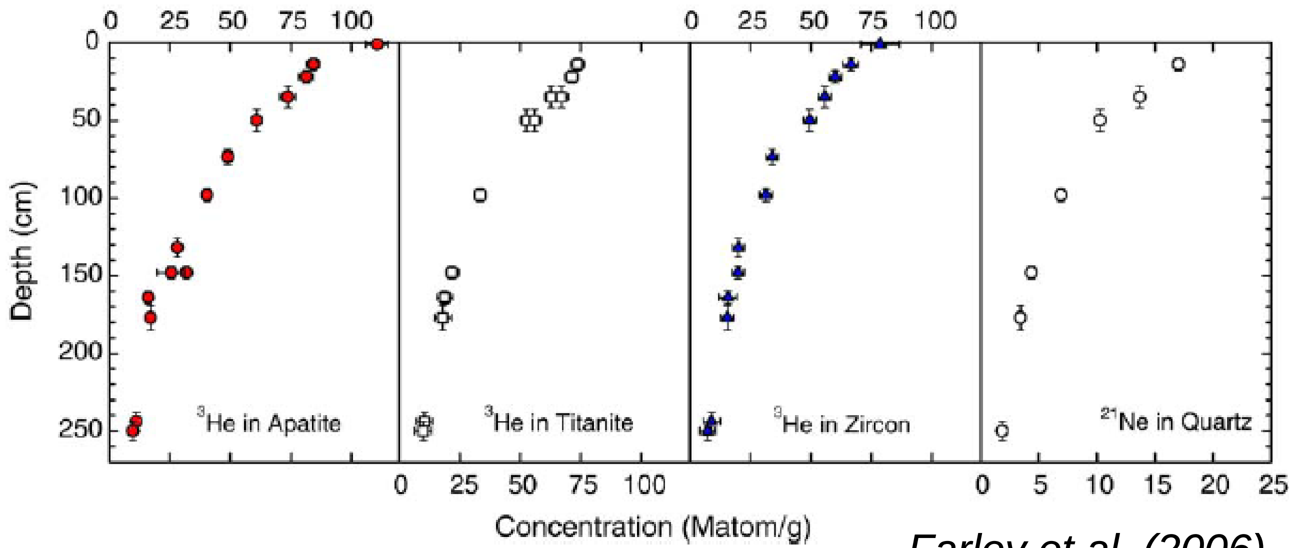

Farley et al. (2006)

Übung 1: Produktionsratenberechnung

^{23}Na wird bei einer konstanten Neutronenflußdichte von 10^{12} cm^{-2} s^{-1} in radioaktives ^{24}Na umgewandelt

Der Wirkungsquerschnitt beim Einfang thermischer Neutronen (*Neutroneneinfangsquerschnitt*) für diese Reaktion beträgt 0.53×10^{-24} cm^2 pro Atom

Wieviel ^{24}Na Atome werden pro g Natrium und pro Sekunde produziert?

Übung 1: Produktionsratenberechnung

^{23}Na wird bei einer konstanten Neutronenflußdichte von 10^{12} cm^{-2} s^{-1} in radioaktives ^{24}Na umgewandelt: $^{23}Na(n,\gamma)^{24}Na$

Der Wirkungsquerschnitts für den Einfang thermischer Neutronen (*Neutroneneinfangsquerschnitt*) für diese Reaktion beträgt 0.53×10^{-24} cm^2 pro Atom

Wieviel ^{24}Na Atome werden pro g Natrium und pro Sekunde produziert?

Pro Sekunde werden $0.53 \times 10^{-24} \times 10^{12}$ = $\mathbf{0.53 \times 10^{-12}}$

^{24}Na Atome produziert

Übung 1

In einer Sekunde werden $0.53 \times 10^{-24} \times 10^{12}$ = **0.53×10^{-12}**

^{23}Na Atome produziert

1Mol Na enthält 6.023×10^{23} Atome (Avogadro-Zahl)

Na hat das Atomgewicht 23 → Gewicht von 6.023×10^{23} Atomen entspricht also 23 g

→ $0.53 \times 10^{-12} \times 6.023 \times 10^{23} / 23$ = **1.387×10^{10}** Atome ^{24}Na werden pro Sekunde pro g Natrium produziert

Übung 2: Berechnung der Probenmenge für Expositionsaltersbestimmung

^{10}Be Produktionsrate in Quarz: 5 Atome pro Jahr

Geschätztes Alter der Oberfläche 6000 Jahre

^{10}Be Konzentration in Quarz?

Für AMS Messung:

Gewünschtes ^{10}Be/^{9}Be-Verhältnis: 5×10^{-14}

gewünschte Menge an (reinem) BeO: 0.5 mg

Vieviel g Quarz wird für die Messung gebraucht?

Assuming no erosion….

…the exposure age can be determined using the following equation:

$$T = \frac{\ln(1 - C\lambda/P)}{-\lambda}$$

T = the length of irraditation (i.e., exposure age),

C = number of cosmogenically produced atoms

P = cosmogenic isotope production rate

λ = decay constant

Production rates, considering erosion

$C = P_\Lambda / D$

C = concentration of cosmogenic nuclide
P = production rate
Λ = penetration length scale
D = denudation rate

$N_{(0)} = [P_{(0)}/(\lambda + \rho\varepsilon/L_0)]$

$N_{(0)}$ = concentration at surface
$P_{(0)}$ = production rate at surface
λ = decay constant
ε= (constant) erosion rate
ρ = density
L_0 = attenuation length

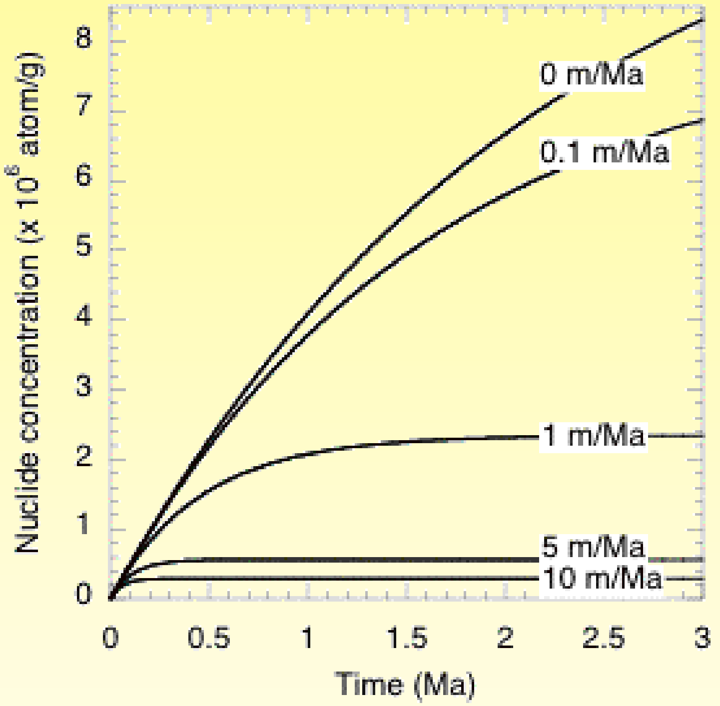

Surface concentration of in-situ cosmogenic stable isotope (^{10}Be) for steady-state erosion rates ranging from 0 to 10 m/Ma.

Exposure age dating and erosion

Assumptions:

- No *inheritance* of nuclide concentrations
- Steady state erosion or no erosion
- Simple exposure history (e.g. no shielding)
- Production rate can be constrained

Questions:

- Exposure age of a surface
- Exposure age of terraces (bedrock and deposits)
- Erosion rate of exposed bedrock
- Soil production rates

Banana plot 1/2

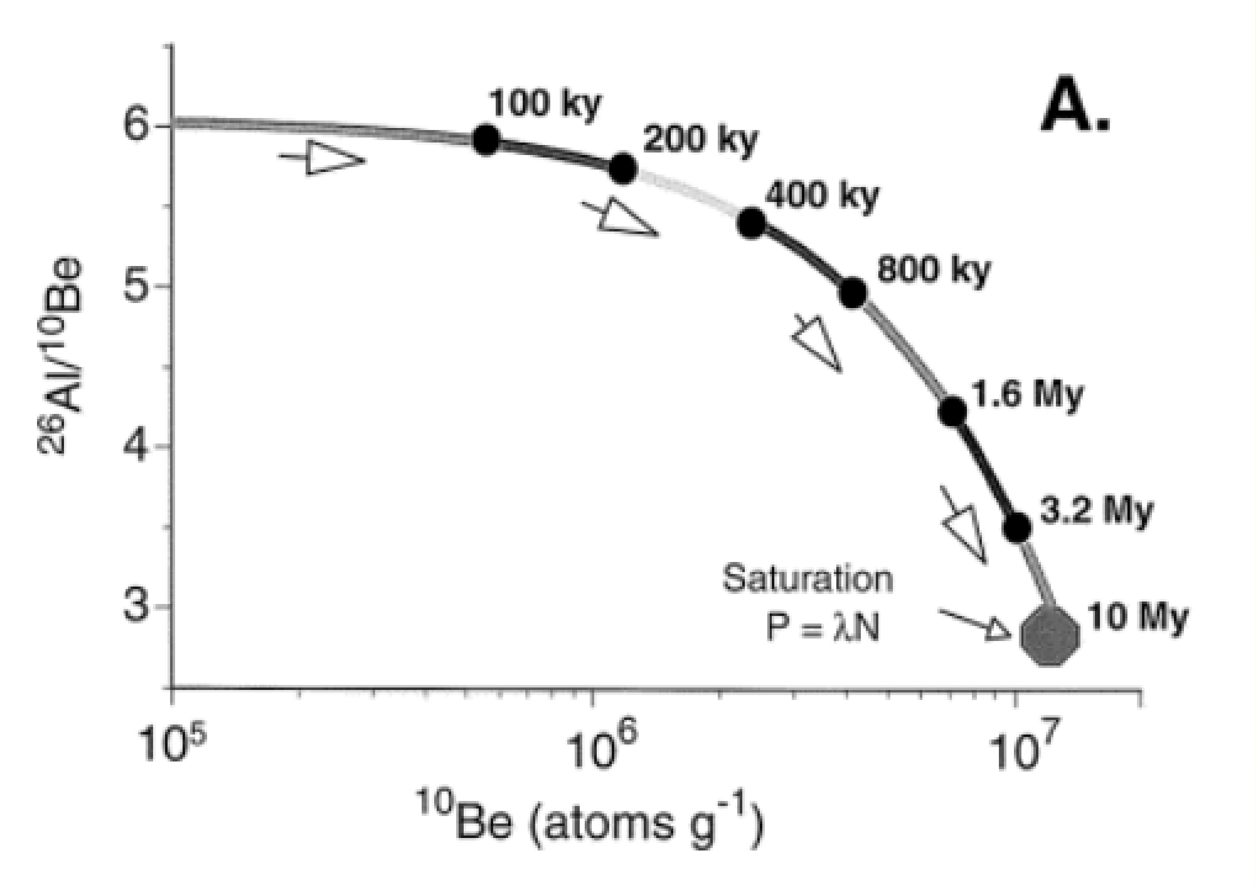

^{26}Al is produced six times faster than ^{10}Be, but ^{26}Al decays more quickly (half-life = 0.71 Ma) than ^{10} Be (half-life = 1.5 Ma)

Long dashed curve: decay of ^{26}Al
Short dashed curve: decay of ^{10}Be
Solid: ^{26}Al/^{10}Be ratio

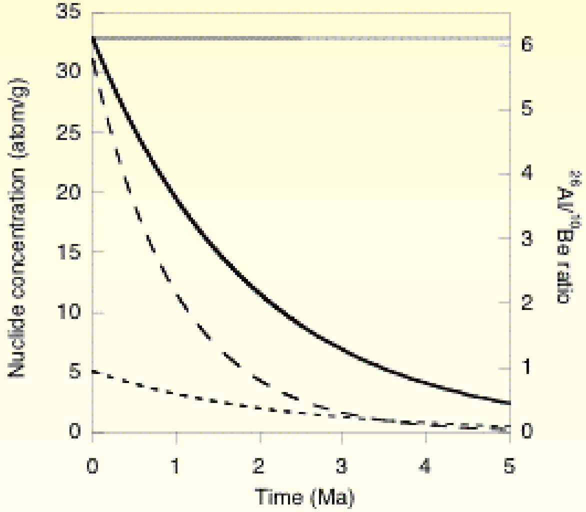

The line is the isotopic trajectory of non-eroding sample exposed continuously at the surface. Numbers to right of curve are exposure ages.
Trajectory ends at saturation where in situ production is equal to decay. In reality, saturation is rarely reached as nuclides are lost by surface erosion.

Banana plot 2/2

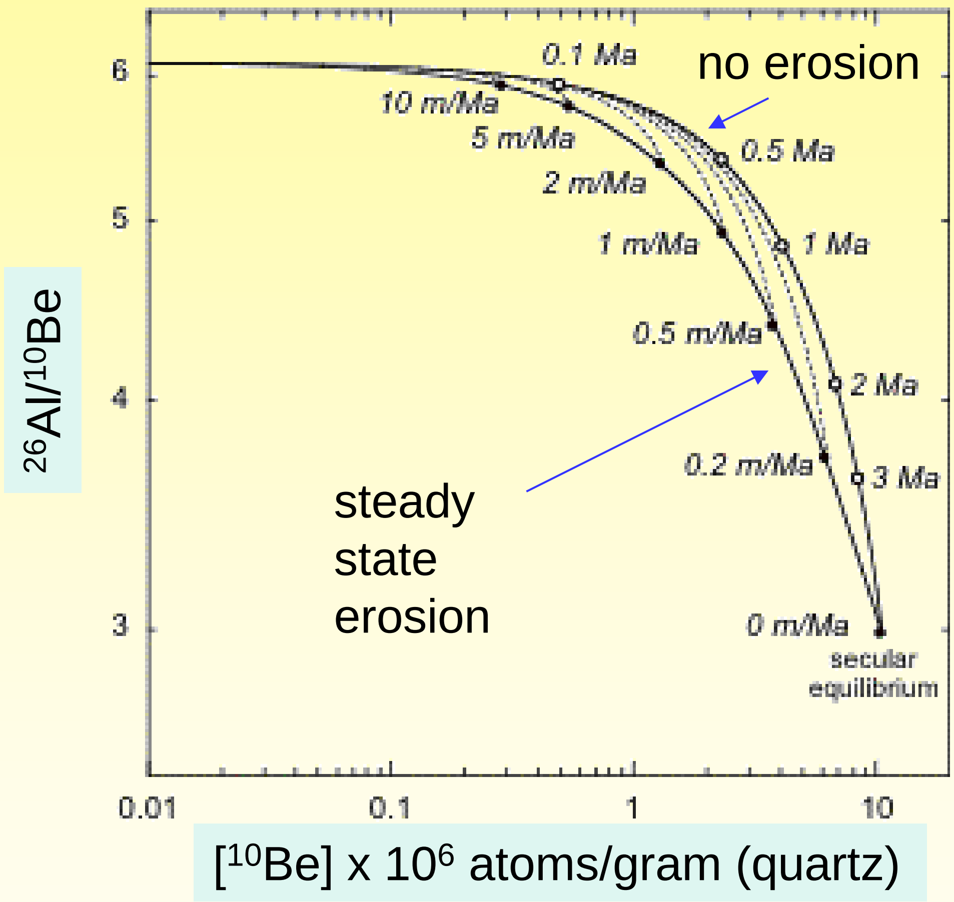

Continuously exposed samples fall on the curve connecting the open circles labelled with exposure time (same as in last figure)

Steadily eroding samples lie on the lower curve connecting the labelled steady-state erosion end points (solid dots).

Dashed curves show the trajectory of samples within the ^{10}Be concentration vs. $^{26}Al/^{10}Be$ space for the given steady-state erosion rates.

Samples that have been shielded will plot below the "*banana- window*" i.e., below the line of steady-state erosion

Burrial dating

Burrial dating plot

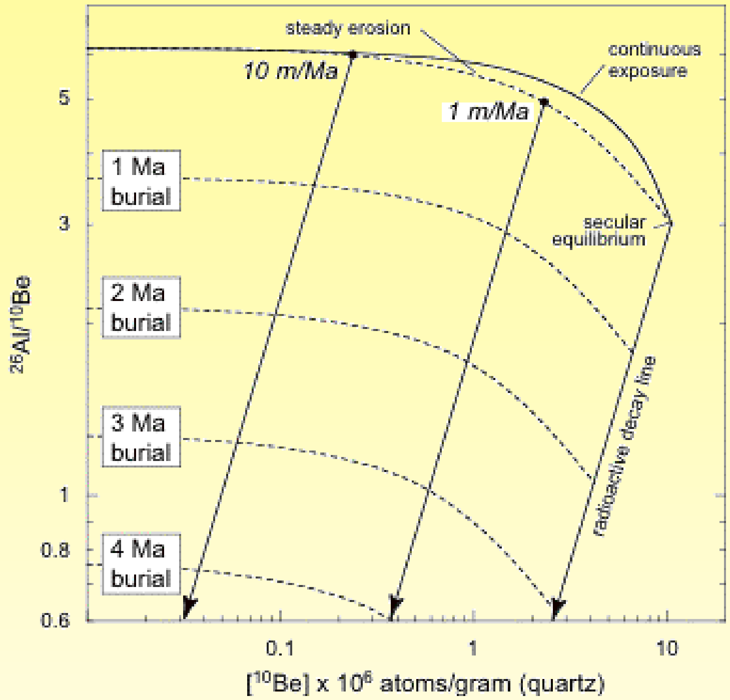

A mineral with no burial history should plot between the steady erosion and continuous exposure curves (i.e., in the “banana-window”)

For completely buried and shielded minerals, the $^{26}Al/^{10}Be$ decreases along a line parallel to the solid "radioactive decay line".

Measured $^{26}Al/^{10}Be$ ratio in a sample determines the burial time, and can also be used to calculate the pre-burial erosion rate.

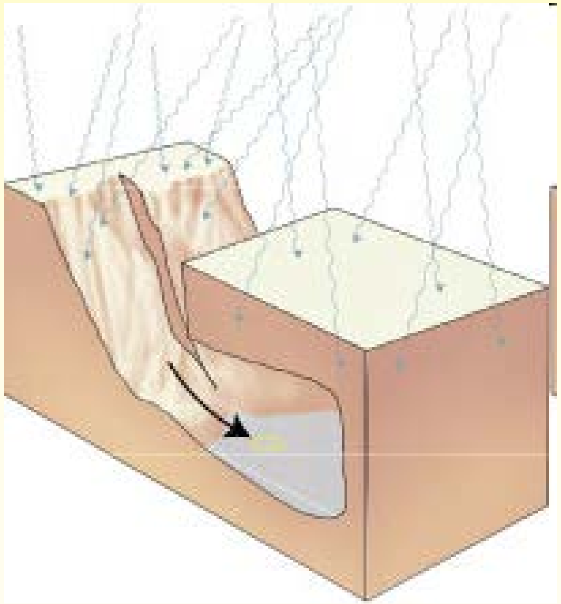

Applications

1. Dating Quaternary basalt volcanism
2. Timing of landslides
3. Tectonic displacement
4. Glaciers and ice-sheets
5. Meteorite impacts
6. Sedimentation rates
7. Ground water dating
8. (Sea water dating)
9. Age of landscapes
10. Erosion rates

Exposure age dating

1. Dating Quaternary volcanism

Radiocarbon dating (if charcoal in between)
or: cosmogenic ^{3}He

Lascar, N-Chile

2. Timing of landslides

A: After landslide, cosmic rays build up in the rocks exposed in the landslide scar and on the surface of the deposit

B: after boulder fall, cosmogenic isotopes build up on the upper surface of the boulder and in the scar left behind

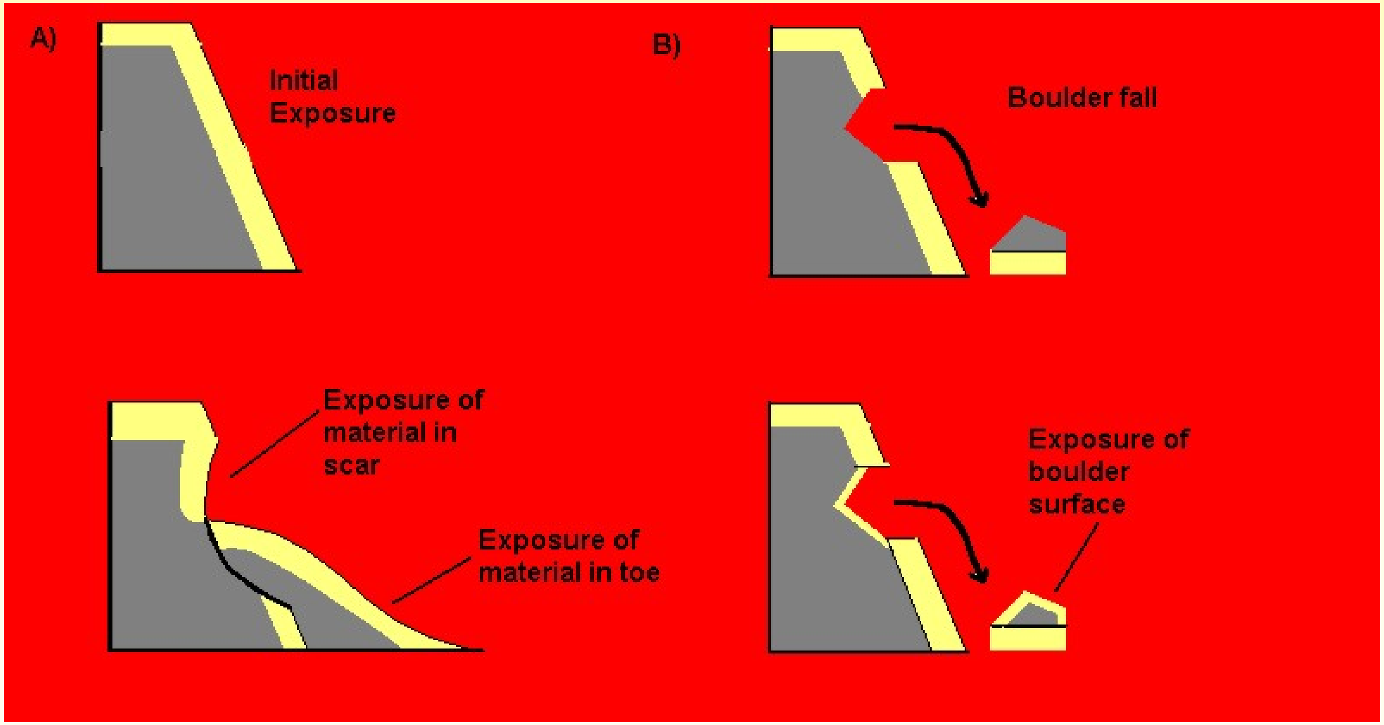

2. Timing of landslides

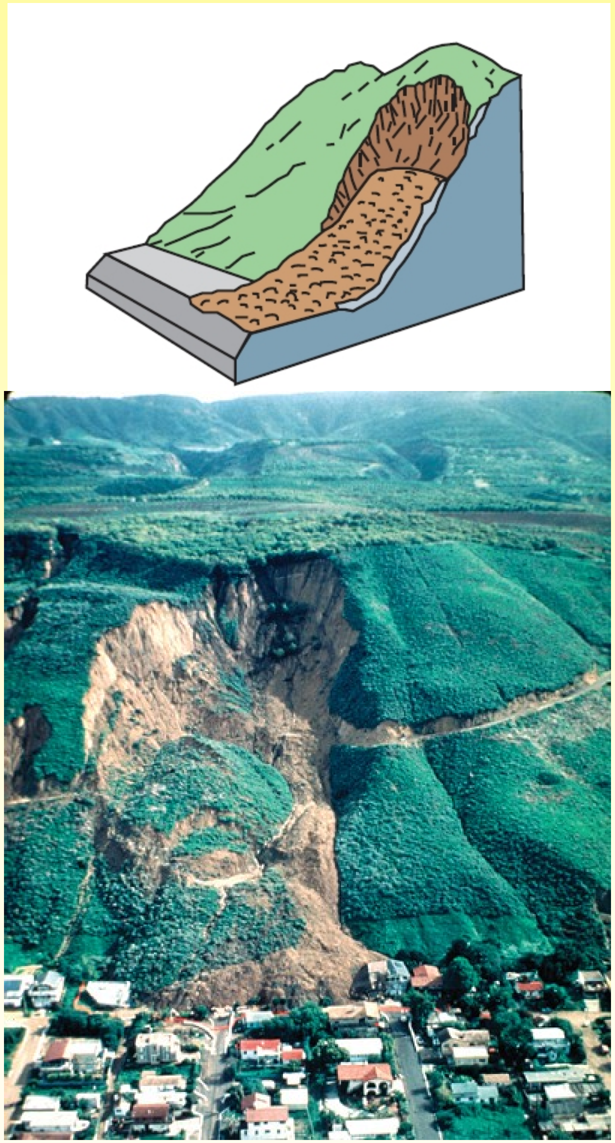

La Conchita landslide (1995) California

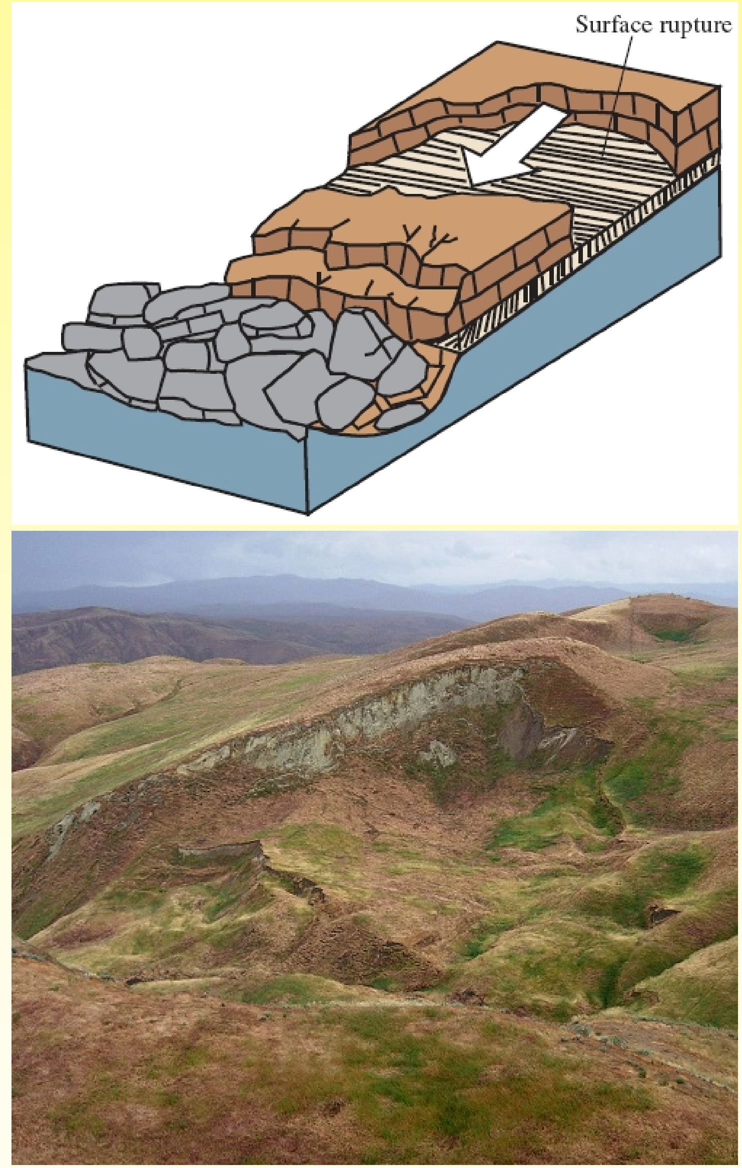

Panoche Hills, California

2. Timing of landslides

3. Tectonic displacement

dating of ancient earthquakes

Movement along fault planes usually occurs during earthquakes.

Exposure ages increase from bottom to top, and can cluster into discrete groups or steps representing the episodic nature of faulting events.

The number and magnitude and recurrence interval of the faulting events which produced the scarp can be determined.

(Zreda & Noller 1998, Science 282)

3. Tectonic displacement

Sparta fault, Greece

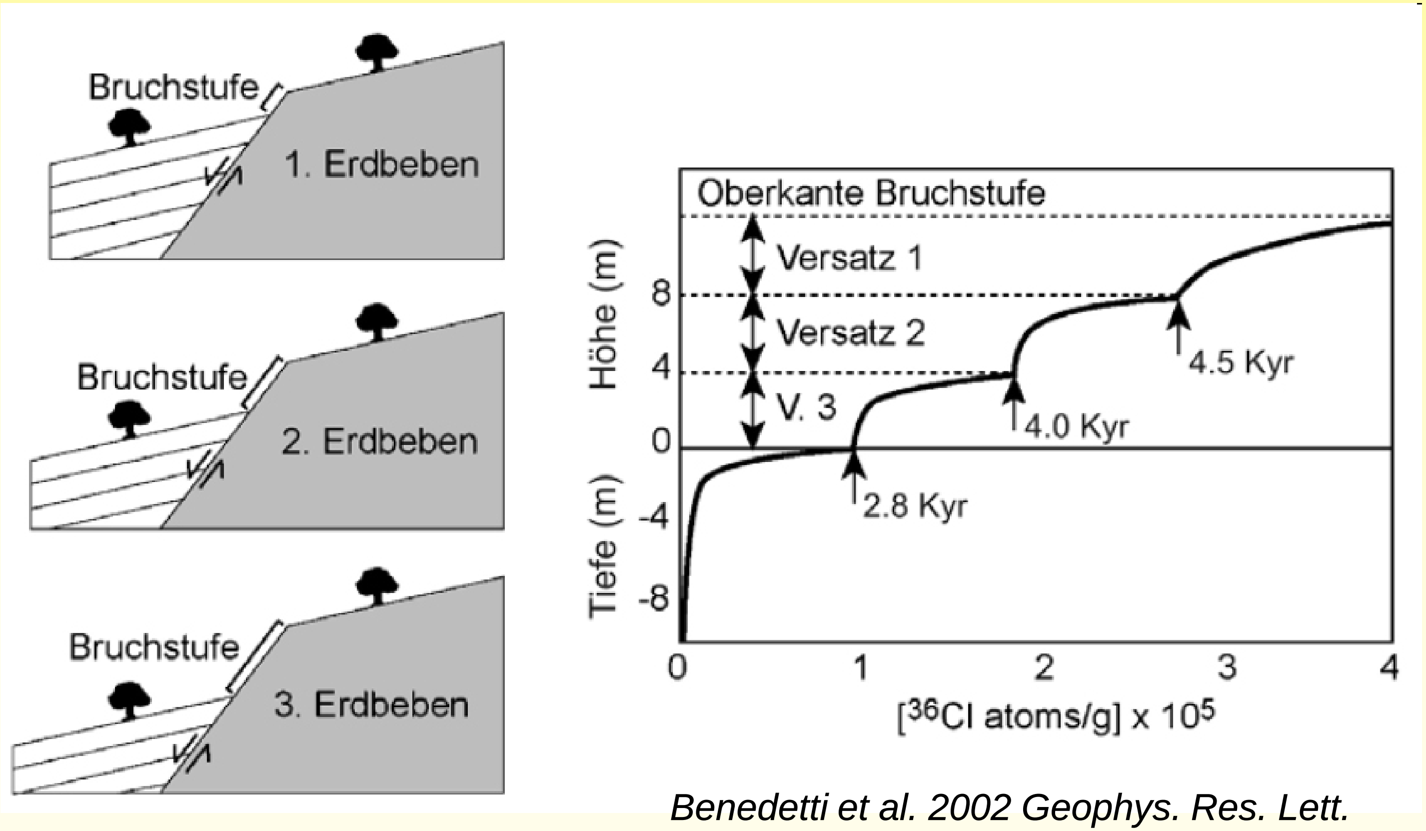

Benedetti et al. 2002 Geophys. Res. Lett.

3. Tectonic displacement

Magnola fault, Apennines

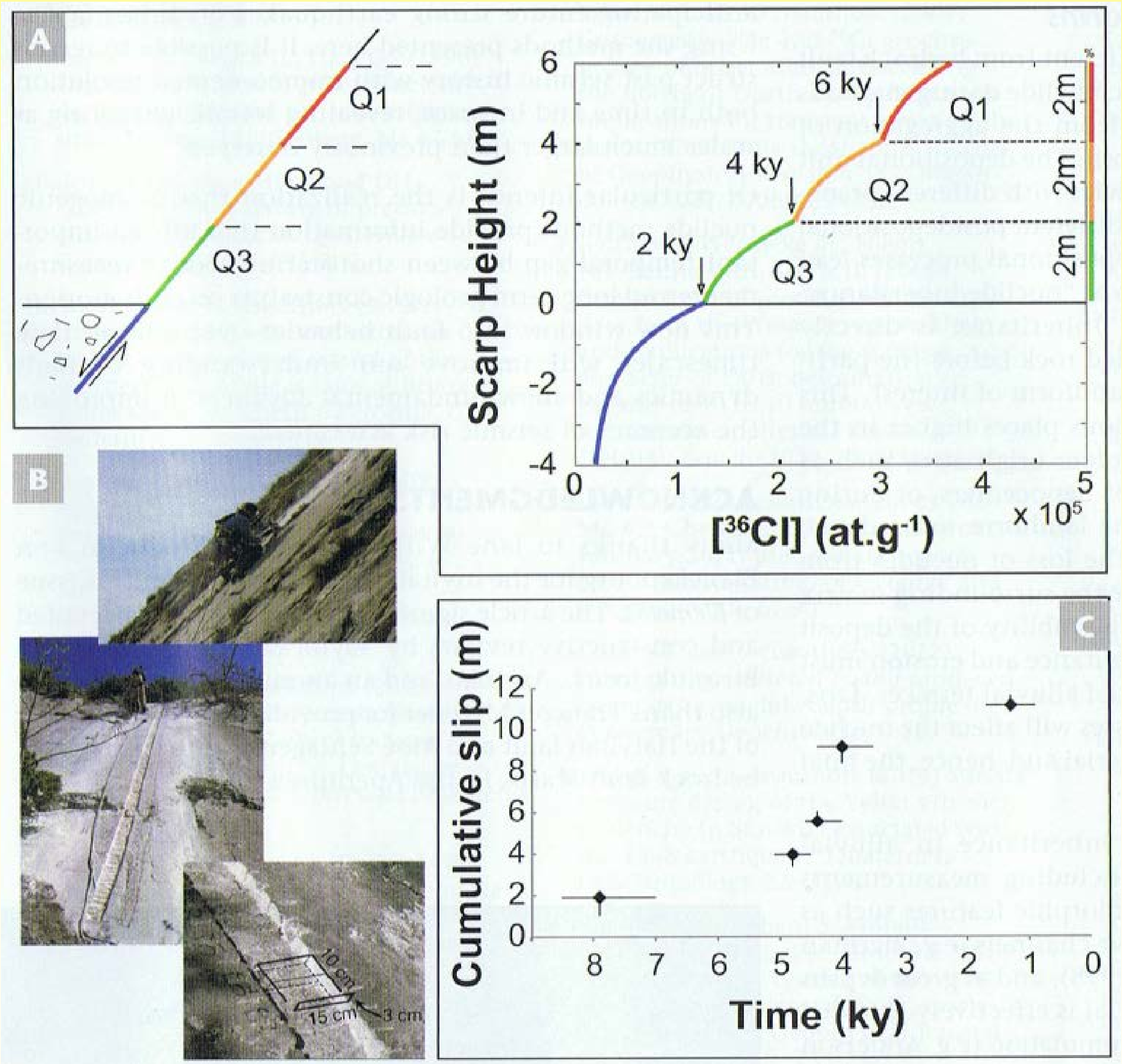

Schlagenhauf et al. (2011), EPSL 307

4. Glaciers and ice sheets

Courtsey H. Hann

4. Glaciers and ice sheets

Pasterzenzunge, Großglockner (3798 m)

1900

2000

Assuming that boulders have been exposed continuously since the retreat of the ice, the glacial retreats can be dated

4. Glaciers and ice sheets

Morteratsch

1867

2007

4. Glaciers and ice sheets

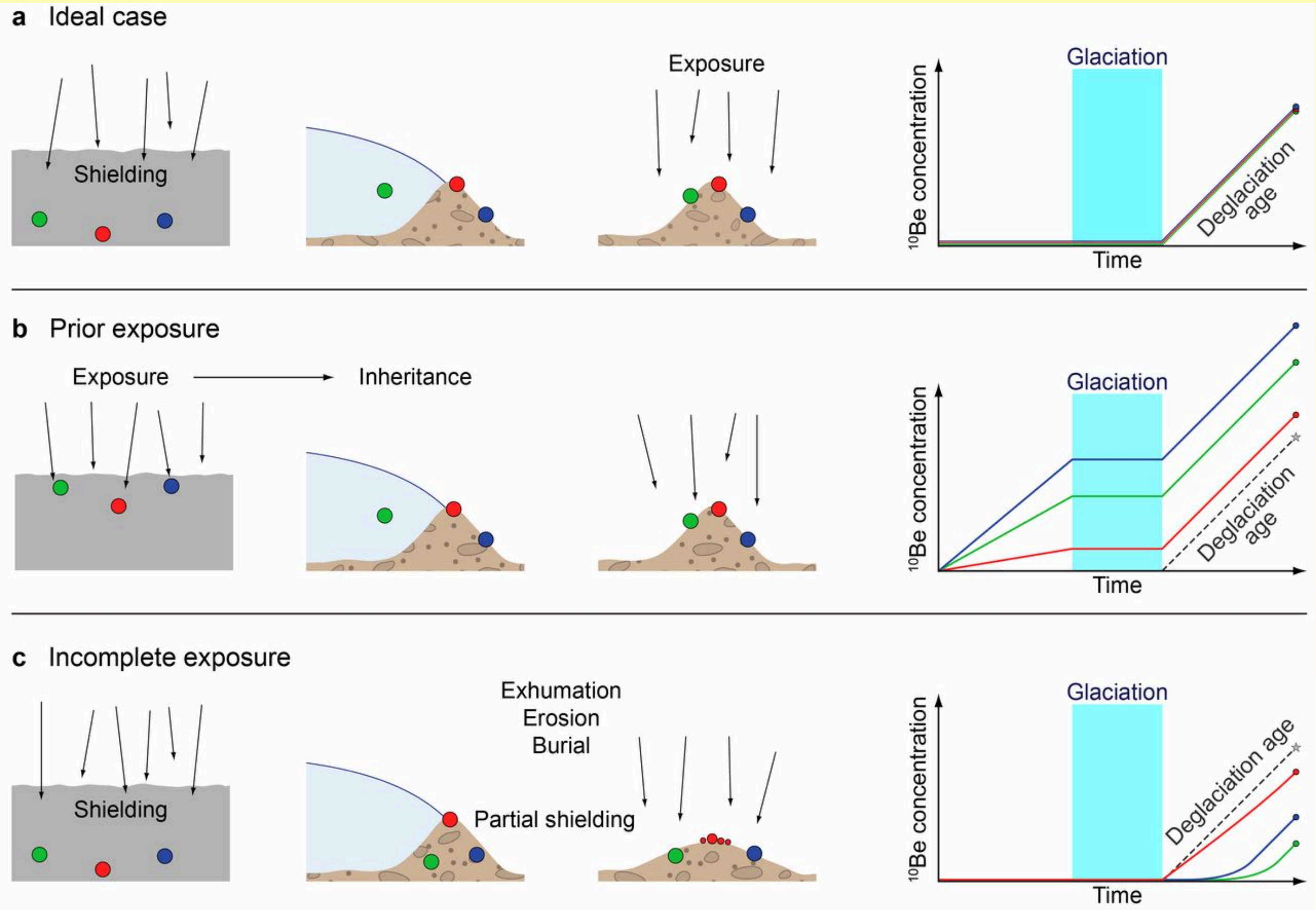

Ivy-Ochs & Briner:
Elements (2014)

4. Glaciers and ice sheets

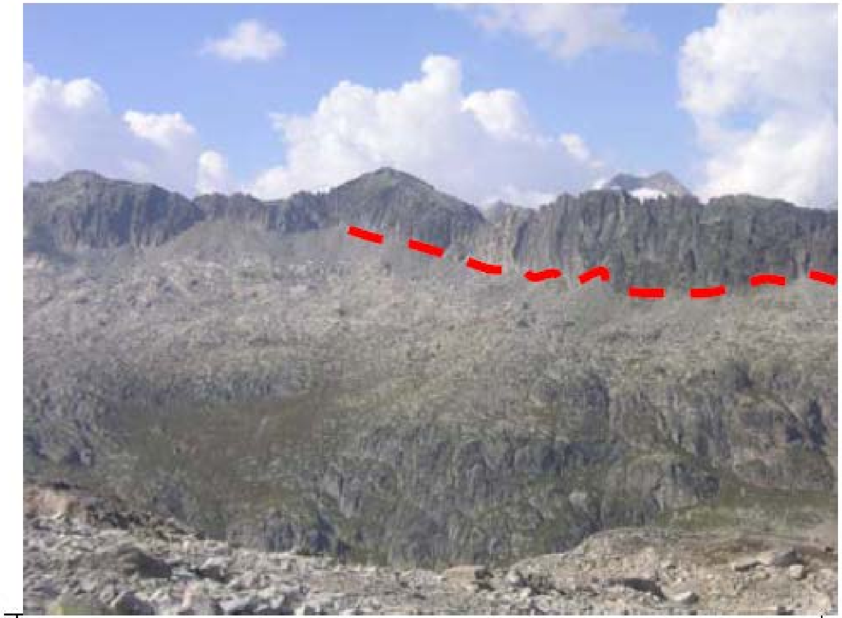

Grimselpass, Schweiz

former active ice surface

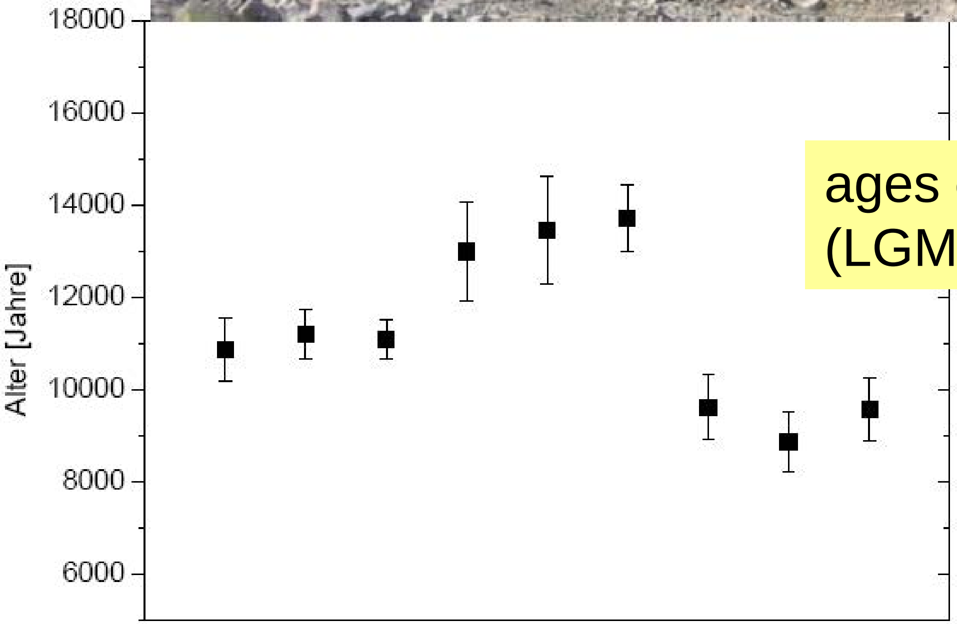

ages correspond to the last glacial maximum (LGM) → Younger Dryas

Kelly et al. 2004 J.Quaternary Sci.19: 431

5. Meteorite impacts

Dating a hole in the ground

The Barringer Meteorite Crater of the Arizona desert.

49.2 ± 1.7 ka, based on ^{10}Be and ^{26}Al exposure age of samples from the crater walls and ejecta blocks at the crater rim *(Nishiizumi et al. 1991).*

49 ± 0.7 ka, based on ^{36}Cl exposure age of for dolomite ejecta on the crater rim *(Phillips et al. 1991).*

6. Sedimentation and growth rates

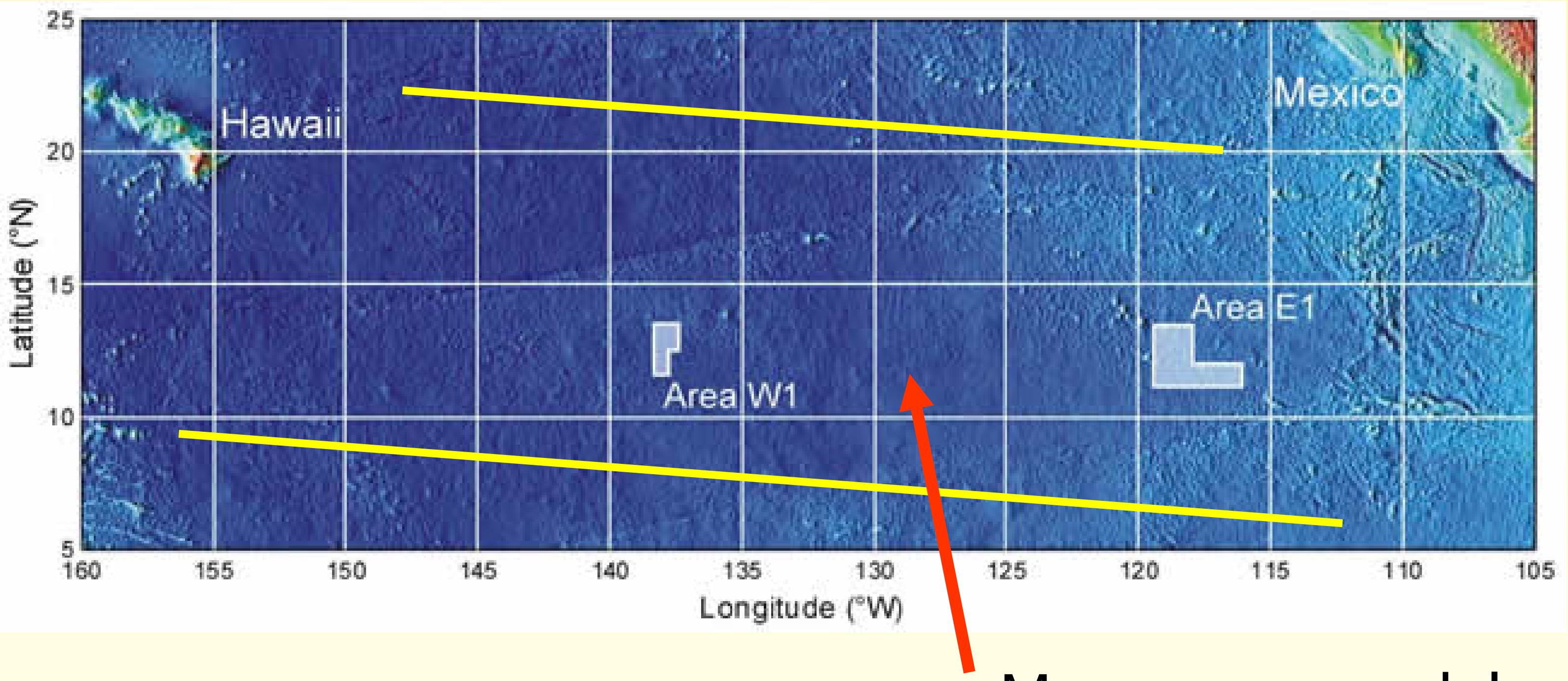

Manganese nodules

6. Sedimentation rates

The down-core decrease of $^{10}Be/^{9}Be$ yields an average sedimentation rate of 14.5 ± 1 m/Ma and a gap in sedimentation between 9.4 and 11.6 Ma

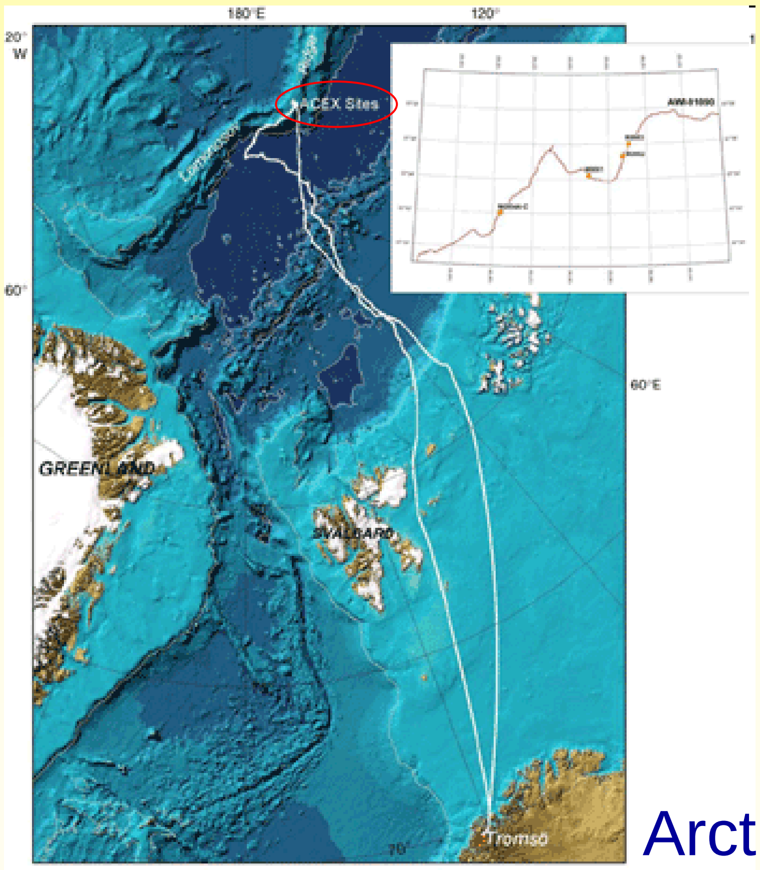

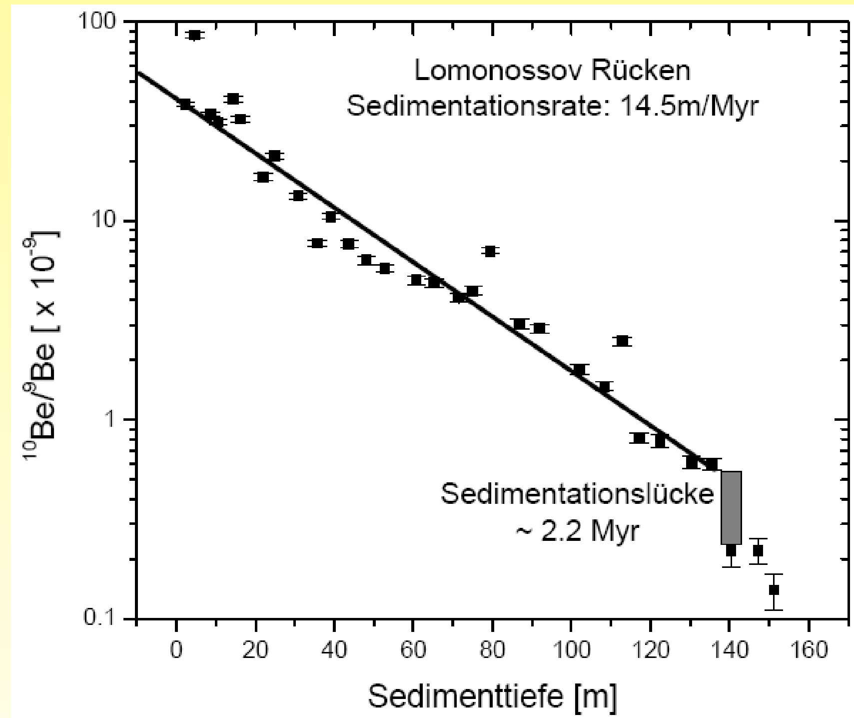

Frank et al. 2008

Arctic Coring Expedition 2004

http://www.eso.ecord.org/expeditions/302/302.htm

6. Growth rates

Manganese nodules are dark, potato-shaped little balls where metals and other minerals have accumulated around a core.

They contain a relatively high percentage of metals, i.e. **Nickel, Copper, Cobalt, Manganese** and **Iron** and are mostly found in water depths of 4000-6000 metres a few thousand km from the closest continent shores.

Manganese nodules

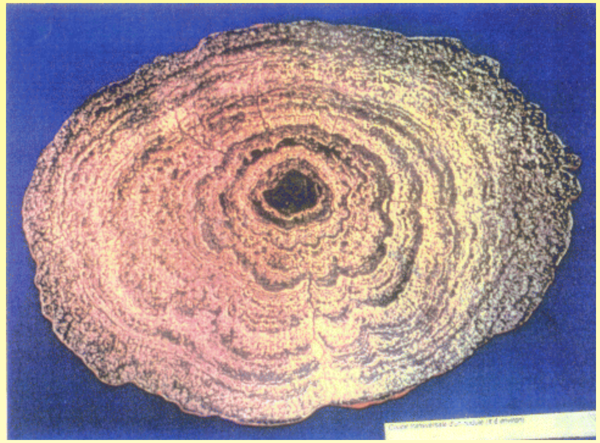

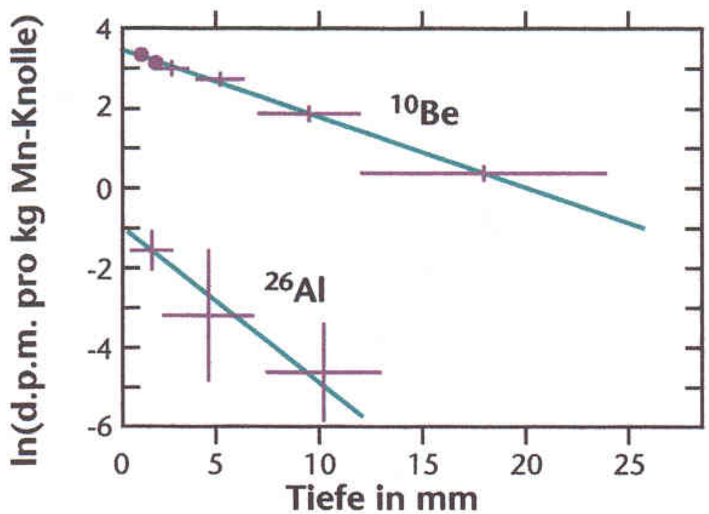

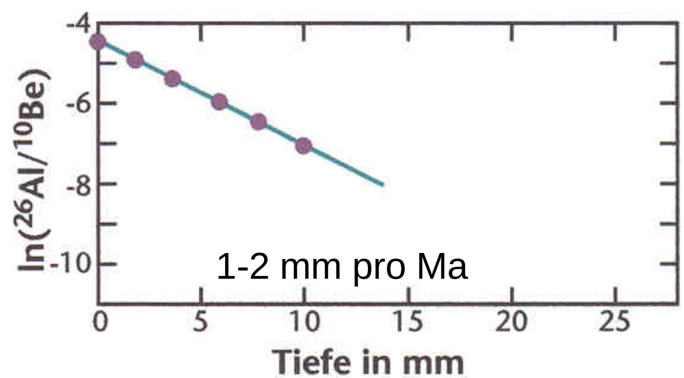

Guichard et al. (1978) Nature 272

7. Ground water dating – ^{36}Cl

Great Artesian Basin (Eastern Australia)

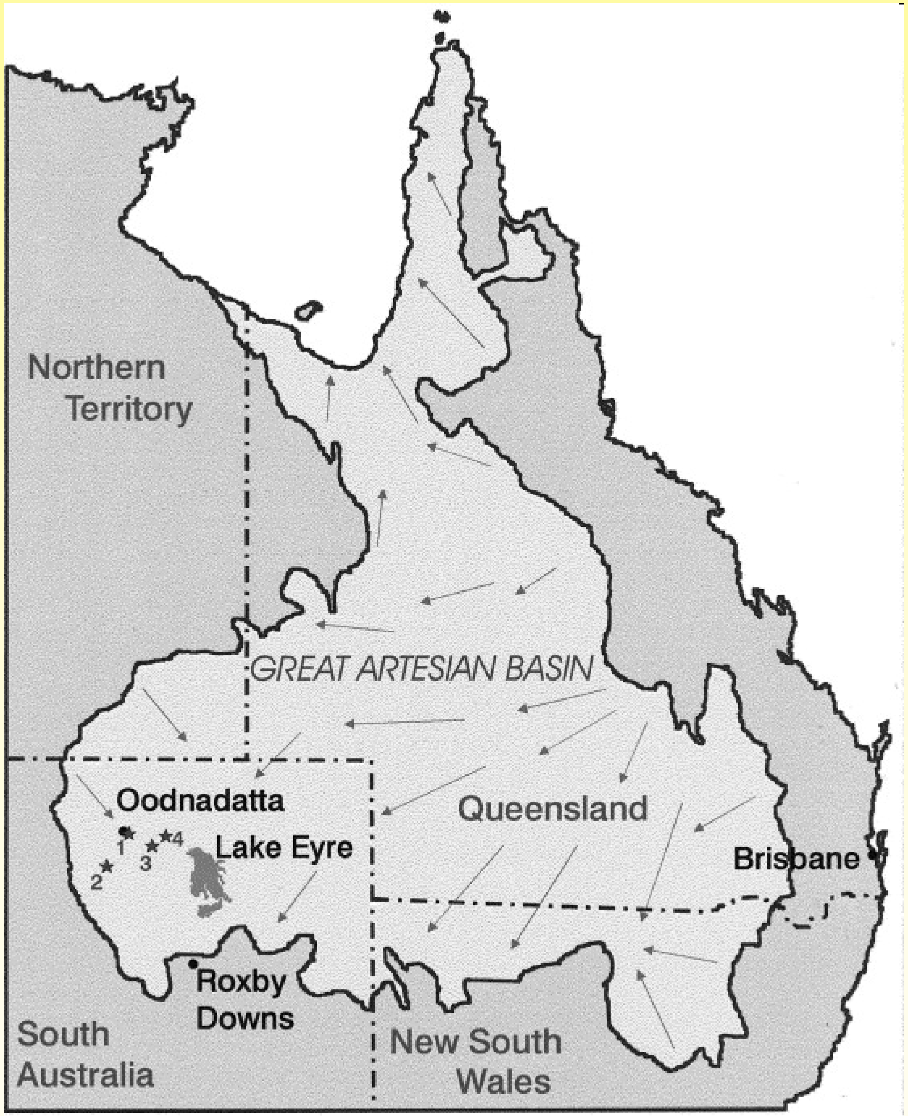

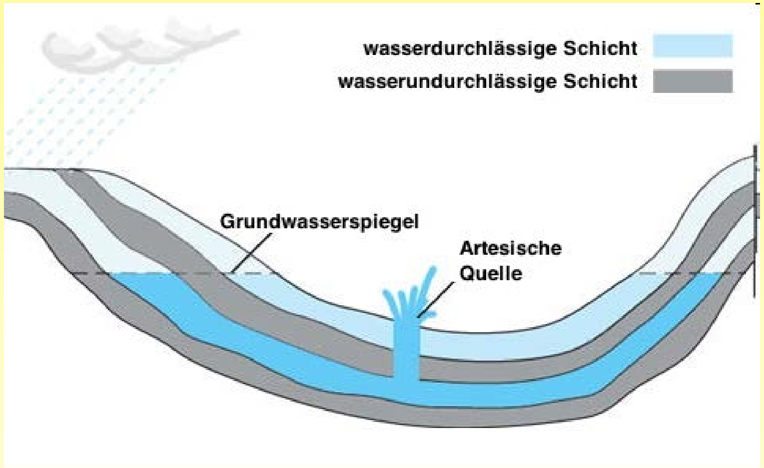

Collon et al. (2000)

7. Ground water dating – ^{36}Cl

Great Artesian Basin (Eastern Australia)

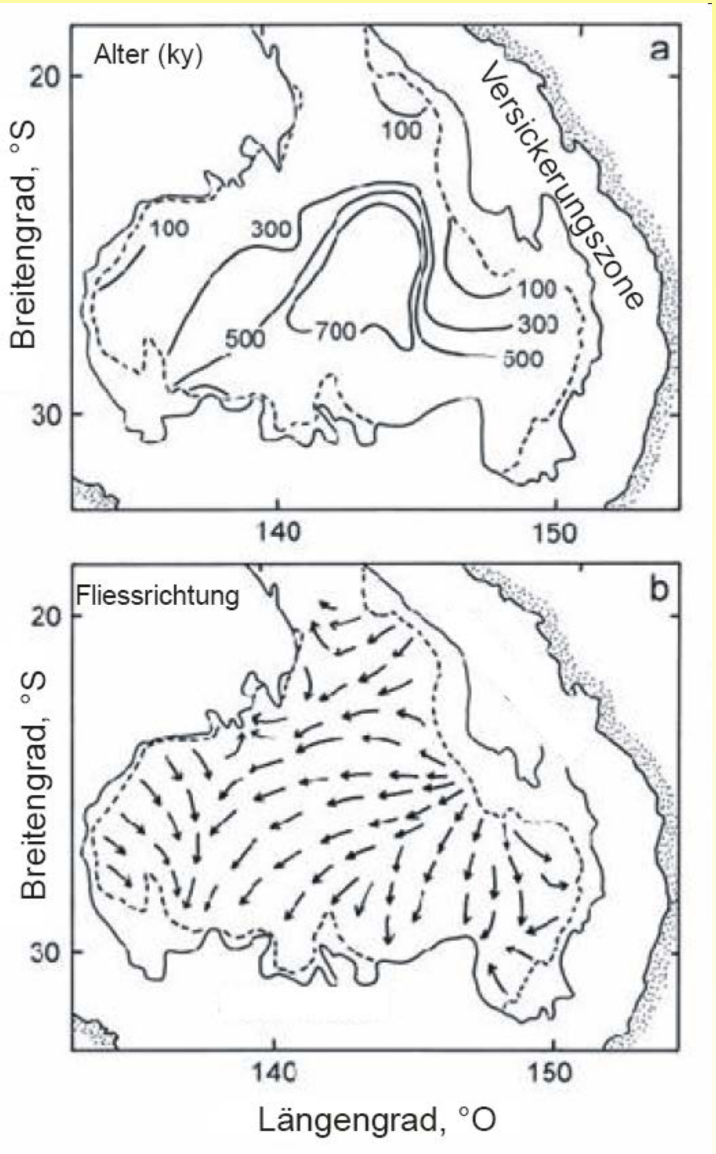

a) ^{36}Cl ground water dating (ages in 10^3 years)

b) reconstructed ground water flow directions

Torgersen et al. (1991), Love et al. (2000)

8. Sea water dating – ^{14}C

Great Ocean Conveyor

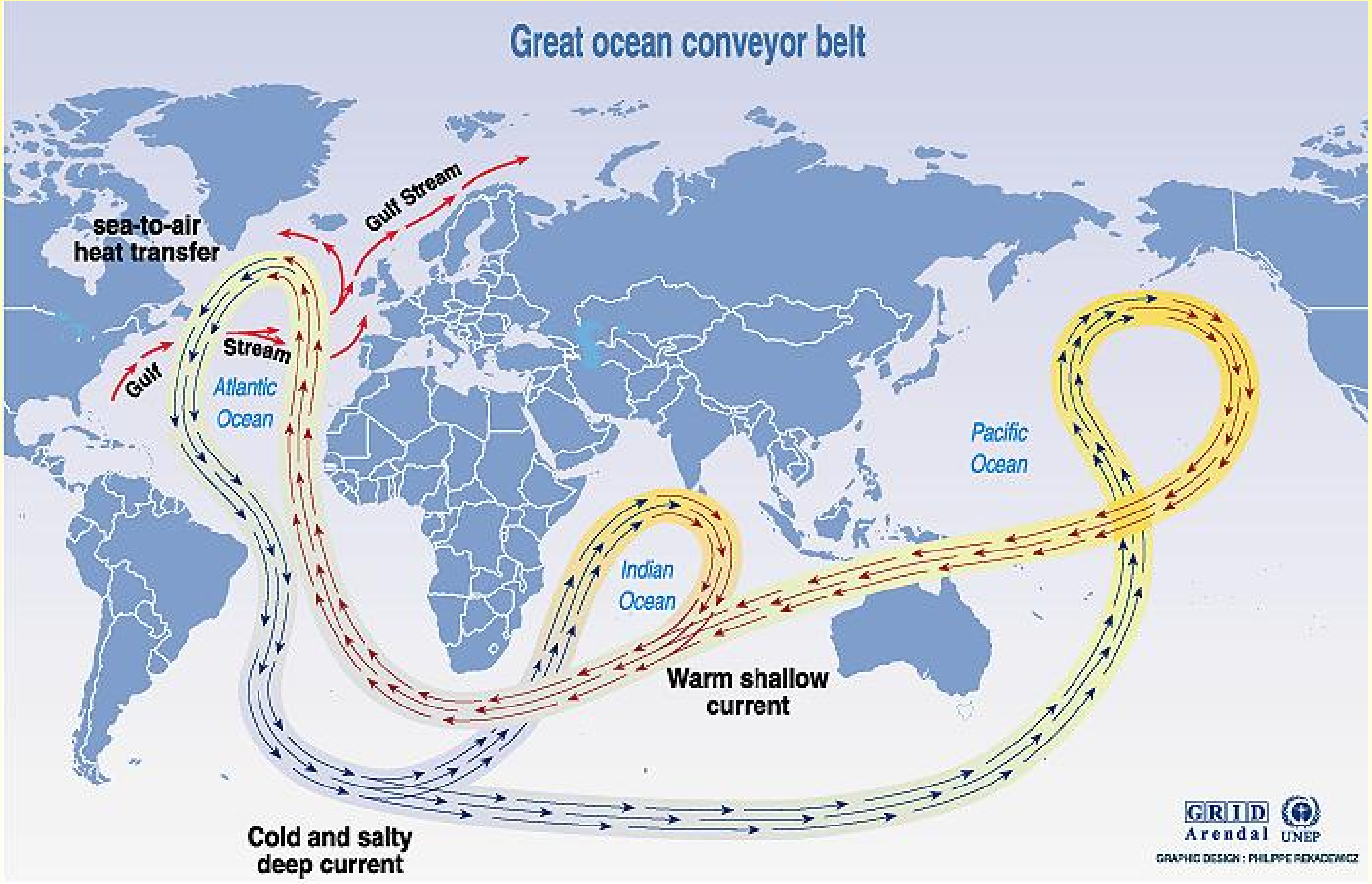

Source: Broecker, 1991, in Climate change 1995, Impacts, adaptations and mitigation of climate change: scientific-technical analyses, contribution of working group 2 to the second assessment report of the intergovernmental panel on climate change, UNEP and WMO, Cambridge press university, 1996.

8. Sea water dating – ^{14}C

Great Ocean Conveyor

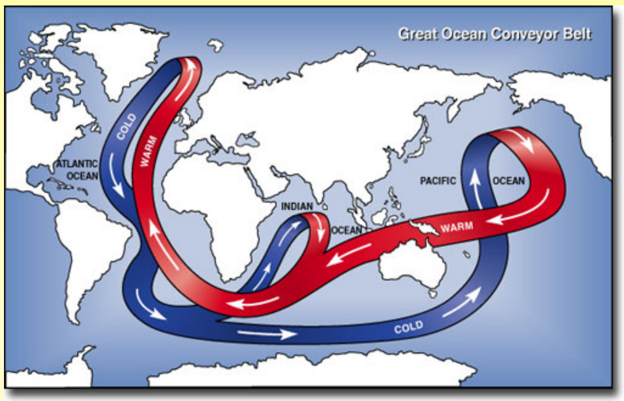

At high latitudes surface sea water becomes denser as it cools

Carbon dioxide in the atmosphere reacts with carbonate ions in sea water to form bicarbonate:

$CO_2 + CO_3^{2-} + H_2O \rightarrow 2HCO^{3-}$

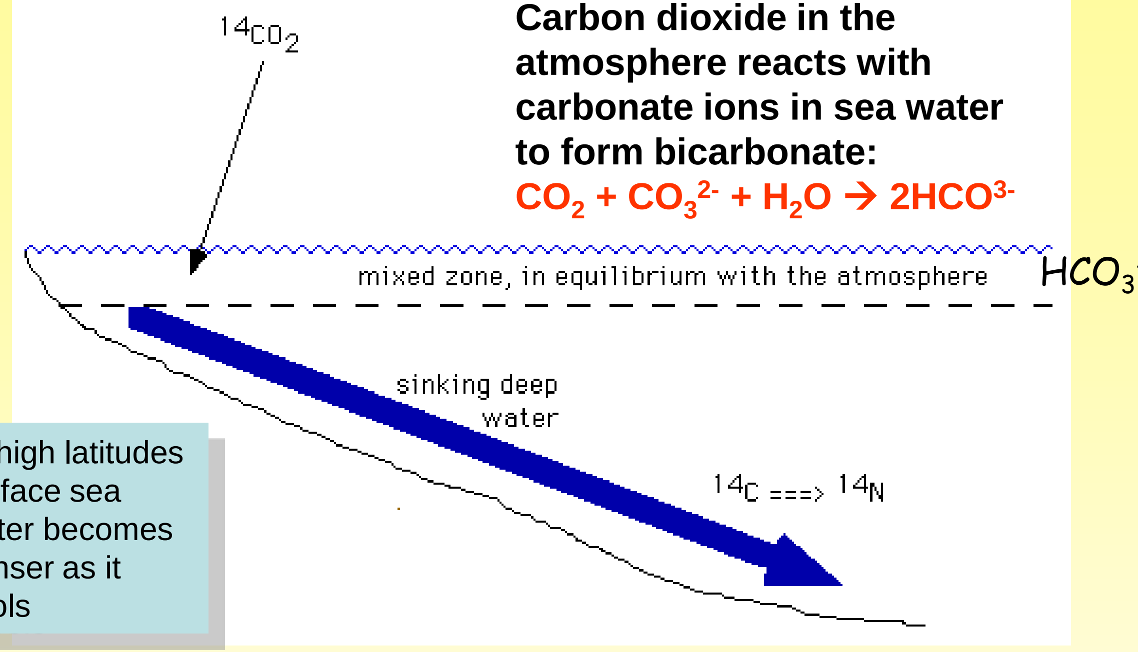

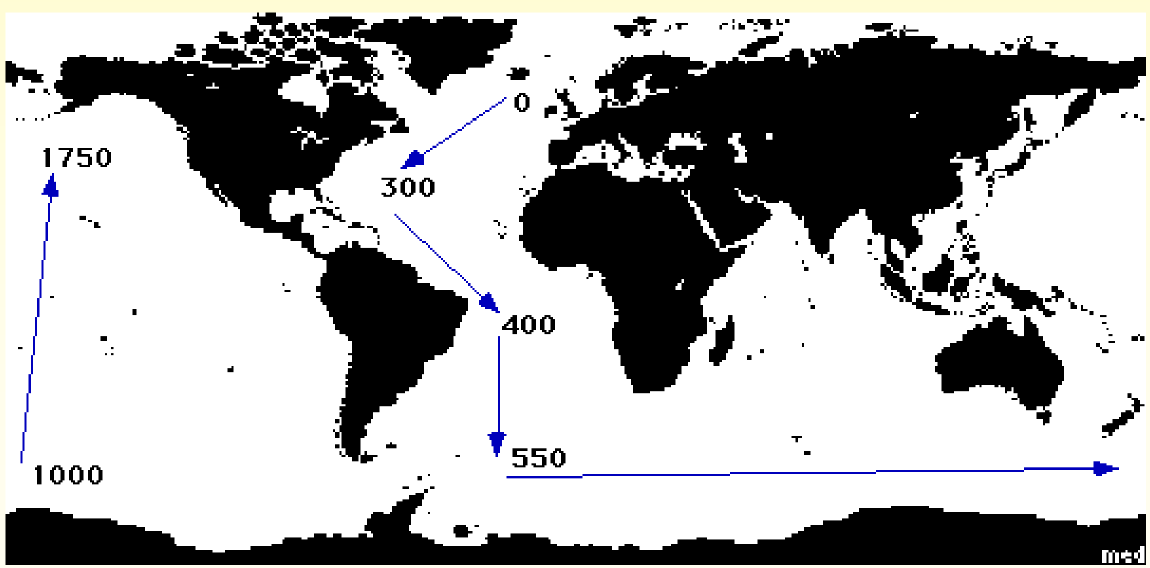

The major source of this bottom water is in the North Atlantic

9. Age of landscapes

Tropical inselbergs

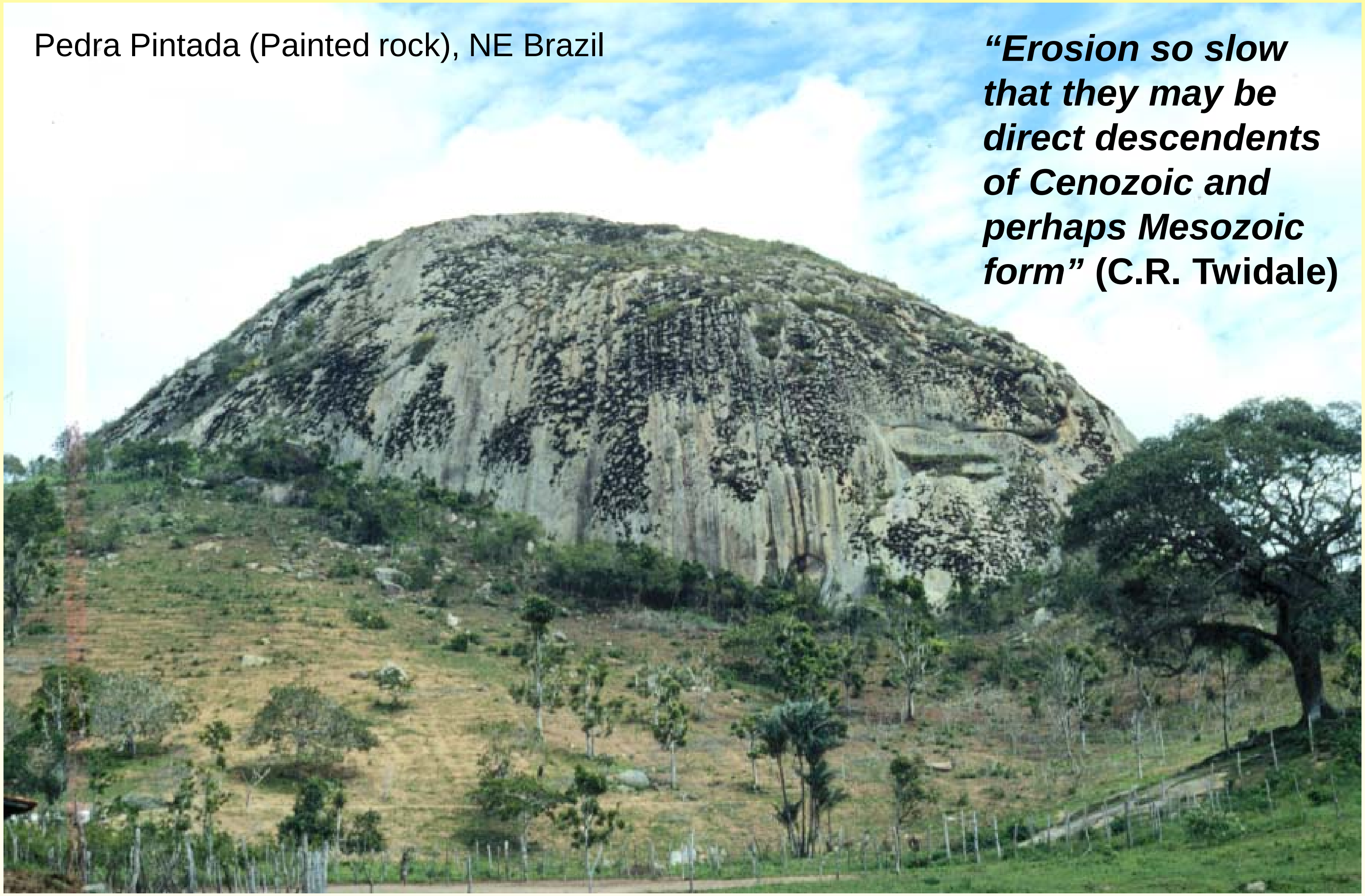

9. Age of landscapes

Arid environments

Inselbergs in the central Namib desert:
mean denudation rate of the order of 5 m/m.y.
(Cockburn et al., 1999)

Atacama desert, Chile:
~2 m/m.y. to <0.2 m/m.y.
(Caffee, 2005)

9. Age of landscapes

Martian surface: 78 ± 30 Ma *(Farley et al. 2013 Science 24)*

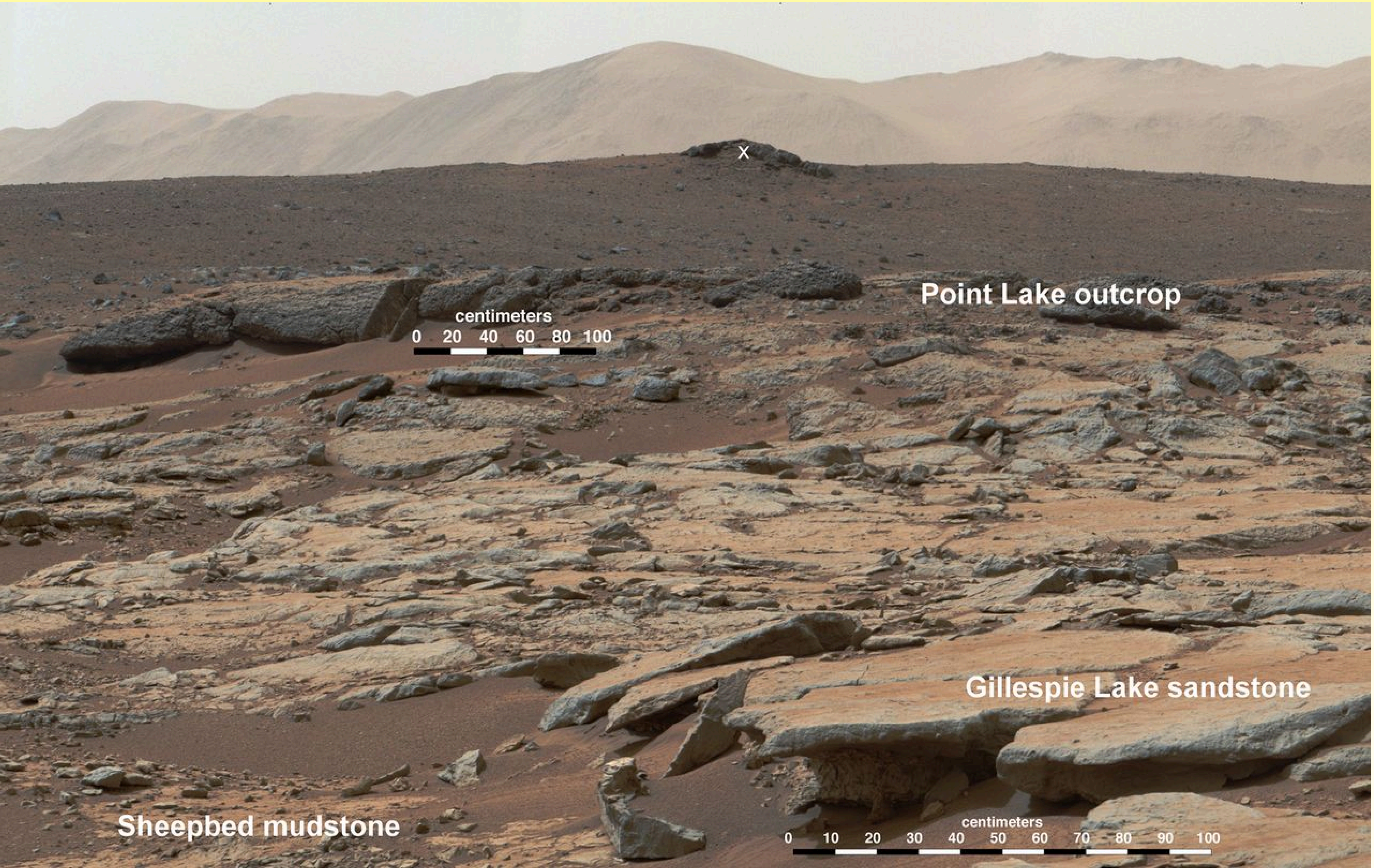

10. Erosion rates

How many years must a mountain exist
Before it is washed to the Sea?

The answer, my friend, is blowing in the wind…

Bob Dylan's song cited in:
Cerling and Craig (1994): Annu. Rev. Earth Planet. Sci 22: 273-317

…for geomorphologists the answer is provided by cosmogenic isotopes…

10. Erosion rates

What processes regulate chemical weathering and physical erosion?

What are the driving forces for landscape denudation?

Climate?
Precipitation?
Tectonics?
or combination?

Does erosion drive weathering or does weathering drive erosion?

10. Catchment wide denudation rates

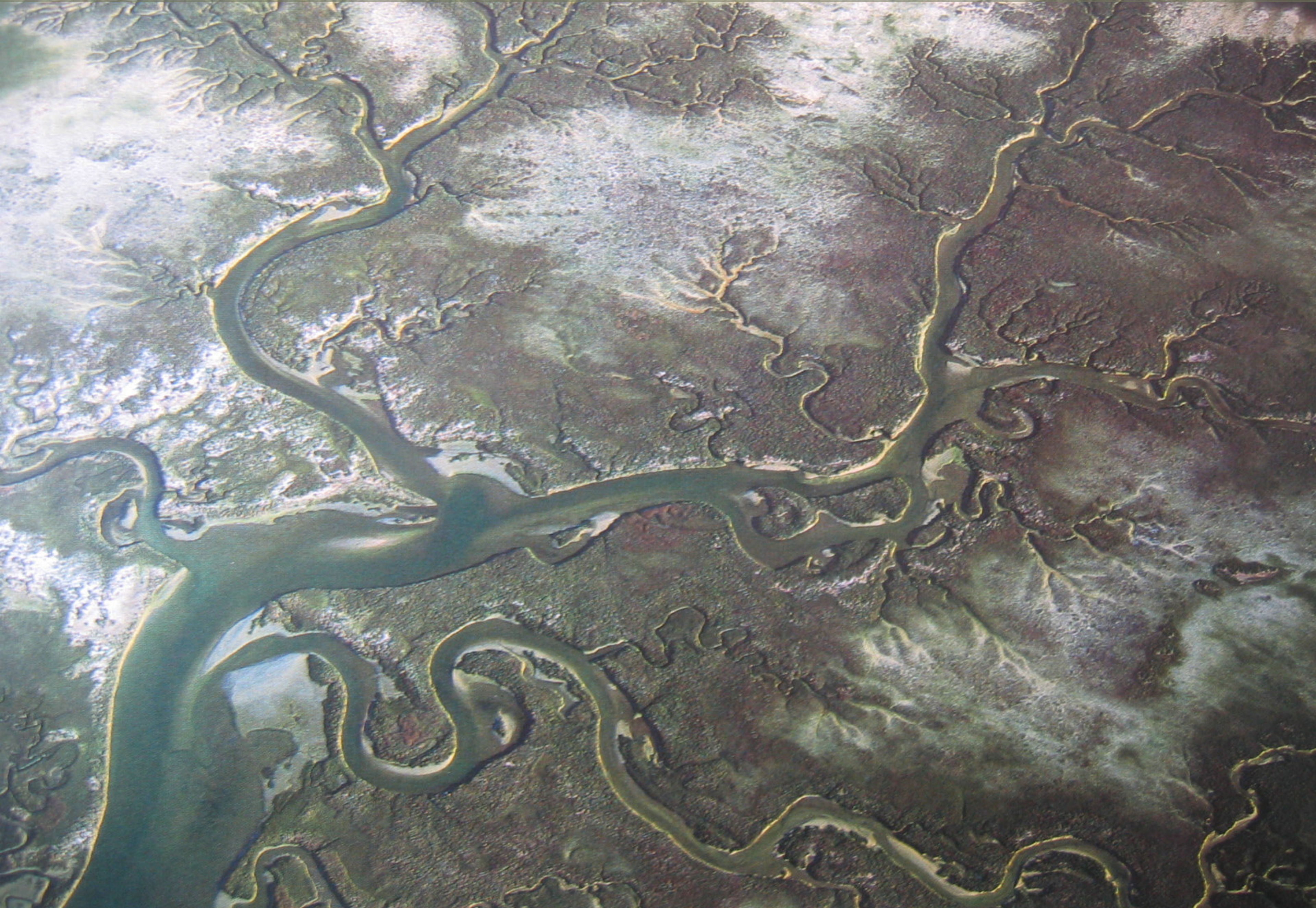

10. Catchment wide denudation rates

10. Catchment wide erosion rates

Erosionsraten aus *in situ*- produzierten kosmogenen Nukliden

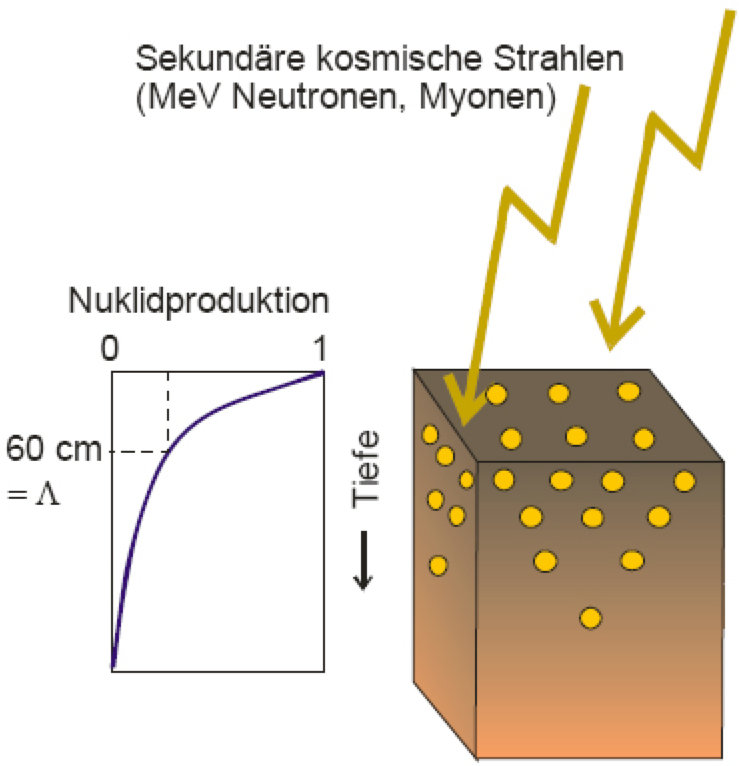

$$C = \left(\frac{P_o}{\varepsilon/\Lambda + \lambda} \right)$$

ε : Erosionsrate

C : Nuklidkonzentration

P_o : Nuklid Produktionsrate an der Gesteinsoberfläche

Λ : Mittlere Abschirmtiefe

λ : Zerfallskonstante

10. Catchment wide erosion rates

derived from river loads:

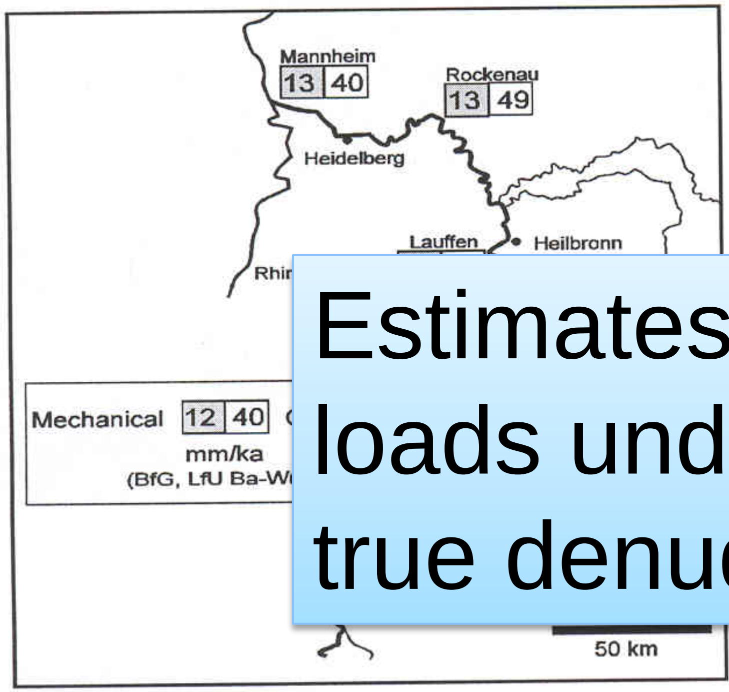

Fig. 1: Neckar denudation rates from river load data

von Blanckenburg et al.

derived from alluvial sediments:

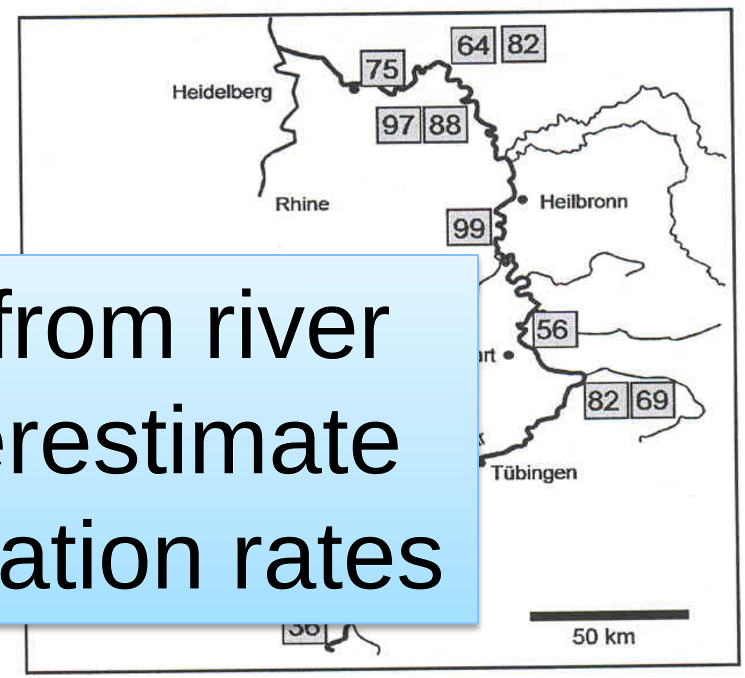

Fig. 2: Neckar total denudation rates from cosmogenic nuclides

Estimates from river loads underestimate true denudation rates

Cosmogenic isotopes measure total denudation rate - chemical part and physical part

10. Catchment wide denudation rates

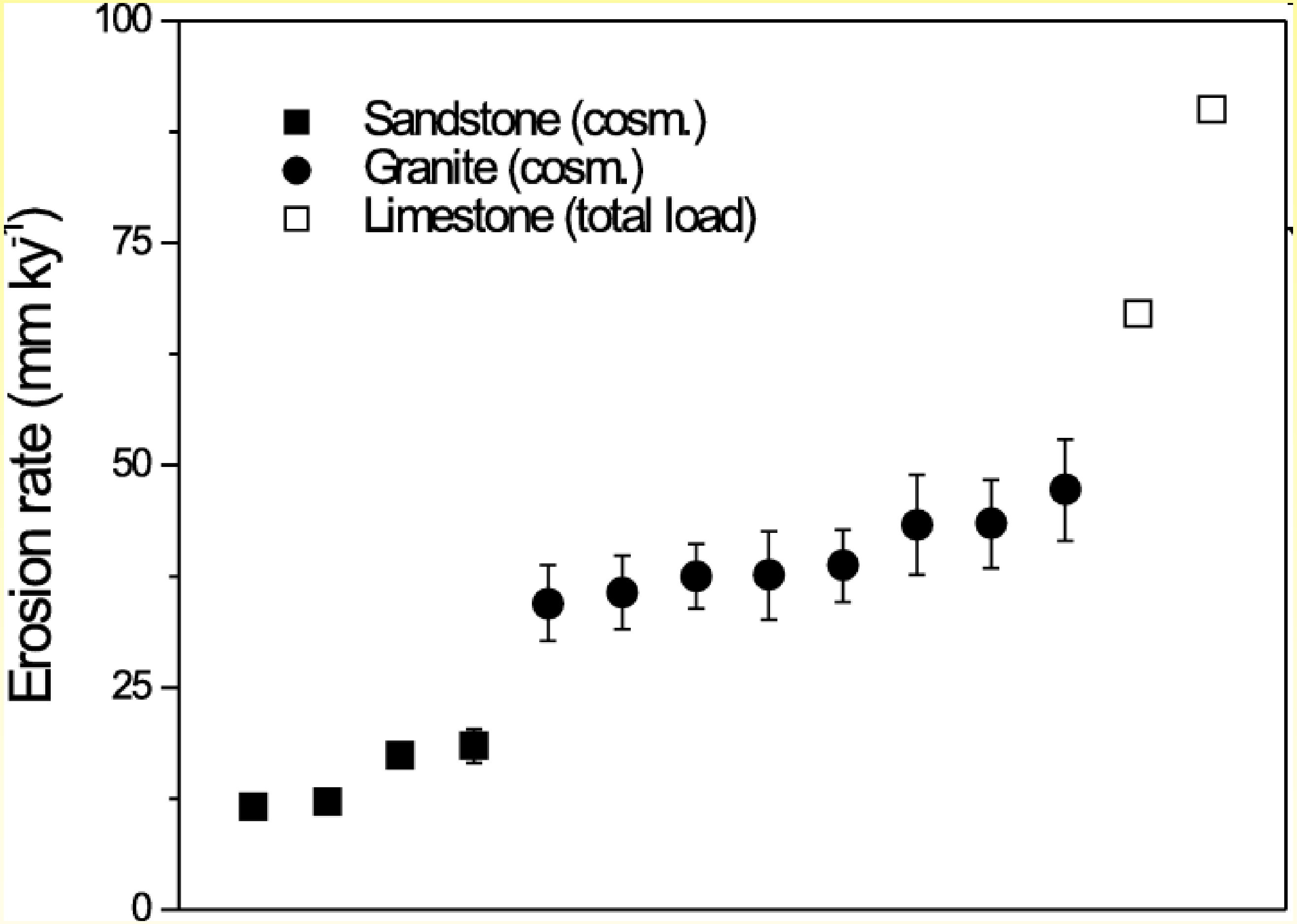

Lithological dependence of erosion rates as determined from cosmogenic nuclides and river load data (Bauer 1993, Morel et al. 2003)

10. Catchment wide denudation rates

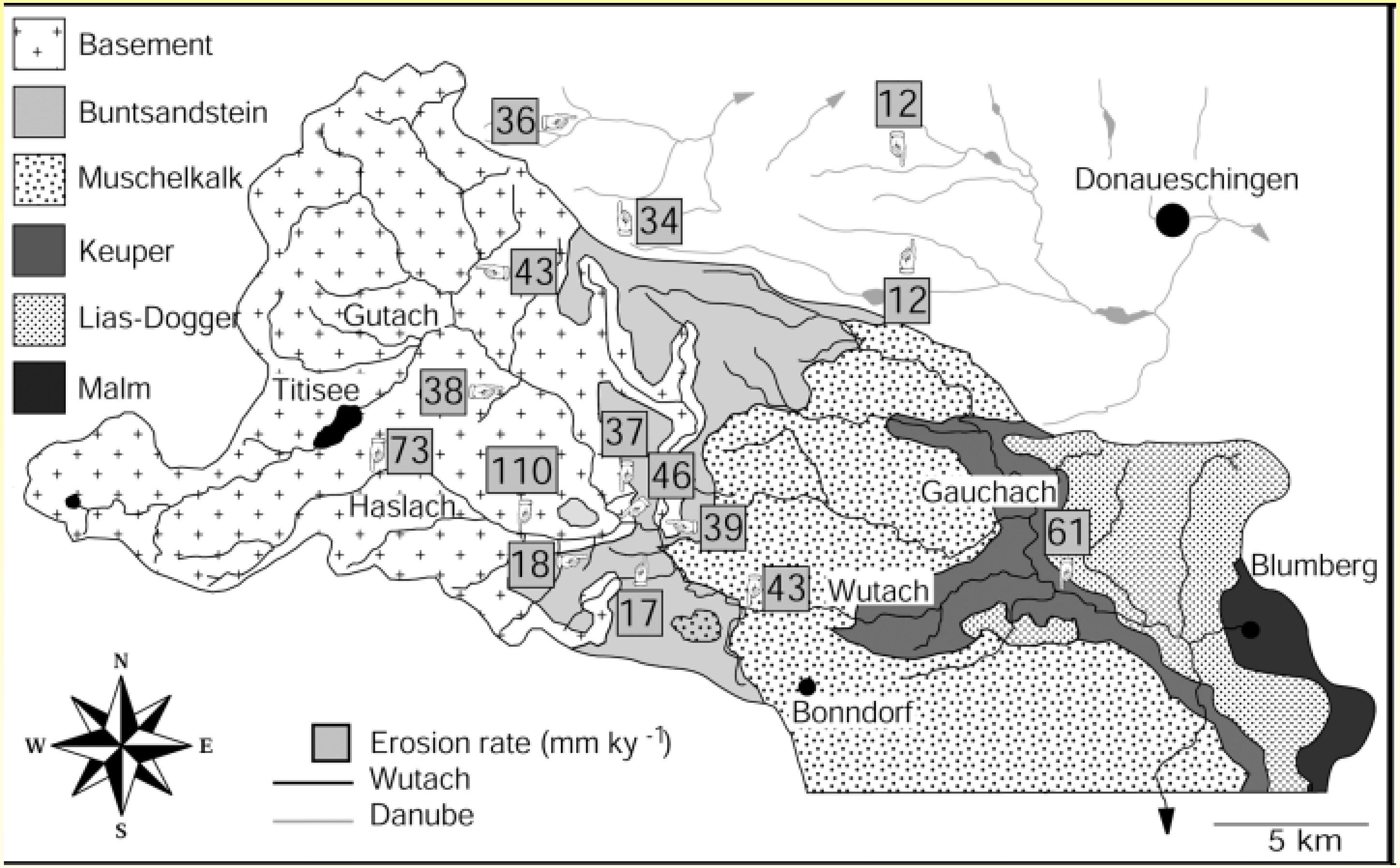

Morel et al. 2003 Terra Nova

Geological map of the Wutach basin, with erosion rates from cosmogenic nuclides (mm kyr^{-1}).

10. Catchment wide erosion rates

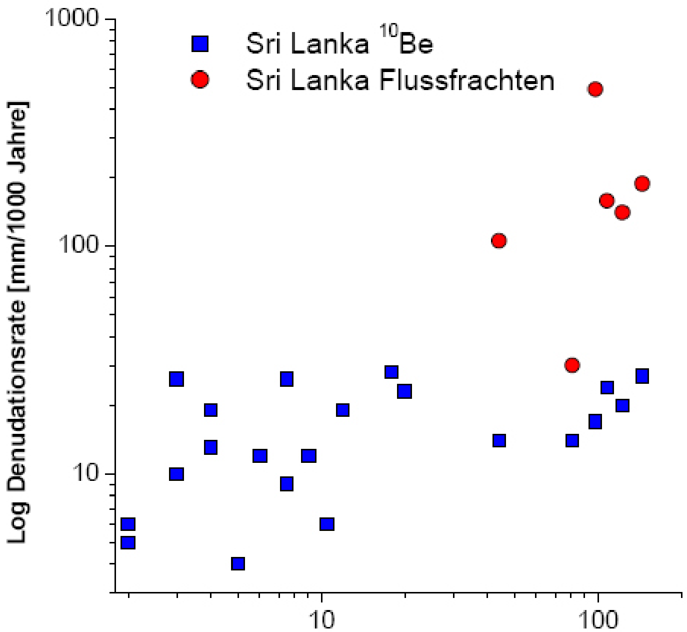

Fläche des Einzugsgebietes (km2)

von Blanckenburg 2008 GMIT 33

Sri Lanka: antropogenic increase of soil erosion

10. Catchment wide erosion rates

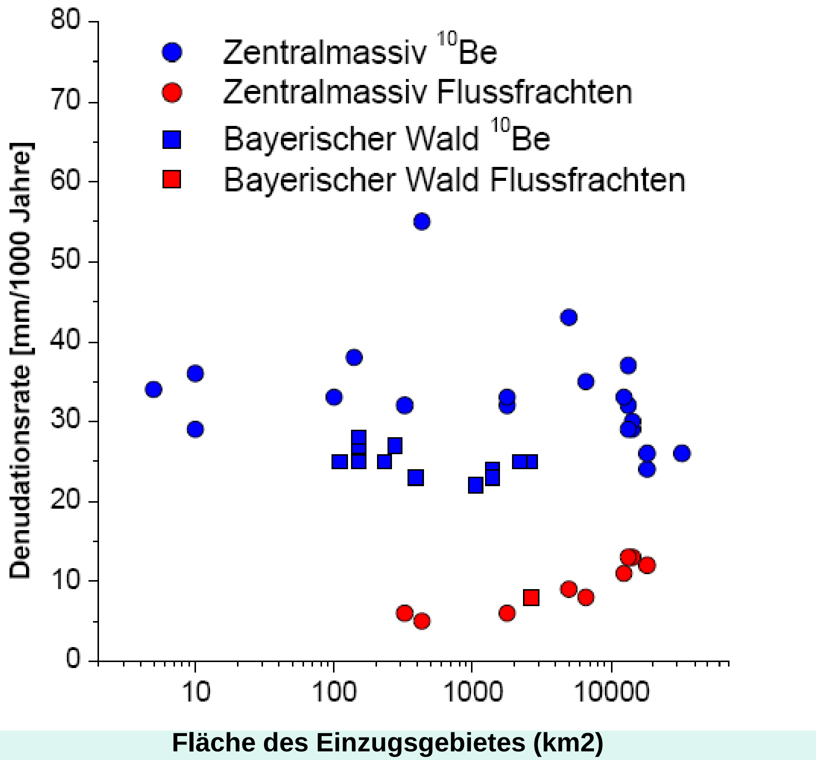

von Blanckenburg 2008 GMIT 33

European midlands:

Higher denudation rates as in Sri Lanka!

Why?????

Quarternary tectonic activity (uplift and rift formation) in central Europe
Ski Lanka: stable shield area

10. Catchment wide erosion rates

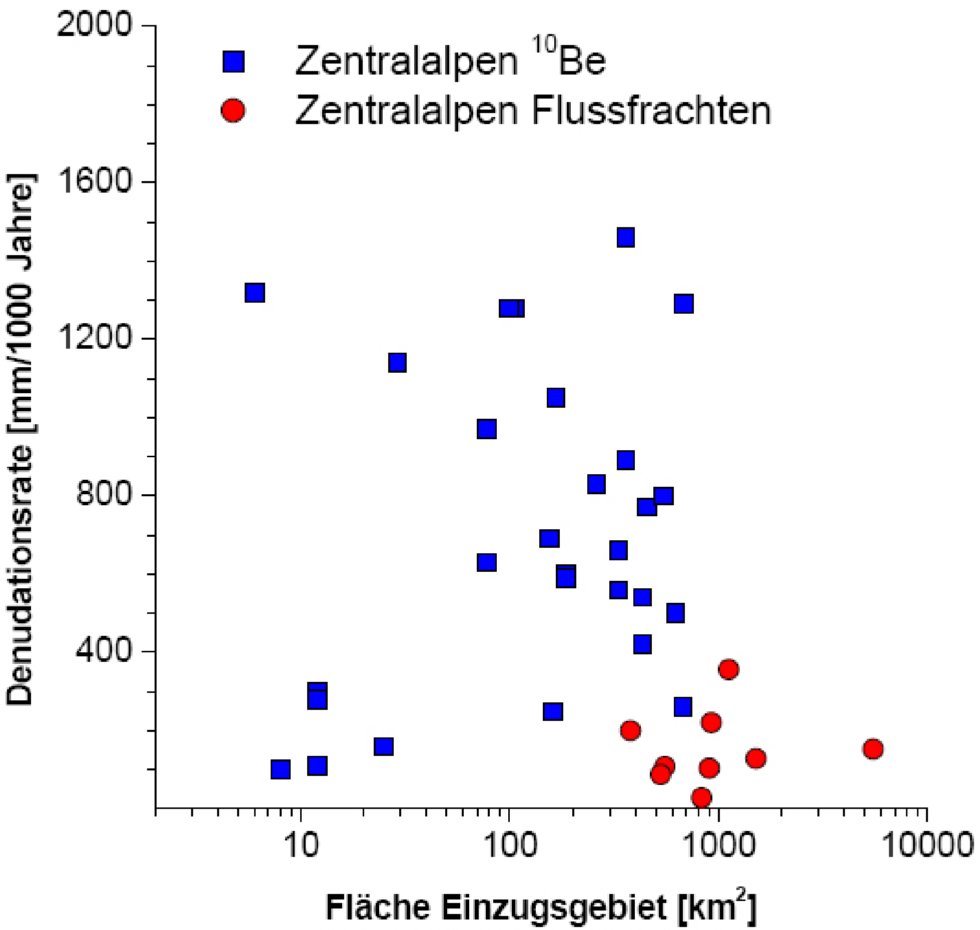

von Blanckenburg 2008 GMIT 33

Swiss Alps:

Very high cosmogenic denudation rates

River load underestimates true erosion rates

Reason: isostatic rebound following deglaciation

10. Catchment wide erosion rates

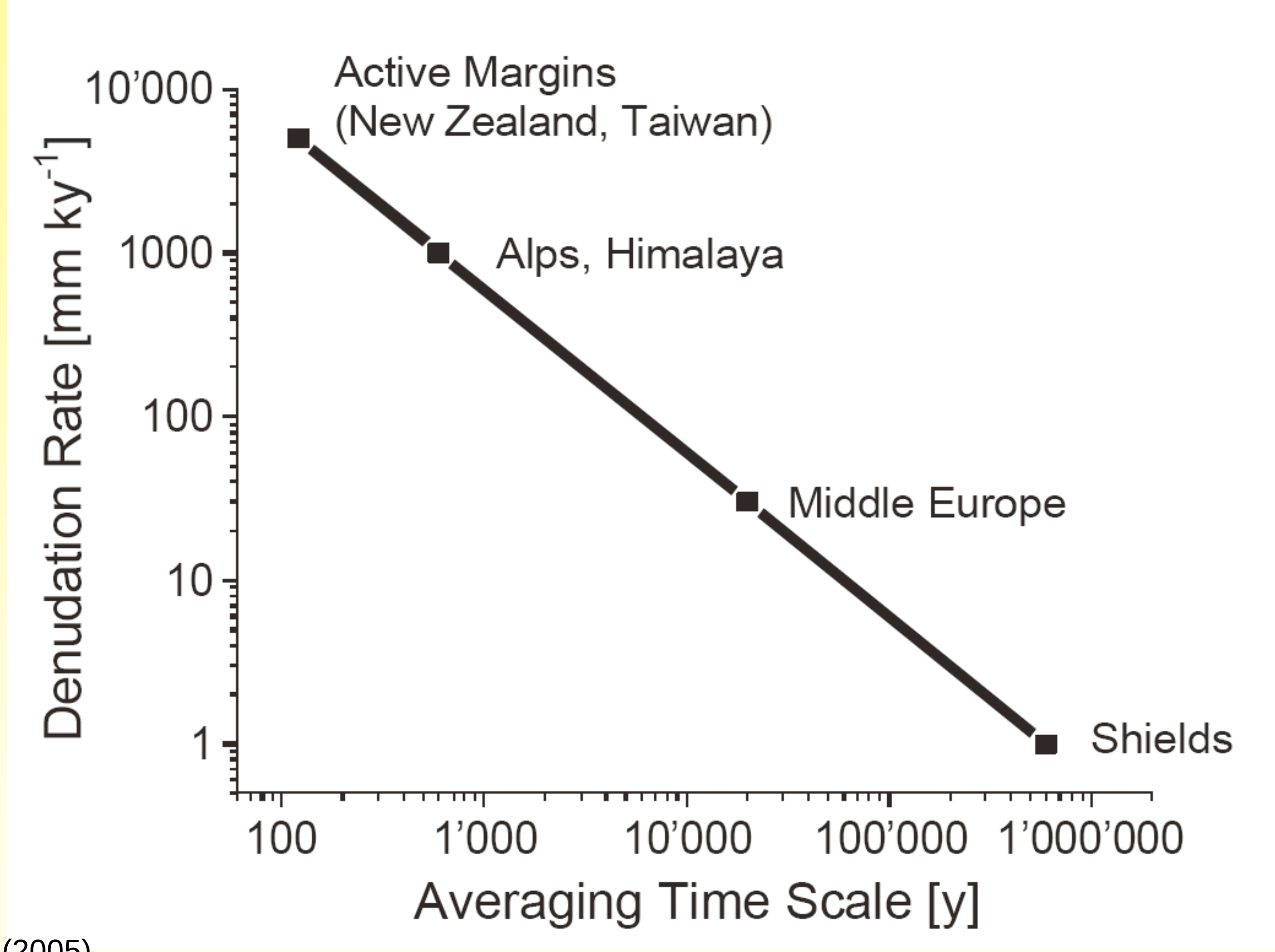

von Blankenburg (2005)

the time it takes to erode the upper 0.6 m of bedrock, or ca. 1.0 m of soil

10. Climate, erosion and rock weathering

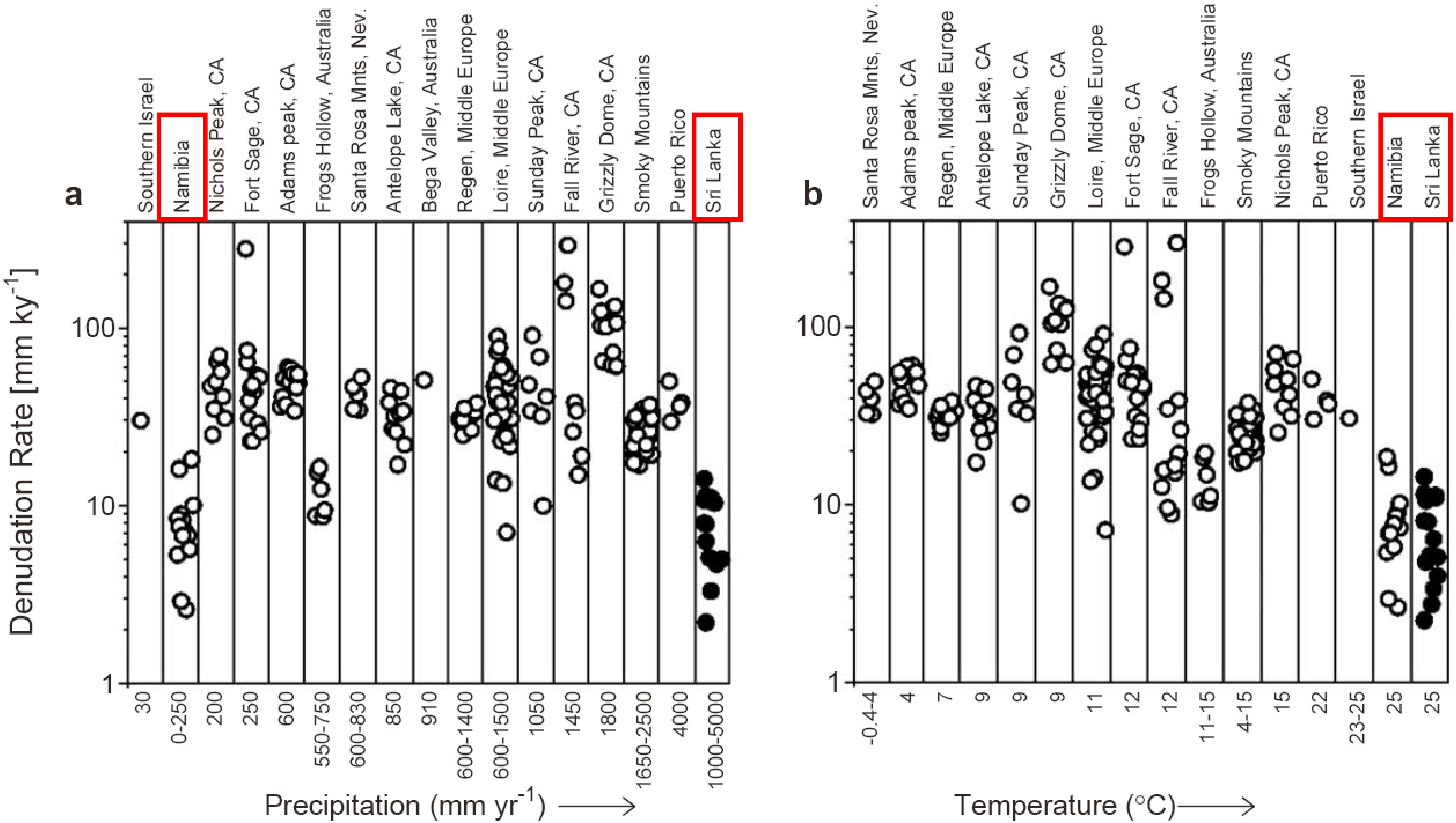

In order to avoid lithology-dependent effect only granitic catchments are shown

von Blanckenburg 2005

10. Catchment wide erosion rates

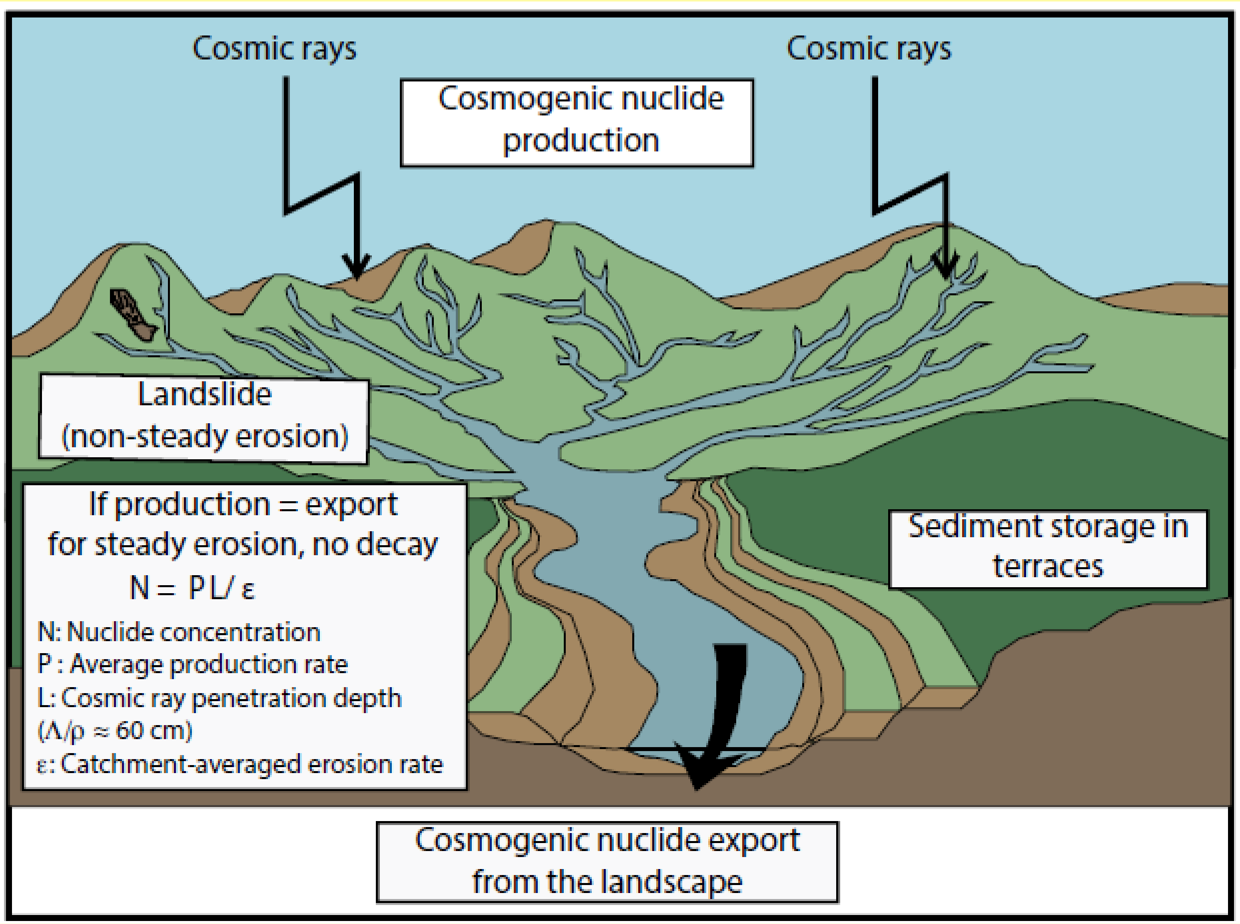

Granger & Schaller: Elements (2014)

„Nature does the averaging“

10. Catchment wide erosion rates

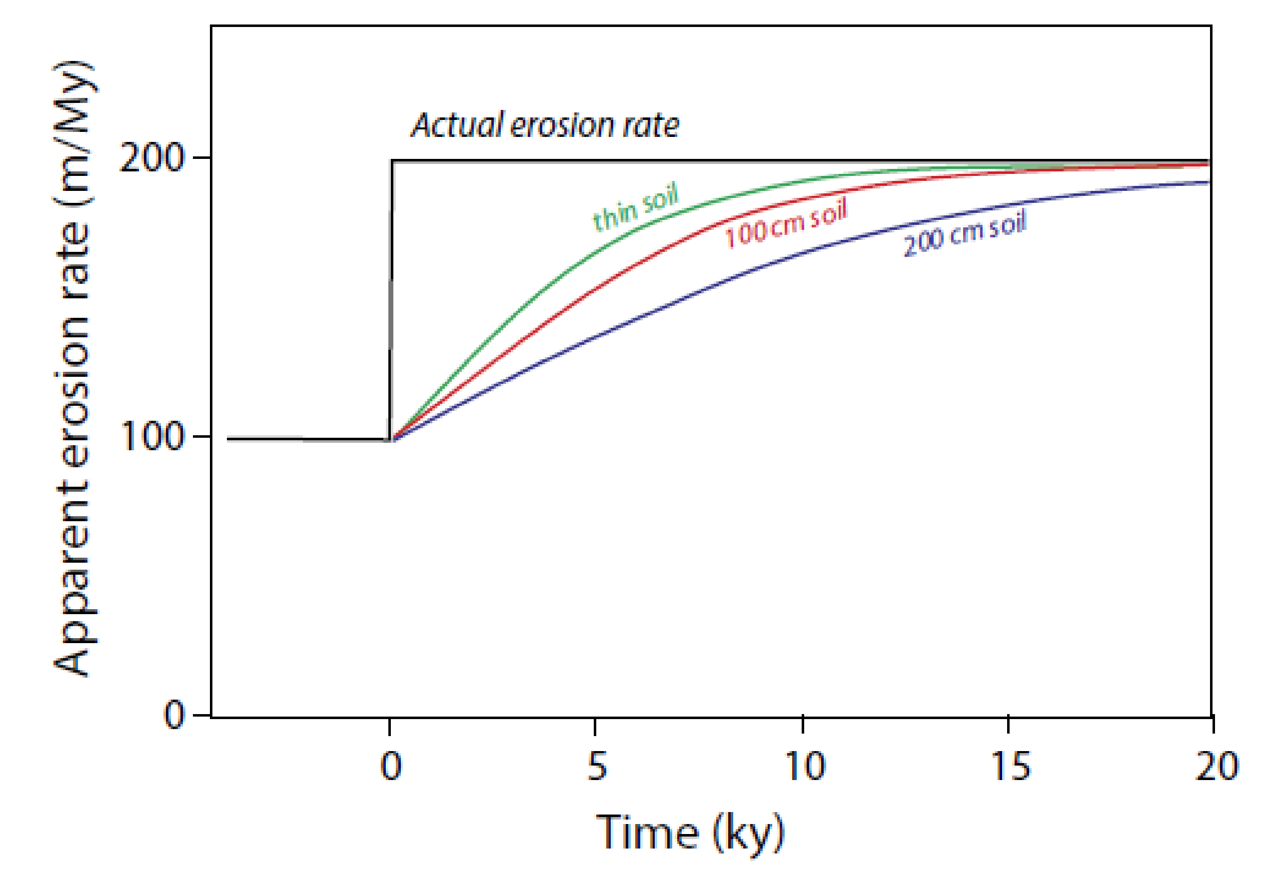

Granger & Schaller: Elements (2014)

10. Palaeo-erosion rates

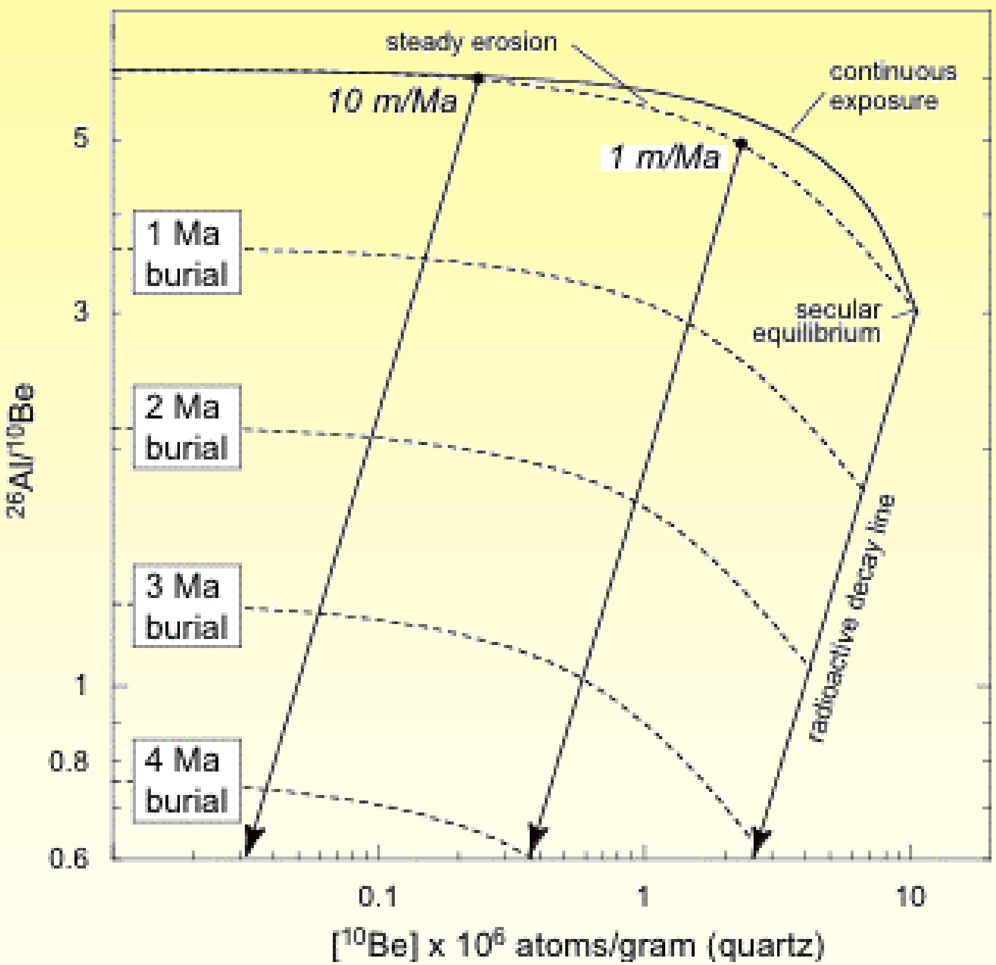

For completely buried and shielded minerals, the $^{26}Al/^{10}Be$ decreases along a line parallel to the solid "radioactive decay line".

Measured $^{26}Al/^{10}Be$ ratio in a sample determines the burial time, and can also be used to calculate the pre-burial (or palaeo) erosion rate.

10. Palaeo-erosion rates

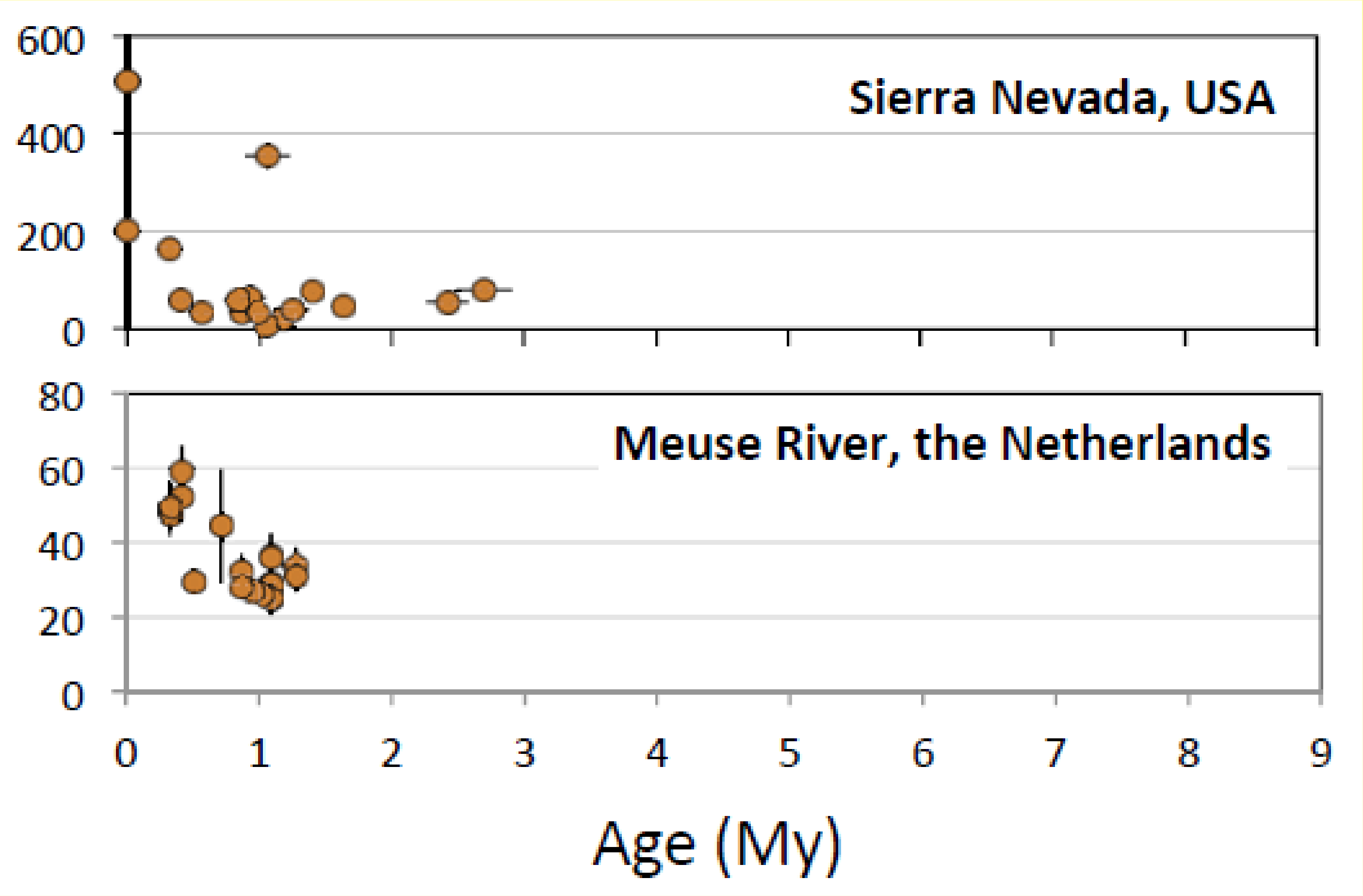

Granger & Schaller: Elements (2014)